A VERSATILE DESIGN PLATFORM FOR MULTI-HETEROCYCLIC IONIC LIQUID SYNTHESIS

by

DAVID MARTIN DRAB

A DISSERTATION

Submitted in partial fulfillment of the requirements
for the degree of Doctor of Philosophy
in the Department of Chemistry
in the Graduate School of
The University of Alabama

TUSCALOOSA, ALABAMA

2011

ABSTRACT

Ionic liquids (ILs, briefly defined as salts exhibiting melting points below 100 ^{o}C) have been extensively researched in the past few decades, where properties controllable through selective variation in ion structure have supported a variety of discoveries in materials design. The modular combination of available 'IL-forming' cations and anions provides retention of properties inherent to ILs such as low melting points, good thermal stability and negligible vapor pressure. Additionally, the dual-functional nature of ILs, whereby the design of functionalized ions is compartmentalized, can target specific physicochemical properties. Such transformable chemistry provides access to new design options from which contemporary problems in materials synthesis and applications may be strategically addressed.

Due to the potential to reduce environmental health and safety hazards as well as access the systematic design of energetic materials, energetic ionic liquids (EILs) are identified as a class of materials which may afford new and improved alternatives to conventional propellants, explosives, and fuels. Rather than aiming to synthesize new energetic materials, the effort of this research was to develop a working knowledge of how to affect changes in EIL properties through modification of ion structure and composition, as well as to develop new design concepts that could provide effective strategies for future EIL synthesis.

The approach to the investigations described here was two-fold, where the synthesis of EILs was achieved by either a conventional dual-functional strategy or multi-heterocyclic ionic

liquid (MHIL) design. The main focus for this work includes (i) the synthesis of *N*-cyanoalkyl-functionalized imidazolium salts with different energetic anions for examination of effects on IL thermal properties and reactivity, (ii) the conceptual development and experimental demonstration of a new design platform for MHIL synthesis with variable structure, charge, and symmetry, and (iii) the expansion of MHIL design to include new IL structures and to explore novel synthetic methodologies.

DEDICATION

I would like to dedicate this work to my wife Andrea Drab and our children, Pablo and Anastasia; whose loving support provided me with the endurance and dedication necessary to meet all of my goals. I also give thanks to my father, Anthony Drab, my mother, Irene Drab, and both of my brothers, Michael Drab and Peter Drab, for their encouragement over the years as I sought my fortune in pursuing a career in chemical research.

LIST OF ABBREVIATIONS AND SYMBOLS

$[X]^-$	Variable anion
$[Az]^-$	Azolate anion
$[BF_4]^-$	Tetrafluoroborate anion
$[NO_3]^-$	Nitrate anion
$[NTf_2]^-$	Bistrifylamide anion
$[N(CN)_2]^-$	Dicyanamide anion
$[OH]^-$	Hydroxide anion
$[OTf]^-$	Triflate anion
$[PF_6]^-$	Hexafluorophosphate anion
$[ZnCl_4]^{2-}$	Tetrachlorozincate anion
$[1,3\text{-diMeIM}]^+$	1,3-Dimethylimidazolium cation
%	Percent
$\boldsymbol{\delta}$	Chemical shift
δ^+	Partial positive charge
λ	Wavelength
π	Pi
μ	Letter Mu (Greek), indicating bridging ligand
Å	Angstrom 1×10^{-10} m

K	Kappa
α	Alpha
β	Beta
γ	Gamma
Δ	Delta, “change in”
$\boldsymbol{\nu}_{max}$	Frequency of absorption in wavenumbers (1/cm)
AcOH	Acetic acid
AFRL	Air Force Research Laboratory
AG 1-X8	Analytical grade strongly basic anion exchange resin; 100-200 mesh, 8% divinylbenzene copolymer cross-linkage
ATR	Attenuated total reflection
Az	Azole
bis	Twice (Latin)
ca.	“Approximately” (Latin)
calcd	Calculated
cat.	Catalytic amount
catena	Chain (Latin)
cm	Centimeter
CCD	Charge coupled device
CCDC	Cambridge Crystallographic Data Centre
CH_3CN	Acetonitrile
CO_2	Carbon dioxide
DAIL	Dicationic acidic ionic liquid

D_2O	Deuterium oxide
D.I.	Deionized
DMSO-d_6	Deuterated dimethylsulfoxide
DNB	Dinitrobenzene
DSC	Differential scanning calorimetry
DSSC	Dye-sensitized solar cell
EIL	Energetic ionic liquid
e.g.	"For example" (Latin)
EM	Energetic material
Eq.	Equivalent
ESD	Electrostatic discharge
et al.	"And others" (Latin)
etc.	"And so forth" (Latin)
Et_3N	Triethyl amine
Et_2O	Diethyl ether
EtOH	Ethanol
F	Structure factor
FT-IR	Fourier transform infrared
g	Grams
h	Hours
C	Specific heat (J/g)
HA	Unspecified Brönsted acid
HCl	Hydrochloric acid

Het	Heterocycle
HNO_3	Nitric acid
Hz	Hertz
ID	Inner diameter
i.e.	"That is" (Latin)
IL	Ionic liquids
in situ	"In the place" (Latin)
IRA-400	Strongly basic anion exchange resin (16-50 mesh, 8% divinylbenzene copolymer cross-linkage
J	Joules
J	J coupling, or indirect dipole-dipole proton coupling (^{1}H NMR)
K	Kelvin
$K_2[Hg(CNS)_4]$	Potassium tetrathiocyanatomercurate(II)
kg	Kilogram
L	Liter
M	Molar (moles/liter)
MeOH	Methanol
meq	Milliequivalent
mg	Milligram
MHIL	Multi-Heterocyclic Ionic Liquid
MHz	Megahertz
min	Minutes
mL	Milliliter

mm	Millimeter
mmol	Millimole
MoK_{α}	Molybdenum kappa alpha
mol	Moles
mol%	Molar percent concentration
mp	Melting point
MW	Molecular weight
mW	Milliwatt
N	Normal (equivalent/liter)
N	Newton
nm	Nanometer
NMR	Nuclear magnetic resonance
n.s.	Not synthesized
ORTEP	Oak Ridge Thermal Ellipsoid Plot Program
PEG	Poly(ethylene glycol)
per se	"In itself" (Latin)
PFPAE	Perfluropolyalkylether
pH	Negative logarithm of proton concentration
pK_a	Negative logarithim of the acid dissociation constant
ppm	Parts per million
psi	Pounds per square inch
RDX	Research Department Explosive (1,3,5-trinitroperhydro-1,3,5-triazine)

RT	Room temperature
RTIL	Room temperature ionic liquid
s	Seconds
SADABS	Siemens Automated Diffractometer (sad) Absorption (abs) Correction
SHELXTL	Sheldrick X-ray software (SHELX); Crystal (XTL)
SMART	Siemens Molecular Analysis Research Tool
$\boldsymbol{T}_{5\%onset}$	Onset temperature for 5% decomposition
$\boldsymbol{T}_{cryst}$	Temperature of onset of crystallization
$\boldsymbol{T}_{d}$	Temperature of thermal decomposition
$\boldsymbol{T}_{g}$	Glass transitions
$\boldsymbol{T}_{l\text{-}l}$	Temperature of onset for liquid-to-liquid transition
$\boldsymbol{T}_{m}$	Melting point of single component
$\boldsymbol{T}_{onset}$	Temperature of onset for thermal decomposition
TGA	Thermogravimetric analysis
TNT	Trinitrotoluene
TriHet	1-(2-(5-Tetrazolidyl)ethyl)-3-(5-1*H*-tetrazolyl)methylimidazolium
US AFOSR	United States Air Force Office of Scientific Research
V	Volt
via	"By way of" (Latin)
vide infra	"See below" (Latin)
VOC	Volatile organic solvent
vs.	Versus

v/v	Volume-to-volume ratio
W	Watts
w/w	Percent concentration by weight of solute to weight of solution
XRD	X-ray diffraction
(s)	Strong absorption (FT-IR)
(b)	Broad absorption (FT-IR)
(m)	Medium absorption (FT-IR)
(w)	Weak absorption (FT-IR)
(vs)	Very strong absorption (FT-IR)
s	Singlet (^{1}H NMR multiplicity)
d	Doublet (^{1}H NMR multiplicity)
t	Triplet (^{1}H NMR multiplicity)
td	Triplet of doublets (^{1}H NMR multiplicity)
m	Multiplet (^{1}H NMR multiplicity)
pent	Pentet (^{1}H NMR multiplicity)
1D	One-dimensional
2D	Two-dimensional
3D	Three-dimensional

ACKNOWLEDGEMENTS

I would like to thank Professor Robin D. Rogers, who has served as my research advisor for the duration of my residency at The University of Alabama. Along with providing me with the necessary funding for my research and education, Dr. Rogers has also supported and guided my initiation into the exciting field of ionic liquids. I am thankful for his invitation to participate in high-level, interdisciplinary projects of interest to both our group and our collaborators, where he has also advised my scientific writing and presentation that are essential for effective and professional communication. Perhaps most importantly, he has encouraged me not to settle for merely meeting expectations but, rather, to strive for excellence in all my career objectives.

I also would like to express my gratitude to all members of Dr. Rogers's group, both present and past, for enhancing my graduate experience with their fellowship. For their support of my work with the Air Force research team, I thank Dr. Marcin Smiglak and Dr. Julia L. Shamshina for advising my projects as well as for their assistance in the preparation of my work for publication. Special thanks go out to Dr. Gabriela Gurau, Dr. Marcin Smiglak, and Dr. Ning Sun for their generous gift of time and effort to help with the formatting and editing of the dissertation document. In addition, I thank Dr. Ning Sun, Mirela Maxim, Steven P. Kelley, C. Corey Hines, Dr. Nicholas J. Bridges, Dr. Whitney L. Hough, Jane-Holly Hines, Dr. Meghna Dilip, Dr. Keith E. Gutowski, Dr. W. Matthew Reichert, Dr. Richard P. Swatloski, Dr. Gabriela Gurau, Dr. Violina Cocalia, Dr. Scott T. Griffin, Dr. Ying Qin, Dr. Mustafizur Rahman, Dr. Melanie L. Moody, Dr. Hui Wang, Dr. Xiaosi Zhou, Dr. Asako Narita, Parker McCrary, T.

Gannon Parker, Preston Beasley, and John Canada for their companionship over the years in our group. Also, I would like to thank the visiting scholars that I have had the pleasure to work with, including Dr. Christiaan Rijksen, Dr. Diego Fort, Dr. Andreas Metlen, Dr. David B. Cordes, Sohail Nadeem, and Dr. Héctor Rodríguez. I value our shared friendship and research experiences during all of our days together, and they will not very soon be forgotten.

I am thankful to each member of my committee, including Dr. Robin D. Rogers, Dr. Michael P. Jennings, Dr. Timothy S. Snowden, Dr. Kevin H. Shaughnessy, and Dr. Gregory W. Drake for showing patience and wisdom throughout their critique of my research progress. To Dr. Jennings, Dr. Snowden, and Dr. Shaughnessy, I give further mention here for their excellent formal instruction in my organic chemistry curriculum which has been invaluable in providing a theoretical foundation for all of my research endeavors. Likewise, I thank Dr. Drake for offering his time and expert opinion to effectively address the priority needs of the Air Force when developing my own research agenda.

For their support throughout my time at The University of Alabama, I would like to thank the United States Air Force Office of Scientific Research for their generous funding of my research (US AFOSR Grant F49620-03-0357 and FA9550-10-1-0521). In addition, I thank my collaborators Dr. Tommy W. Hawkins and Dr. Stefan Schneider (Air Force Research Laboratory, Edwards Air Force Base, CA) for their dedication and cooperation when assisting me to achieve my research goals. By sharing their knowledge and extensive experience from working with energetic materials synthesis and characterization, they have helped me to form synthetic strategies while enriching my conceptual knowledge through our various exchanges. Additionally, Dr. Hawkins and Dr. Schneider have provided impact, friction, and electrostatic

discharge sensitivity testing data for all dicyanamide salts presented in this work, and for this I extend my gratitude.

I am also thankful to Prof. Leonard R. MacGillivray (University of Iowa, Iowa City, Iowa) for serving as my MS advisor as I began my graduate research, where his passion for solid-state organic synthesis and crystallographic studies provided me with a foundation of theory and practice from which I could effectively address structural issues in my work at The University of Alabama. I also am thankful to Dr. Scott T. Griffin, C. Corey Hines, Dr. David B. Cordes, and Steven P. Kelley for their analysis and refinement work in all single crystal X-ray structures that have been solved for my research. Finally, I am grateful to Dr. Ken Belmore for his help at The University of Alabama's NMR Facility with the operation of instrumentation and interpretation of data.

TABLE OF CONTENTS

LIST OF TABLES

LIST OF FIGURES

LIST OF SCHEMES

CHAPTER 1

INTRODUCTION

1.1 Abstract

An account of the recent growth of a new family of ionic liquids, namely, multi-heterocyclic ionic liquids (MHILs) is presented here. Bridged MHILs, in particular, have been shown to provide unique access to highly directed properties through both symmetric and asymmetric structures which enable flexible modifications at the site of the heterocycle, substituent, bridging units, as well as the type of counter-ion. A representative selection of new advances in symmetric and asymmetric bridged MHILs are showcased here, where emphasis is made in describing the reported properties trends from the modification of MHIL structures and findings which indicate high performance applications.

1.2 Introduction

Initially, ionic liquid (IL, or salt with melting point below 100 ^{o}C[1]) synthesis had emphasized the combination of available cations and anions (Figure 1.1) and further identifying what structural changes were associated with observed trends in properties.[2-7] More recently, the 'second evolution' of IL discovery focused on (i) the systematic preparation of new functionalized ionic liquids to target specific properties as well as (ii) the development of novel synthetic methodologies for the safe and efficient production, transportation, and storage of ILs. Here, the *dual-functional nature* of ILs – whereby both the cation and anion may be modified in

a compartmentalized fashion – enables a high degree of synthetic flexibility, where functional groups can be selectively incorporated to influence IL properties.[8] The capacity for ILs to target specific properties inspired concentrated investigations for high-performance applications. For example, the United States Air Force Office of Scientific Research (US AFOSR) has a vested interest to understand the nature of properties inherent to ILs (e.g., low melting points, negligible vapor pressures, high thermal stability) as well as other 'tunable' features achieved by further modification of cation and anion structure (e.g., high density,[9] low viscosity,[10] hypergolicity,[11,12] high heat of formation).[13] Significant efforts were made to develop new and improved candidates for energetic materials, where examples of ions under consideration for this category of energetic ionic liquids (EILs) are illustrated in Figure 1.1.

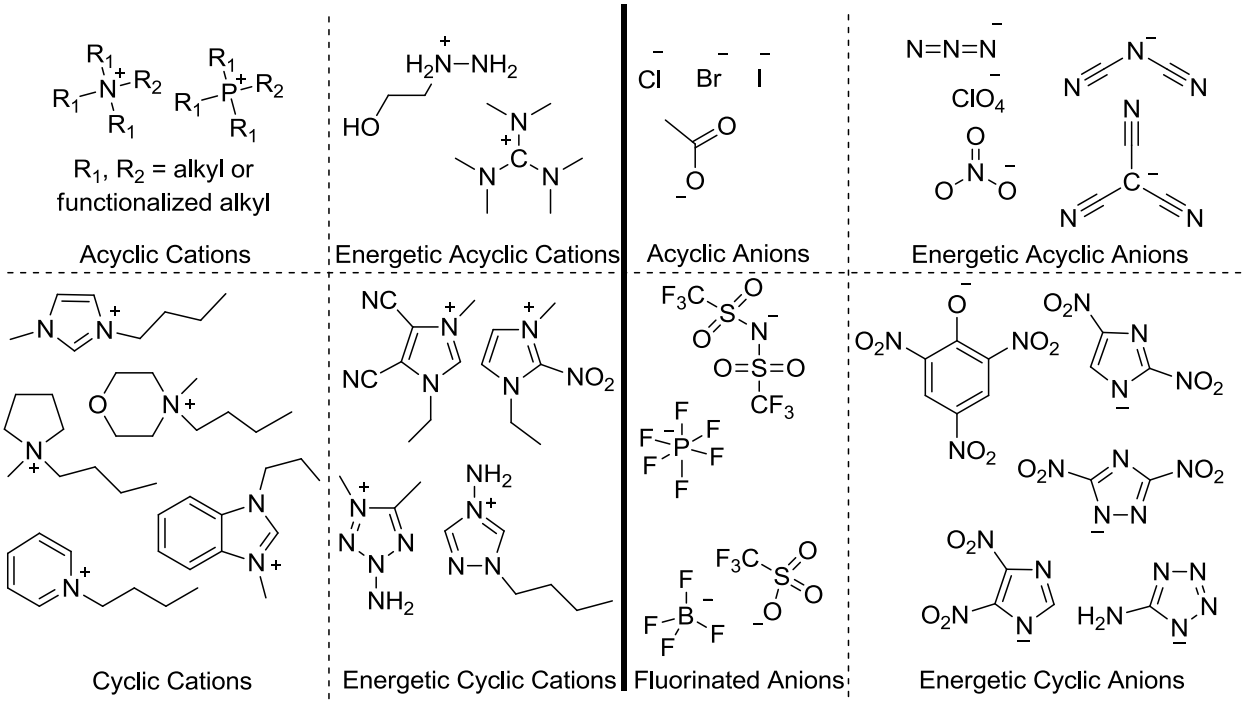

Figure 1.1. Examples of cations and anions used for the formation of ILs and energetic ILs.

As a result of their recognition as materials capable of a high level of compartmentalized design,[14,15] new forms of ILs have been highly sought after to (i) expand the number of known structures that exhibit IL-type behavior as well as (ii) gain a deeper understanding of ionic liquid chemistry at a fundamental level. In the former case, increasing IL structural diversity would enable identification of specific trends in IL behavior.[16-18] Considering the latter, developing an improved comprehension of the nature of ILs and identifying emergent applications are both highly sought after (e.g., What is it about ionic liquid structure that makes them liquids?).[19]

Multi-heterocyclic ionic liquids (or MHILs) are a relatively new class of ILs to recently receive acclaim and are the subject for this review. To begin, a brief definition and overview of MHILs are presented (Section 1.3), including a discussion of both symmetric (Section 1.3.1) and asymmetric (Section 1.3.3) bridged MHILs. Research highlights that target properties and identify potential applications are illustrated by example (Section 1.3.2). Although the majority of MHILs reported here are bi-heterocyclic in form, a short survey of tri- and poly-heterocyclic MHILs follows (Section 1.3.4). Efforts towards the systematic design of MHILs are then showcased to demonstrate how the dual-functional nature of ILs may be incorporated into new synthetic approaches (Section 1.4). To conclude, future directions for MHIL synthesis and applications are proposed based on the current state-of-the-art (Section 1.5).

1.3 Multi-Heterocyclic Ionic Liquids (MHILs)

As previously mentioned, there exists a persistent drive to identify new synthetic targets that exhibit IL-type properties. One such class is that of *multi-heterocyclic ionic liquids* (MHILs), here defined as salts with (a) melting points below < 100 ^{o}C and (b) cations and/or anions composed of more than one heterocyclic in a fused, spiro, bridged, or non-bridged

configuration (Figure 1.2). Synthetic diversity is achieved at numerous levels, including (i) type and number of heterocycles, (ii) composition of bridging unit (if present), (iii) sign and multiplicity of charge, (iv) symmetry, and (v) structure of counter ion.

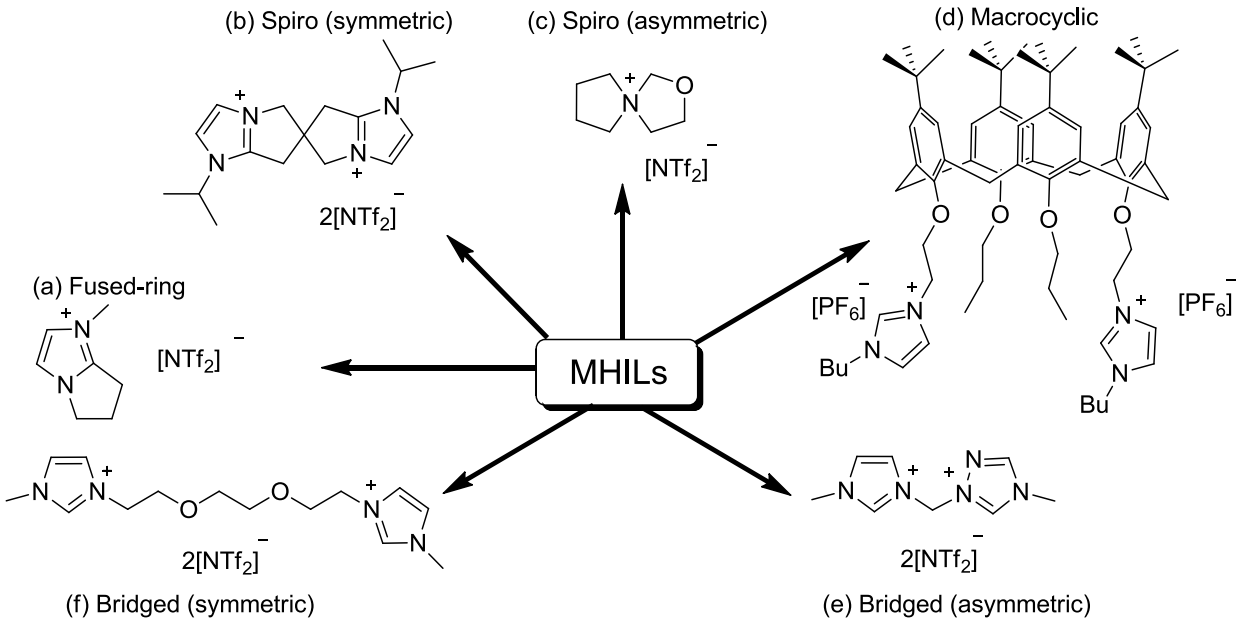

Figure 1.2. Examples of MHILs from the literature, including fused-rings,[20] (a), symmetric,[21] (b) and asymmetric,[22] (c), spiro heterocycles, macrocycles,[23] (d), and asymmetric,[24] (e), and symmetric,[25] (f), bridged multi-heterocycles.

Given the possible structural variations, MHILs suggest a high level of control in their design, where the presence of multiple heterocycles may enable regional differences in heterocyclic reactivity across the same ion, especially with increasing asymmetry. Although the fused-ring IL[26-29] (Figure 1.2a), spiro-IL[30,31] (Figure 1.2b-c), and macrocyclic (Figure 1.2d) classes are capable of forming MHILs, the bridged asymmetric (Figure 1.2e) and bridged symmetric (Figure 1.2f) MHILs have been selected as the focus for this review in part from our group's own interest in the exploration of these compounds.

1.3.1 Symmetric Bridged MHILs: Physicochemical Properties

Similar to trends in monocyclic IL synthesis, investigators have probed the effects of modifying the structure of bridged MHILs on observed physicochemical properties. For example, Armstrong and co-workers have reported numerous 'bolo' or geminal ILs, where *bis*(imidazolium), *bis*(pyrrolidinium), and *bis*(pyridinium) dications were reported featuring interchangeable bridge units (e.g., poly(ethylene glycol), or (PEG),[32] alkyl[33]), substituents on the heterocyclic cations (e.g., *N*-methyl, *N*-butyl, *N*-2-hydroxyethyl), and several different anions by exchange (e.g., Br^-, $[NTf_2]^-$, $[BF_4]^-$, $[PF_6]^-$) (Figure 1.3). Higher thermal stabilities were generally observed in comparison with analogous monocationic ILs ($\boldsymbol{T}_d$ = 330-400 ^oC *vs.* 145-185 ^oC, respectively). Melting points were found to decrease in a regular fashion by (i) increasing the length of the bridging unit,[34] (ii) selecting an appropriate anion ($\boldsymbol{T}_m$: $[NTf_2]^- < [BF_4]^- < [PF_6]^- < Br^-$), or (iii) selecting an appropriate heterocycle ($\boldsymbol{T}_m$: imidazolium < pyrrolidinium).

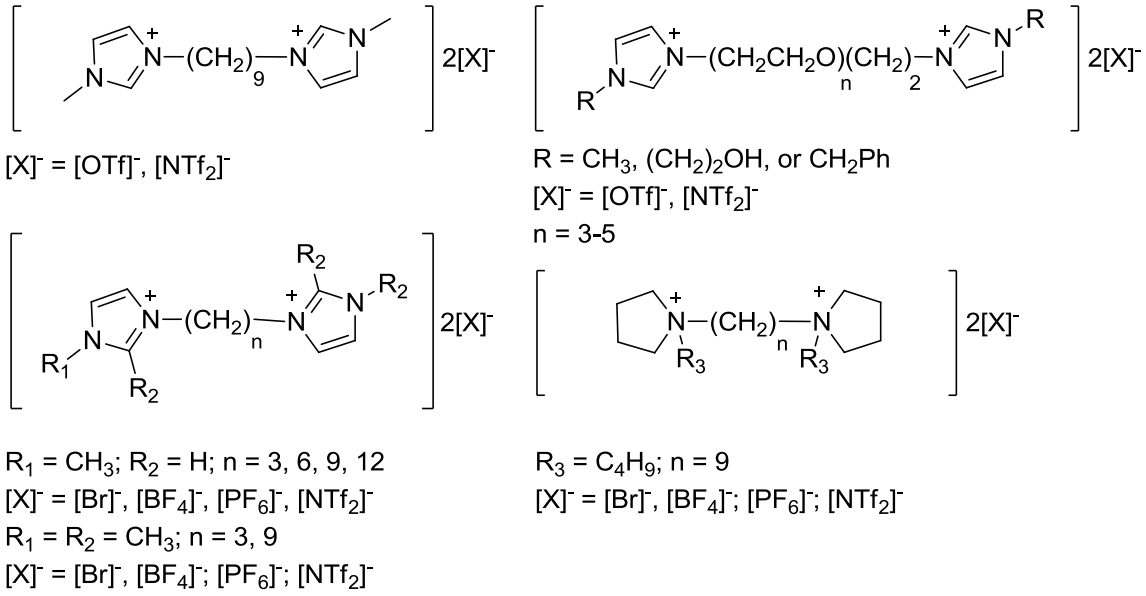

Figure 1.3. Symmetric alkyl-bridged MHILs based on *bis*(imidazolium)alkyl[33] or *bis*(imidazolium)poly(ethylene glycol)[32] dicationic structure.

Shreeve and co-workers have also extensively investigated the physicochemical properties of MHILs,[35] where *bis*(imidazolium) cations were modified with PEG (Figure 1.4a), fluoroalkyl (Figure 1.4b), or fluorinated benzene (Figure 1.4c) bridge units. Hydrocarbon and fluorinated substituents were compared when determining various properties, where it was found that the solubility of MHILs could be affected by altering the length and composition of *N*-alkyl substituents as well as bridge units. For example, the substitution of longer alkyl chains or fluorinated benzene bridges resulted in dicationic species that were miscible in toluene, whereas shorter or non-fluorinated *N*-alkyl and bridging substituents showed a more hydrophilic nature. In addition, increasing density was observed for shorter substituents and fluorine-containing bridges. Similarly, melting points determined for dicationic MHILs showed dependence on size and content of the bridge units and substituents as well as the type of anion (e.g., where $[NTf_2]^-$

showed low melting points as with mono-heterocyclic ILs, presumably due to the diffusion of negative charge across the anion[36]). Although it was observed that viscosity increased with the longer chains and higher fluorine content, this class of MHILs has been considered as safer alternatives to perfluropolyalkylethers (PFPAEs) used in industry as heat transfer fluids with negligible vapor pressure and high viscosity to prevent containment leakage.[37]

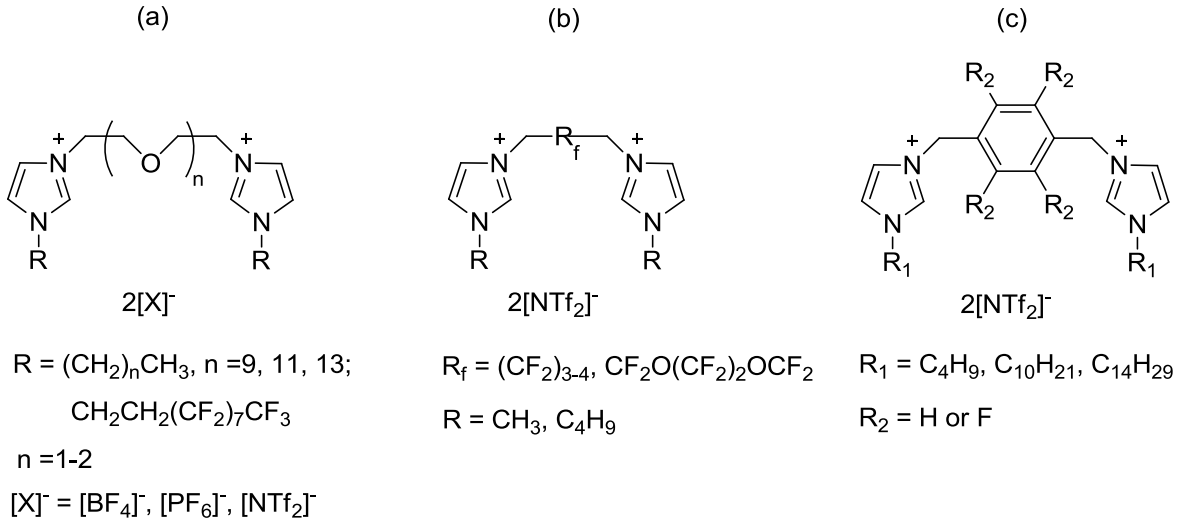

Figure 1.4. Dicationic *bis*(imidazolium) MHILs, including poly(ethylene glycol)-bridged, (a), fluoroalkyl-bridged, (b), and fluorinated benzene-bridged, (c), structures.[35]

From properties trends revealed as a result of systematic changes in symmetric dication structure, numerous applications were explored where specific ranges of performance are requisite. Here as with monocyclic ILs, the capacity to target properties by dual-functionalization enables an IL to meet needed performance criteria.

1.3.2 Symmetric Bridged MHILs: Applications

One of the very first symmetric, bridged MHILs was reported by our group (see Figure 1.2f), where greater partitioning capabilities for the Hg(II) cation from aqueous solutions were observed in comparison with analogous monocyclic ILs.[25] PEG linkers were found to protect the

C2 position through hydrogen bonds formed with ether oxygen atoms, and the capability for bridged *bis*(azolium) dications to bind to metals was later to become a major application for symmetric, bridged MHILs. For example, Shreeve and co-workers had utilized symmetric *bis*(imidazolium) and *bis*(1,2,4-triazolium) dications as bi-dentate "pincers" for the *in situ* formation of carbene complexes with Pd(II) as catalysts for Heck cross-coupling reactions of aryl halides with butyl acetate (Figure 1.5).[38]

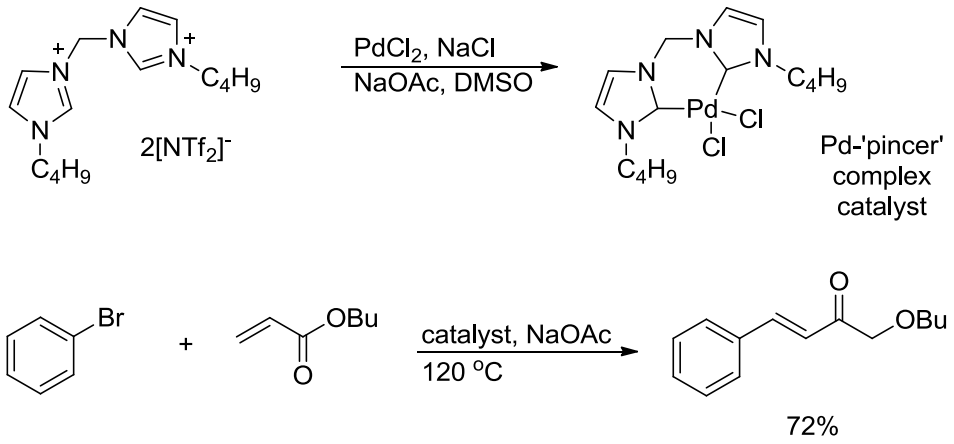

Figure 1.5. *In-situ* formation of Pd(II)-complexed Heck coupling catalyst with *bis*(imidazolium) MHIL for the coupling of aryl halides with butyl acetate.[38]

There have also been reports of symmetric MHILs utilized as reaction media[39] as well as organocatalysts. For example, the use of MHILs for chemical partitioning was reported by Sheldon and co-workers for the separation of phenol from water,[40] demonstrating how MHILs could effectively address a current industrial challenge. Recently, the partitioning ability of PEG-bridged dicationic acidic ionic liquids (DAILs) was reported in temperature-dependent, phase-separation systems with toluene.[41] For this work, the use of DAILs was demonstrated as an ideal reaction media for the efficient synthesis of benzopyrans (Figure 1.6).

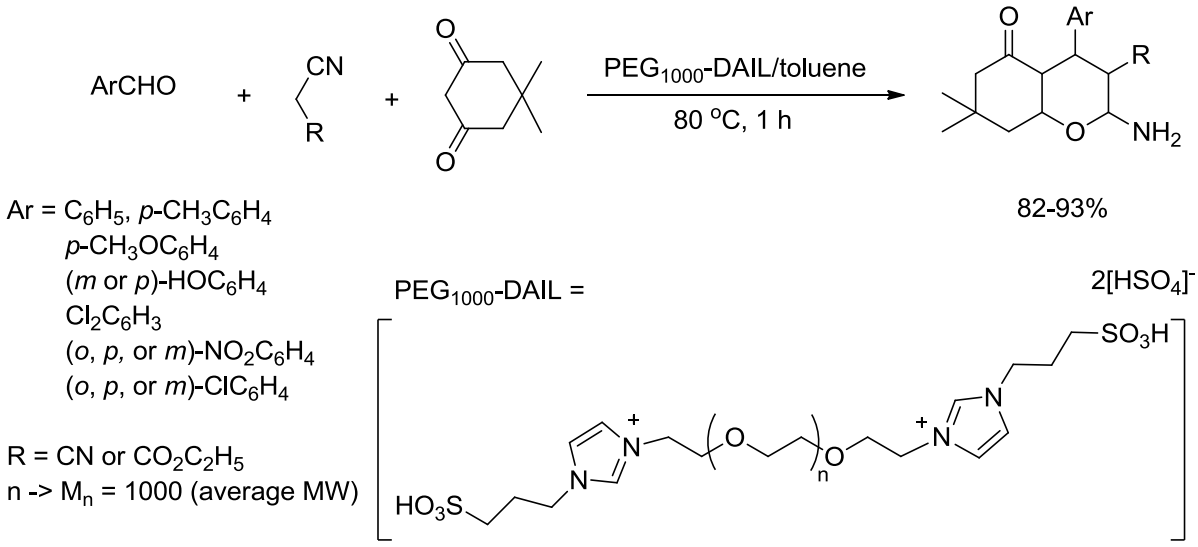

Figure 1.6. PEG-bridged DAIL used as phase-separated reaction medium for the synthesis of benzopyrans from a general class of aromatic aldehydes and nitriles.[41]

Symmetric bridged MHILs have found successful materials applications, including energetic materials,[42] electrical energy storage,[43,44] nanostructure functionalization,[45] and surfactants,[46] to name a few. For example, Savafi and co-workers showed that gold nanoparticles undergo long-term stabilization with dicationic *bis*(imidazolium)-type MHILs, where low polydispersity in particle size (diameter = 10.1 ± 4.2 nm) is observed.[47] It was concluded that the dications formed a charged bilayer, which enabled the nanoparticles to solvate in aqueous media. In other work, thixotropic gels (i.e., convertible to sols under mechanical stress) were prepared by Kim and co-workers from PEG-bridged MHILs.[48] These materials showed good photovoltaic performance and long-term stability, suggesting MHILs as satisfactory, leak-resistant alternatives for future dye-sensitized solar cell (DSSC) development.

1.3.3 Asymmetric Bridged MHILs

The main difference, and often a synthetic advantage, between symmetric and asymmetric bridged MHILs is the presence of regional reactivity on the same ion. This feature

can be exploited to affect changes in MHIL physical properties (melting point or thermal stability) or to enable preferential interaction of one terminus of the bridged structure for reaction media or catalysis applications. The properties and applications will be described in the following discussion.

As might be expected, introducing asymmetry into MHIL structures opens new design options for available properties and applications. Perhaps one of the most prominent applications discovered for asymmetric MHILs is in the field of asymmetric catalysis, where MHILs can serve as recyclable supports for asymmetric homogeneous catalysts in organic synthesis.[49] For example, Itoh and co-workers had synthesized different imidazolium salts functionalized with either D-proline or L-proline, which induced enantiomeric selectivity in the transesterification reaction of 1-phenylethanol *via* enzyme activation.[50] In another study, Agbossou-Niedercorn's group reported the synthesis of a new family of furanyl- and pyranyl-functionalized imidazolium triflate MHILs, used for the preparation of Pd(II) catalysts and found effective in Tsuji-Trost C-C bond-forming allylic alkylation reactions (Figure 1.7).[51] In addition to offering a halide-free synthetic route, these MHILs showed good recyclability in comparison with symmetric *bis*(imidazolium) salts. It was proposed that the presence of polar and non-polar regions in the same ion may also contribute to the high solubility of reagents, resulting in an observed increase in synthetic yields.

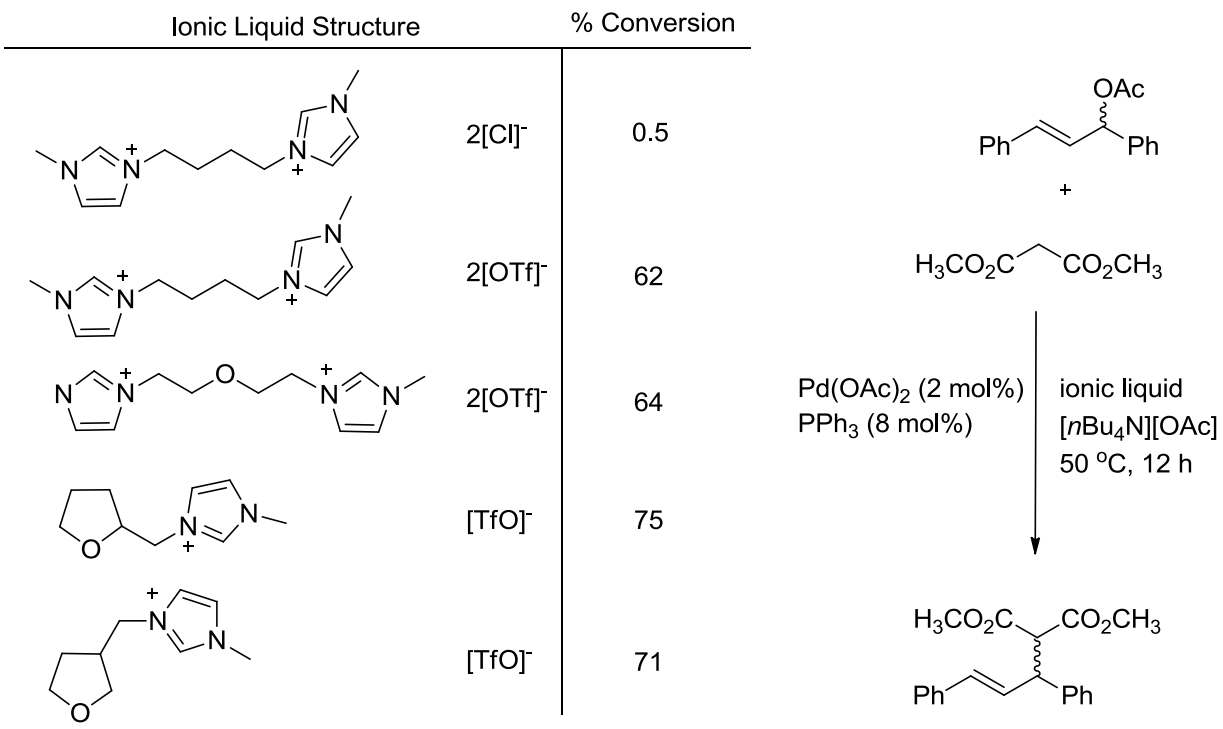

Figure 1.7. Use of asymmetric furanyl-functionalized imidazolium MHILs for Pd(II)-catalyzed allylic alkylation.[51]

Asymmetric MHILs have also found technological applications, where Inoue, *et al.* described the synthesis of amphiphilic, fluorescent carbazole-functionalized imidazolium salts, which were observed to form micelles at low concentrations with good photoconductivity.[52] Song and co-workers have reported MHILs as mono- and diradical species, where their good performance in charge-discharge tests pointed towards potential applications as cathode-active materials in lithium ion batteries.[53] Finally, for investigation as energetic ionic liquids (or EILs), Shreeve and co-workers had reported several methylene-bridged MHILs featuring both monocations and dications with variation in energretic heterocyclic cation and anion structures.[54,55] From these results, it was revealed that higher densities (a property sought after for some energetic materials applications[56]) could be achieved from methylene-bridged dications in comparison with their analogous monocationic EILs.

1.3.4 Other Bridged MHILs: Beyond a 2-Cycle System

When considering MHILs as a new structural class of ILs, it is important to develop an awareness of their synthetic limitations as well as what sort of modifications are capable of eliciting IL-type properties. There have been reports where the numbers of heterocycles have been increased beyond that of bridged bi-heterocycles, such as the tripodal trications synthesized independently by the research teams of Armstrong (symmetric)[57]and Pernak (asymmetric) (Figure 1.8).[58] Commonly observed features for the tripodal structures were very high viscosity and higher melting points compared with bi- and mono-heterocyclic analogues, where these properties were assumed to result from high electrostatic interactions between three cationic head groups and three equivalents of anion per MHIL unit.[57] However, when considering the high thermal stabilities of these salts, application as high temperature chromatographic phases or electrolytes for low-potential batteries were suggested; where high viscosity and liquid-state behavior under high temperature ranges of operation are both considered desirable properties.

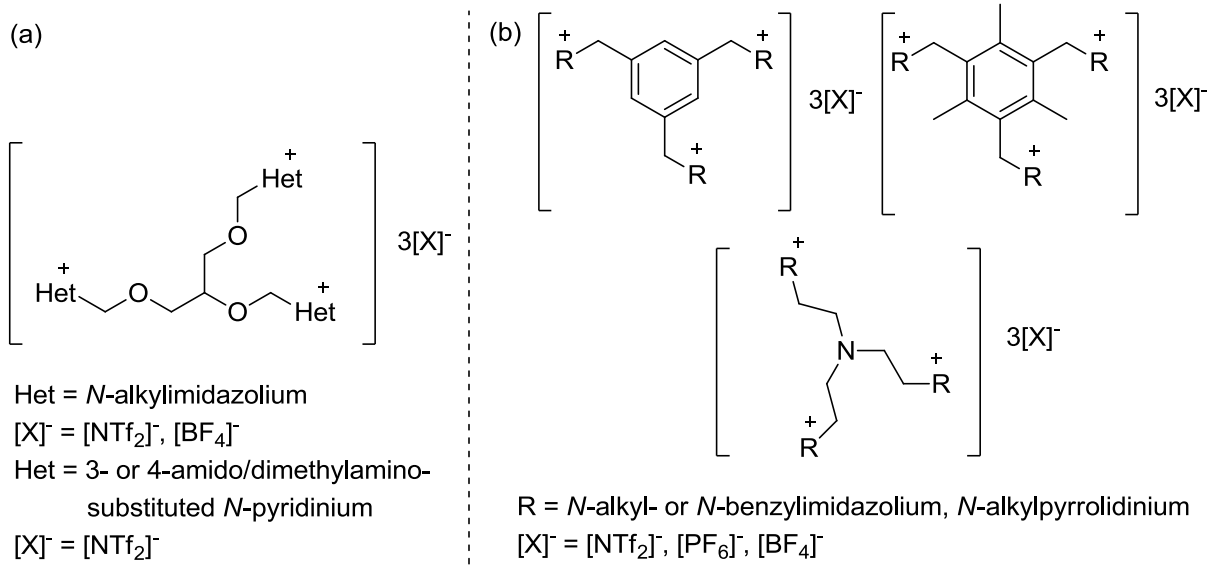

Figure 1.8. Examples of tripodal tricationic asymmetric, (a)[58], and symmetric, (b)[57], MHILs.

In work reported by Shreeve and co-workers, some *p-tert*-butylcalix[4]arene-based salts were found to exhibit IL-behavior when exchanged for appropriate anions (e.g., $[NTf_2]^-$) and featuring specific lower-rim functionalization (Figure 1.9).[59] Results indicated that all MHILs were very thermally stable (T_d > 290 °C), and these materials were successfully tested as media for the selective extraction of alkali metal cations (e.g., K^+ *vs.* Na^+, depending upon the structure of the MHIL cation). The results from this work will potentially find application in the synthesis of *N*-heterocyclic carbenes as well as metal extraction, benefiting from the properties available from calixarenes as well as azolium-based ILs.

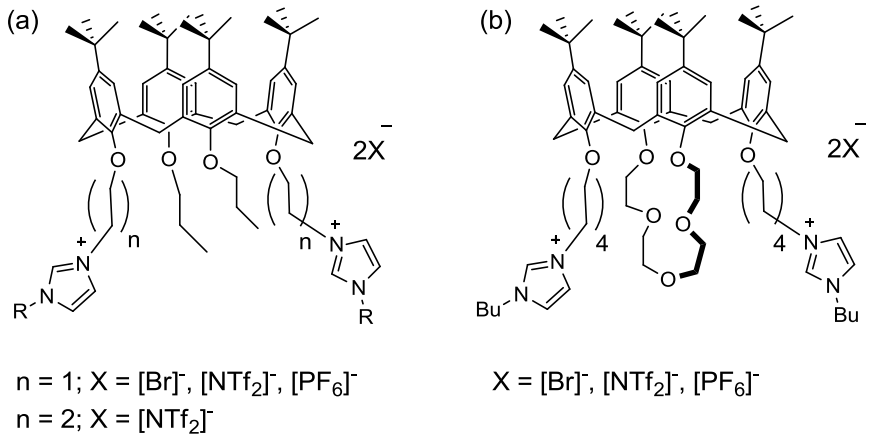

Figure 1.9. Examples of *p-tert*-butylcalix[4]arene-based MHILs featuring either propoxyl-, (a), or crown-5-, (b), functionalized lower-rim.[59]

As shown in the cases reported by Pernak and Armstrong (Figure 1.8, above), increasing the size of multi-heterocyclic cations can frequently restrict IL properties in a salt, where increased melting points and viscosities appear to increase with the size and number of positive charges residing on the cation structure. However, as the flexible, dual-functional nature of ILs permits the modification of either the cation or anion structure, further steps to modify the structure of IL ions can often achieve the desired property in MHILs (e.g., melting point < 100

^{o}C). Such tactics for targeting properties are often the hallmark of IL synthesis,[60] where efforts to develop new platforms for MHIL design is now addressed.

1.4 Strategies to Explore the MHIL Design Space

A more in-depth understanding of MHIL structures allows increasing control over the design options available through multi-heterocyclic systems (e.g., increased number of heterocycles, bridging *vs.* substituent contributions), while still retaining modularity found in more familiar monocyclic ion systems. Considering the potential richness of the design space available for MHILs, it is then perhaps a surprise that there have been only a few reports for the general and systematic synthesis of bridged MHILs. For example, our group has recently reported a new design platform for the synthesis of MHILs *via* a click chemistry approach to tetrazole-based MHILs and their precursors.[61] This approach allowed for the systematic preparation and interconversion of asymmetric bi-heterocyclic cations, anions, and zwitterions. To show how MHILs could be formed by IL-based synthetic strategies, a tri-heterocyclic zwitterion was obtained by a 'double-click' reaction using 1,3-dicyanoalkyl-substituted imidazolium halide (Figure 1.10a) with 2 equivalents of azide anion (Figure 1.10b) which then could be selectively converted to either the cationic (Figure 1.10c) or anionic (Figure 1.10d) forms of MHILs. This demonstration showed a general synthetic approach to multi-heterocycles by known click protocols, where products may be selectively converted to novel MHILs.

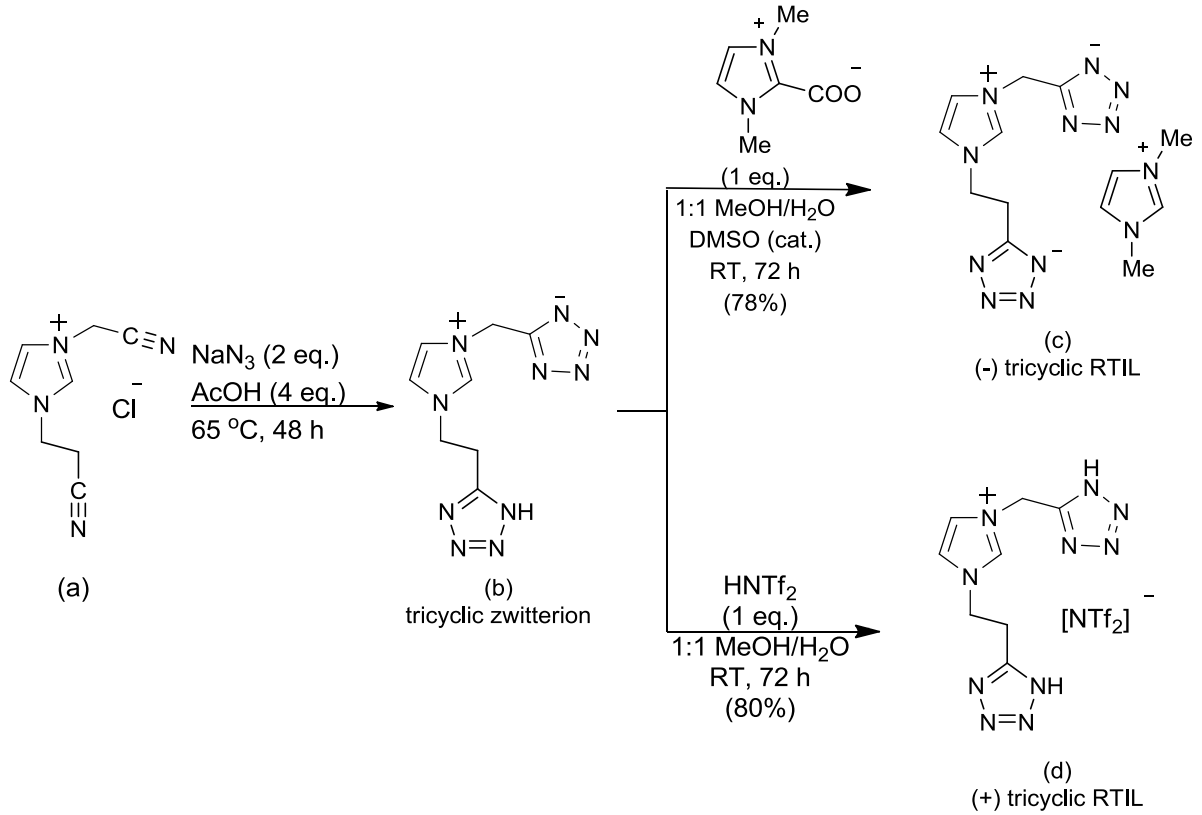

Figure 1.10. A design platform for MHILs as demonstrated by the synthesis of a tri-heterocyclic zwitterion, (b), from the click reaction of 1,3-dicyanoalkyl-functionalized imidazolium chloride with sodium azide, (a), and its selective conversion to either anionic, (c), or cationic, (d), component in room-temperature MHILs.[61]

Recently, we have continued to develop this platform, where we have found that both the bridging and substituent alkyl chain lengths may be modified without loss in click reactivity.[62] Furthermore, a new method for the synthesis of azolium azolate MHILs from the reaction of prepared azolium (1-butyl-3-methylimidazolium, 4-amino-1-butyl-1,2,4-triazolium) azides with neutral nitrile-functionalized azoles (1-(2-cyanoethyl)imidazole and 1,2,4-trizole) has been investigated, where the modular functionalization of the cation and anion structures is shown to provide flexible access to MHILs *via* a metal- and solvent-free protocol.[63]

Others have researched the synthesis of bridged di-[64] or trications[65] with mixtures of anions to gain access to targeted properties by way of formulations rather than pure compounds. For example, Chan and co-workers showed how ionic oligomers could be constructed in a step-wise fashion, where different compositions of anions could be introduced sequentially with oligomer chain lengthening (Figure 1.11).[65]

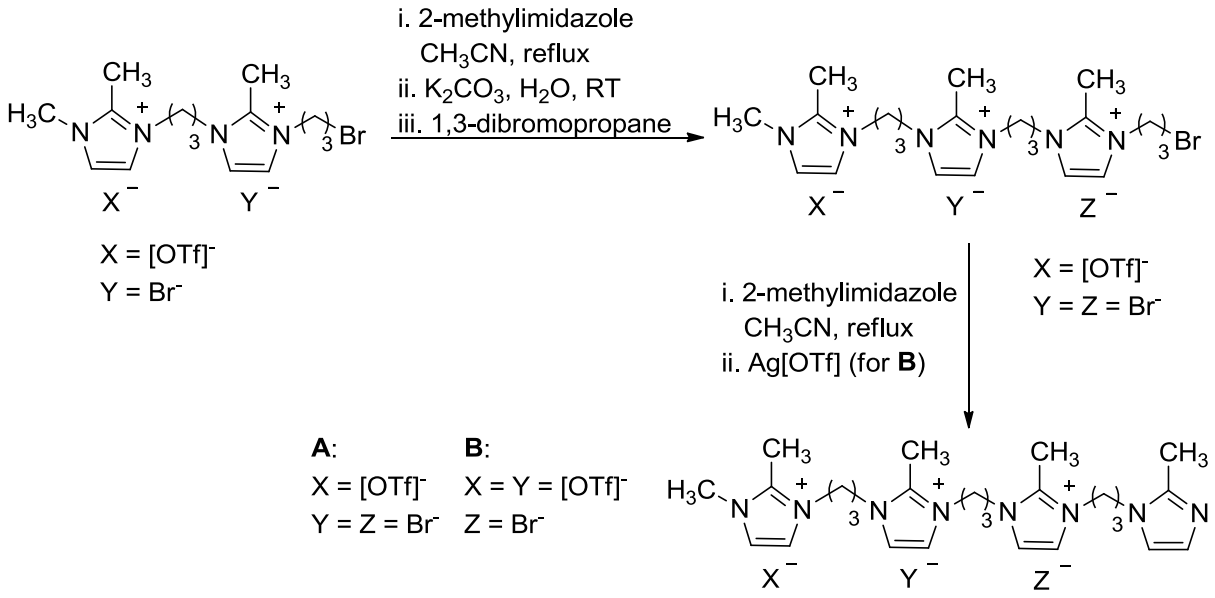

Figure 1.11. Step-wise synthesis of oligomeric MHILs, with selective formulation of anion composition introduced in each step.[65]

In a similar approach, Sun and co-workers have recently reported the synthesis of dicationic MHIL systems featuring mixtures of both hydrophobic and hydrophilic anions with a common dication (Table 1.1).[64] The results indicated that heteroanionic MHILs showed changes in melting point (e.g., higher proportion of asymmetric $[NTf_2]^-$ *vs.* $[PF_6]^-$ anion for greater melting point reduction) and solubility (e.g., water and alcohol miscibility when in the presence of bromide, but not for homoanionic $[PF_6]^-$ and $[NTf_2]^-$ salts) that were dependent on the composition of anions. Interestingly, only a negligible change in thermal stability was observed

between $[PF_6]^-$ *vs.* $[NTf_2]^-$ heteroanions and when comparing between imidazolium-, pyrrolidinium-, and piperidinium-substituted dications.

Table 1.1. Comparison of melting point (Mp) and decomposition temperatures (T_d) for salts and MHILs with changing heteroanion composition and dication structure.[64]

Cation	Anions	Mp (°C)	T_d (°C)
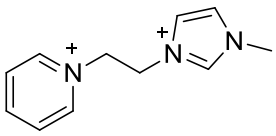	PF_6^-/Br^-	150-151	252
	$[NTf]_2^-/Br^-$	34-35	246
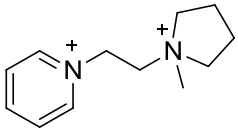	PF_6^-/Br^-	169-170	252
	$[NTf_2]^-/Br^-$	92-93	249
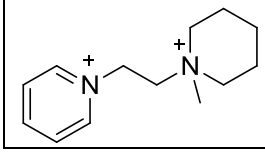	PF_6^-/Br^-	186-187	250
	$[NTf_2]^-/Br^-$	107-108	239

1.5 Conclusions and Perspectives

The rapid growth of IL synthetic methods and the deeper understanding of IL properties and their applications which resulted have encouraged a search for new, IL-forming structures. As a relatively new class, MHILs enable access to structures and, as a result, properties which extend beyond what have previously been achieved with mono-heterocyclic ILs. Bridged MHILs offer several different variables which the chemist may access and manipulate selectively in a unique and flexible design space, where elements of symmetry, heterocycle structure and substituents, bridge length and composition, as well as types of anions may all be interchanged through conventional methods or protocols developed using IL-based synthetic strategies.

From recent reports in the literature demonstrating the diversity possible in MHIL design, structural trends indicate how properties can be targeted for high performance applications (e.g., reaction catalysis, energetic materials synthesis, chemical separations). Yet there still exists an

ongoing need for new and improved methods to systematically prepare MHILs that effectively address the chemical challenges of today. Initial efforts to develop such strategies towards the design of MHIL are promising, but there are still many other possible opportunities to accelerate the growth and innovation of this emerging class of ionic liquids.

Acknowledgements

This research was supported by the Air Force Office of Scientific Research (Grant FA9550-10-1-0521).

References

1 Wasserscheid, P.; Keim, W. *Angew. Chem., Int. Ed.* **2000**, *39*, 3772.

2 Holbrey, J. D.; Reichert, W. M.; Nieuwenhuyzen, M.; Johnston, S.; Seddon, K. R.; Rogers, R. D. *Chem. Commun.* **2003**, 1636.

3 Cooper, E. I.; O'Sullivan, E. J. M. In *Molten Salts*; Gale, R. J., Blomgren, G., Kojima, H., Eds.; The Electrochemical Society Proceedings Series; ECS: Pennington, NJ, 1992; vol. 92–16, p. 386.

4 Wilkes, J. S.; Zaworotko, M. J. *J. Chem. Soc., Chem. Commun.* **1992**, 965.

5 Fuller, J.; Carlin, R. T.; De Long, H. C.; Haworth, D. *J. Chem. Soc., Chem. Commun.* **1994**, 299.

6 Suarez, P. A. Z.; Dullius, J. E. L.; Einloft, S.; de Souza, R. F.; Dupont, J. *Polyhedron* **1996**, *15*, 1217.

7 Larsen, A. S.; Holbrey, J. D.; Tham, F. S.; Reed, C. A. *J. Am. Chem. Soc*. **2000**, *122*, 7264.

8 Smiglak, M.; Metlen, A.; Rogers, R. D. *Acc. Chem. Res.* **2007**, *40*, 1182.

9 Zorn, D. D.; Boatz, J. A.; Gordon, M. S. *J. Phys. Chem. B* **2006**, *110*, 11110.

10 Joo, Y. –H.; Gao, H.; Zhang, Y.; Shreeve, J. M. *Inorg. Chem.* **2010**, *49*, 3282.

11 Schneider, S.; Hawkins, T.; Rosander, M.; Vaghjiani, G.; Chambreau, S.; Drake, G. *Energy Fuels* **2008**, *22*, 2871.

12 Shamshina, J. L.; Smiglak, M.; Drab, D. M.; Parker, T. G.; Dykes, Jr., H. W. H.; Di Salvo, R.; Reich, A. J.; Rogers, R. D. *Chem. Commun.* **2010**, *46*, 8965.

13 Singh, R. P.; Verma, R. D.; Meshri, D. T.; Shreeve, J. M. *Angew. Chem., Int. Ed.* **2006**, *45*, 3584.

14 Zhou, F.; Liang, Y.; Liu, W. *Chem. Soc. Rev.* **2009**, *38*, 2590.

15 Ueno, K.; Tokuda, H.; Watanabe, M. *Phys. Chem. Chem. Phys.* **2010**, *12*, 1649.

16 Martin, J. D. In *Ionic Liquids: Industrial Applications for Green Chemistry*; Rogers, R. D., Seddion, K. R., Eds.; ACS Symposium Series, ACS: Washington, DC, 2002; vol. 818, pp. 413-427.

17 Chiappe, C.; Pieraccini, D. *J. Phys. Org. Chem.* **2005**, *18*, 275.

18 Rooney, D.; Jacquemin, J.; Gardas, R. *Top. Curr. Chem.* **2009**, *290*, 185.

19 Ignat'ev, Nikolai V.; Kucheryna, A.; Bissky, G.; Willner, H. In *Ionic Liquids IV: Not Just Solvents Anymore*; Brennecke, J. F., Rogers, R. D., Seddon, K. R., Eds.; ACS Symposium Series, ACS: Washington, DC, 2007; vol. 975, pp. 320-334.

20 Kan, H. -C.; Tseng, M. -C.; Chu, Y. -H. *Tetrahedron* **2007**, *63*, 1644.

21 Patil, M. L.; Rao, L.; Yonezawa, K.; Takizawa, S.; Onitsuka, K.; Sasai, H. *Org. Lett.* **2006**, *8*, 227.

22 Devarajan, T.; Higashiya, S.; Dangler, C.; Rane-Fondacaro, M.; Snyder, J.; Haldar, P. *Electrochem. Commun.* **2009**, *11*, 680.

23 Jin, C. -M.; Shreeve, J. M. *Inorg. Chem.* **2004**, *43*, 7532.

24 Wang, R.; Gao, H.; Ye, C.; Shreeve, J. M. *Chem. Mater.* **2007**, *19*, 144.

25 Holbrey, J. D.; Visser, A. E.; Spear, S. K.; Reichert, W. M.; Swatloski, R. P.; Broker, G. A.; Rogers, R. D. *Green Chem.* **2003**, *5*, 129.

26 Ishida, Y.; Miyauchi, H.; Saigo, K. *Chem. Commun.* **2002**, 2240.

27 Ishida, Y.; Sasaki, D.; Miyauchi, H.; Saigo, K. *Tetrahedron Lett.* **2004**, *45*, 9455.

28 Kan, H. –C.; Tseng, M. –C.; Chu, Y. –H. *Tetrahedron* **2007**, *63*, 10949.

29 Chiappe, C.; Melai, B.; Sanzone, A.; Valentini, G. *Pure Appl. Chem.* **2009**, *81*, 2035.

30 Patil, M. L.; Rao, C. V. L.; Takizawa, S.; Onitsuka, K.; Sasai, H. *Tetrahedron* **2007**, *63*, 12702.

31 Higashiya, S.; Devarajan, T. S.; Rane-Fondacaro, M. V.; Dangler, C.; Snyder, J.; Haldar. P. *Helv. Chim. Acta* **2009**, *92*, 1600.

32 Huang, K.; Han, X.; Zhang, X.; Armstrong, D. W. *Anal. Bioanal. Chem.* **2007**, *389*, 2265.

33 Anderson, J. L.; Ding, R.; Ellern, A.; Armstrong, D. W. *J. Am. Chem. Soc.* **2005**, *127*, 593.

34 Payagala, T.; Huang, J.; Breitbach, Z. S.; Sharma, P. S.; Armstrong, D. W. *Chem. Mater.* ***2007****, 19, 5848.*

35 Zeng, Z.; Phillips, B. S.; Xiao, J. –C.; Shreeve, J. M. *Chem. Mater.* **2008**, *20*, 2719.

36 Endres, F.; Abedinw, S. Z. *Phys. Chem. Chem. Phys.* **2006**, *8*, 2101.

37 Li, X.; Bruce, D. W.; Shreeve, J. M. *J. Mater. Chem.* **2009**, *19*, 8232.

38 Jin, C. -M.; Twamley, B.; Shreeve, J. M. *Organometallics* **2005**, *24*, 129.

39 Sheldrake, G. N.; Schleck, D. *Green Chem.* **2007**, *9*, 1044.

40 Liu, Q.; van Rantwijk, F.; Sheldon, R. A. *J. Chem. Technol. Biotechnol.* **2006**, *81*, 401.

41 Zhi, H.; Lü, C.; Zhang, Q.; Luo, J. *Chem. Commun.* **2009**, 2878.

42 Jin, C. –M.; Ye, C.; Piekarski, C.; Twamley, B.; Shreeve, J. M. *Eur. J. Inorg. Chem.* **2005**, 3760.

43 Lall, S. I.; Mancheno, D.; Castro, S.; Behaj, V.; Cohen, J. I.; Engel, R. *Chem. Commun.* **2000**, 2413.

44 Pitawala, J.; Matic, A.; Martinelli, A.; Jacobsson, P.; Koch, V.; Croce, F. *J. Phys. Chem. B* **2009**, *113*, 10607.

45 Liu, Y.; Yu. L.; Zhang, S.; Yuan, J.; Shi, L.; Zheng, L. *Colloids Surf., A* **2010**, *359*, 66.

46 Baltazar, Q. Q.; Chandawalla, J.; Sawyer, K.; Anderson, J. L. *Colloids and Surf., A* **2007**, *302*, 150.

47 Safavi, A.; Zeinali, S. *Colloids Surf., A* **2010**, *362*, 121.

48 Kim, J. Y.; Kim, T. H.; Kim, D. Y.; Park, N. –G.; Ahn, K. –D. *J. Power Sources* **2008**, *175*, 692.

49 Ni, B.; Headley, A. D. *Chem. – Eur. J.* **2010**, *16*, 4426.

50 Abe, Y.; Kirakawa, T.; Nakajima, S.; Okano, N.; Hayase, S.; Kawatsura, M.; Hirose, Y.; Itoh, T. *Adv. Synth. Catal.* **2008**, *350*, 1954.

51 Leclercq, L.; Suisse, I.; Nowogrocki, G.; Agbossou-Niedercorn, F. *Green Chem.* **2007**, *9*, 1097.

52 Dong, B.; Gao, Y.; Su, Y.; Zheng, L.; Xu, J.; Inoue, T. *J. Phys. Chem. B* **2010**, *114*, 340.

53 Lee, S. H.; Kim, J. –K.; Cheruvally, G.; Choi, J. –W.; Ahn, J. –H.; Chauhan, G. S. *J. Power Sources* **2008**, *184*, 503.

54 Gao, Y.; Ye, C.; Twamley, B.; Shreeve, J. M. *Chem. – Eur. J.* **2006**, *12*, 9010.

55 Wang, R.; Gao, H.; Ye, C.; Shreeve, J. M. *Chem. Mater.* **2007**, *19*, 144.

56 Tishkoff, J. M.; Berman, M. R., *40th AIAA Aerospace Sciences Meeting & Exhibit*, January 14-17, **2002**, Reno, NV.

57 Sharma, P. S.; Payagala, T.; Wanigasekara, E.; Wijeratne, A. B.; Huang, J.; Armstrong, D. W. *Chem. Mater.* **2008**, *20*, 4182.

58 Pernak, J.; Skrzypczak, A.; Lota, G.; Frackowiak, E. *Chem. – Eur. J.* **2007**, *13*, 3106.

59 Jin, C. –M.; Shreeve, J. M. *Inorg. Chem.* **2004**, *43*, 7532.

60 Rooney, D.; Jacquemin, J.; Gardas, R. *Top. Curr. Chem.* **2009**, *290*, 185.

61 Drab, D. M.; Shamshina, J. L.; Smiglak, M.; Hines, C. C.; Cordes, D. B.; Rogers, R. D. *Chem. Commun.* **2010**, *46*, 3544.

62 Drab, D. M.; Smiglak, M.; Shamshina, J. L.; Kelley, S. P.; Rogers, R. D. **2011**, *in preparation*.

63 Drab, D. M.; Rogers, R. D. **2011**, *in preparation*.

64 Chang, J. –C.; Ho, W. –Y.; Sun, I. –W.; Tung, Y. –L.; Tsui, M. –C.; Wu, T. –Y.; Liang, S. –S. *Tetrahedron* **2010**, *66*, 6150.

CHAPTER 2

SYNTHESIS OF *N*-CYANOALKYL-FUNCTIONALIZED IMIDAZOLIUM NITRATE AND DICYANAMIDE IONIC LIQUIDS WITH A COMPARISON OF THEIR THERMAL PROPERTIES FOR ENERGETIC APPLICATIONS

Taken in part from a published manuscript: Drab, D. M; Smiglak, M.; Shamshina, J. L.; Kelley, S. P.; Schneider, S.; Hawkins, T. W.; Rogers, R. D. *New J. Chemistry* **2010**, submitted.

Acknowledgements: S. Schneider and T. W. Hawkins (Air Force Research Laboratory, Edwards Air Force Base, CA) collected sensitivity testing data for all dicyanamide salts. S. P. Kelley assisted with the final refinement and presentation for all crystal structures.

Abstract

The synthesis of 10 *N*-alkyl-*N*-cyanoalkyl-functionalized imidazolium (*N*-methyl- and *N*-butyl-*N*-((CH_2)$_n$CN)imidazolium; n=1-4) nitrate and 11 *N*-alkyl-*N*-cyanoalkyl-functionalized imidazolium (*N*-methyl-*N*-((CH_2)$_n$CN)imidazolium; n=1-6, *N*-(2-cyanoethyl)-*N*-((CH_2)$_n$CN)-imidazolium; n=1,3-6) dicyanamide salts was achieved *via* *N*-alkylation of substituted imidazoles with commercially available haloalkylnitriles followed by anion exchange. Based on their observed melting points, all dicyanamide salts and all but one nitrate salt (1-cyanomethyl-3-methylimidazolium nitrate) had melting points < 100 ^{o}C, as did 13 of the 17 halide precursors also reported here. Differential scanning calorimetry data indicated that melting points decreased by increasing the *N*-alkyl or *N*-cyanoalkyl chain length or by exchanging with the dicyanamide anion, which produced the lowest melting points in comparison to analogous halide

or nitrate salts. Thermogravimetric analyses indicated that thermal stability increased for longer *N*-cyanoalkyl substituent lengths and decreased significantly for nitrates and more so for dicyanamides bearing short-chain *N*-cyanoalkyl substituents (e.g., *N*-cyanomethyl, *N*-(1-cyanoethyl), and *N*-(2-cyanoethyl)) in comparison to halide precursors. Furthermore, for many of the *N*-cyanoalkyl-substituted salts (especially the dicyanamides), there was a significant production of thermally-stable char – presumably due to by-products formed from the reaction of either *N*-cyanoalkyl substituents, dicyanamide anion, or both, which resulted in thermally-stable polymers or cycles.

Introduction

There exists a high demand for the development of new and improved energetic materials (EMs) for application as propellants, fuels, and explosives, as traditional EMs face problems related to environmental and safety concerns during stages of synthesis, transport, and storage.[1] The Air Force, in particular, is interested in potential replacements of traditional energetic materials, and has recognized that ionic liquids (ILs, salts which have melting points < 100 ^{o}C[2]) are valuable materials in energetic applications.[3,4] ILs often possess broad liquid ranges, negligible vapor pressures, high heats of formation, are thermally stable, and have significantly reduced sensitivity and toxicity characteristics. Additionally, their physical and chemical properties can be carefully tuned *via* the choice of the component ions to target specific performance properties.

As a result of the initial interest of the Air Force in energetic ionic liquids (EILs), intense research efforts have been made in this direction.[5-6] Promising results have appeared in the preparation of EILs with specific properties of interest to the Air Force – for example, high density,[7-8] high heats of formation,[9-10] optimal oxygen balance,[11-12] and hypergolicity.[13-14]

However, there are not many strategies available to access these properties in a predictable manner.

Work in our group has been focused not on the synthesis of EMs *per se* but, rather, on the understanding of IL chemistry at a deeper level. It has long been an interest to identify IL structural patterns with the goal of accessing targeted properties in a systematic and predictable fashion. Previously, we have synthesized azole-based ILs with energetic substituents (e.g., nitro, amino, cyano groups) to identify the effect of azole type and ring substituents on thermal properties of ILs.[15-16] In another study, we established a strategy to incorporate energetic functional groups into either cation or anion, with the consequence that electron-withdrawing nitro- and cyano- groups were observed to deactivate azoles toward formation of cations. [17-19]

Continuing the above efforts, in this paper we report systematic studies of thermal properties for two series of *N*-cyanoalkyl-functionalized imidazolium salts. Although there have been reported examples of *N*-cyanoalkyl-functionalized imidazolium halides,[19,20] nitrates,[21] and dicyanamides,[18,20,22] to the best of our knowledge these classes have not been examined systematically or comparatively with respect to homologous changes in structure.

Three types of systematic modifications to *N*-cyanoalkyl-functionalized imidazoliums have been made here. First, we believed that the length and branching of the alkyl chains in the *N*-cyanoalkyl-functionalized imidazolium cation would influence the liquid state, as others have reported melting point reduction as alkyl length increases.[23] We also hypothesized that the melting points of *N*-cyanoalkyl-functionalized imidazolium salts would be higher when compared with 1,3-dialkylimidazolium analogs, due to possible intra- and intermolecular organization from the π-electron system and lone-pair electrons available in the cyano group.[16]

Secondly, for the same reason, we varied the *N*-alkyl substituent on the imidazole ring to probe for trends similar to those reported in the literature, where melting points typically decrease and thermal stabilities remain largely unaffected from *N*-methyl to *N*-butyl substitution.[23,24] Lastly, we investigated the effect of different energetic anions: nitrate and dicyanamide. Nitrate was chosen because of the oxidizing nature of the $[NO_3]^-$ anion, which facilitates thermal decomposition of the salt.[25] In turn, dicyanamide anions were expected to decrease melting points and increase thermal stability when compared to halide analogs.[26] In addition, the nitrate and dicyanamide anions were selected for their reputed IL-forming abilities and physicochemical properties suitable for EILs. These nitrile-functionalized salts are also excellent precursors to novel mixed heterocyclic species, as we have recently illustrated.[27]

Synthesis

The starting halide salts were obtained by alkylating commercially available methyl-, butyl-, or 2-cyanoethyl-substituted imidazole (Scheme 2.1: **1**, **2**, **3**, respectively)[28] with haloalkylnitriles *via* a classical quaternization reaction. Given the wide variety of commercially available haloalkylnitriles, this was considered a logical starting point for the synthesis of imidazolium salts with variable *N*-cyanoalkyl side-chain lengths as described here.[29] The *N*-cyanoalkyl-functionalized imidazolium nitrate (**4-7**, **10-15[NO_3]**), and dicyanamide (**4-9**, **16-20[$N(CN)_2$]**) salts were prepared by metathesis of the analogous halides *(***4-20[X]**), either by using an ion exchange resin (nitrate salts) or a silver salt (dicyanamide salts).

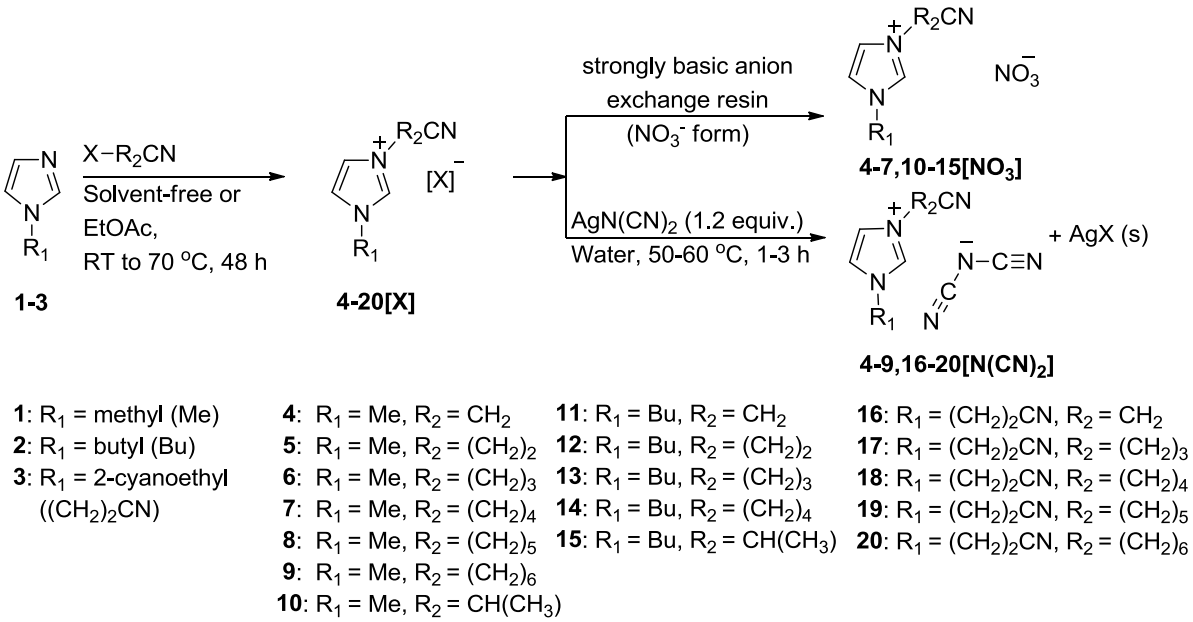

1: R_1 = methyl (Me)
2: R_1 = butyl (Bu)
3: R_1 = 2-cyanoethyl ($(CH_2)_2CN$)

4: R_1 = Me, R_2 = CH_2
5: R_1 = Me, R_2 = $(CH_2)_2$
6: R_1 = Me, R_2 = $(CH_2)_3$
7: R_1 = Me, R_2 = $(CH_2)_4$
8: R_1 = Me, R_2 = $(CH_2)_5$
9: R_1 = Me, R_2 = $(CH_2)_6$
10: R_1 = Me, R_2 = $CH(CH_3)$

11: R_1 = Bu, R_2 = CH_2
12: R_1 = Bu, R_2 = $(CH_2)_2$
13: R_1 = Bu, R_2 = $(CH_2)_3$
14: R_1 = Bu, R_2 = $(CH_2)_4$
15: R_1 = Bu, R_2 = $CH(CH_3)$

16: R_1 = $(CH_2)_2CN$, R_2 = CH_2
17: R_1 = $(CH_2)_2CN$, R_2 = $(CH_2)_3$
18: R_1 = $(CH_2)_2CN$, R_2 = $(CH_2)_4$
19: R_1 = $(CH_2)_2CN$, R_2 = $(CH_2)_5$
20: R_1 = $(CH_2)_2CN$, R_2 = $(CH_2)_6$

Scheme 2.1. Synthesized *N*-cyanoalkyl-functionalized imidazolium halide (**4-20[X]**), nitrate (**4-7, 10-15[NO_3]**), and dicyanamide (**4-9, 16-20[$N(CN)_2$]**) salts.

The 17 *N*-cyanoalkyl-functionalized imidazolium halide salts (**4-20[X]**) were synthesized according to literature protocols,[30,31] where 1-alkylimidazole starting materials (**1-3**) were alkylated with haloalkylnitriles generally under solvent-free conditions at 70 °C for 48 h in a sealed, high-pressure vial (except as noted below). Since the main focus of the work was to investigate how the properties of the nitrate and dicyanamide salts are affected by changing the *N*-cyanoalkyl substituent, the uniformity of the halide anion in the synthesis of **4-20[X]** was not considered essential and was established by the availability of commercial haloalkylnitriles.

Minor changes were implemented in the published reactions. The synthesis of **4[Cl]**, **11[Cl]**, and **16[Cl]** were conducted at room temperature to avoid the thermal degradation of the substrates. In addition, **8[Br]**, **9[Br]**, and **17-20[X]** were all prepared using ethyl acetate as solvent to allow for easy product phase separation from the solvent layer. Upon washing **4-20[X]** with ethyl acetate or acetone, and subsequent removal of residual solvent under high vacuum overnight, the halide salts were obtained in fair to excellent yields (82-97%) with the

exception of **11[Cl]** (yield = 57%) and **14[Cl]** (yield = 45%, as a result of inadvertent loss of sample when removing residual starting materials).

Many of the intermediate halide salts have been synthesized previously including, **4[Cl]**,[19,31] **5[Br]**,[32] **6[Cl]**,[19] **7[Cl]**,[19] **12[Br]**,[33] and **16[Cl]**.[27] Since these compounds were typically only used as intermediates in further IL synthesis, important data such as melting points, glass transition temperatures, thermal stability, and synthetic yields were frequently not reported. Here, we report the thermal properties and yields for these intermediates and, where possible, compare them with the literature. To the best of our knowledge, the nitrate (**4-7**, **10-15[NO_3]**) and dicyanamide (**4**, **5**, **7-9, 16-20[$N(CN)_2$]**) salts were not previously reported, with the exception of **6[$N(CN)_2$]**.[20]

Nitrate salts **4-7**, **10-15[NO_3]** were prepared from the halide precursors using the strongly basic anion exchange resin BioRad AG 1-X8 (100-200 mesh with 8% divinylbenzene copolymer cross-linkage). The resin has an exchange capacity of 2.6 meq/g dry resin and an appropriate amount of resin was prepared to exchange 3.2 to 6.4 mmol of halide precursor. The commercially available chloride resin was converted to (NO_3^-)-form following the manufacturer's protocol,[34,35] where the resin was loaded into a column (1 cm diameter x 10 cm tall) and washed with 5 bed volumes of 0.5 N sodium nitrate solution. To check for the completeness of nitrate anion exchange, the presence of halide in the eluted solution was spot checked frequently with a 1.0 M silver nitrate solution. When no halide was indicated as evident by the lack of white, cloudy precipitate, final conditioning of the nitrate-exchanged resin column was completed by washing with 2 bed volumes of deionized water.

With the (NO_3^-)-form of the resin in hand, halide samples were dissolved in 100 mL of deionized water and eluted through the column followed by an additional 2 bed volumes of

deionized water in the final rinse. For both nitrate loading and sample elution, the linear flow rate was maintained at approximately 2 cm/min through the bed volume. Each of the eluted fractions was qualitatively screened for the presence of halide by spot-testing each eluted fraction with 1.0 M silver nitrate solution. Once separated, the 'halide-free' fractions were then purified by removal of water from the nitrate salts using an air stream followed by final drying under high vacuum for 24 h. The final 10 products **4-7**, **10-15[NO_3]** were obtained in fair to excellent yields (76-95%).

The dicyanamide salts **4-9, 16-20[$N(CN)_2$]** were obtained by metathesis using silver dicyanamide (prior attempts to obtain dicyanamide salts using sodium dicyanamide by literature protocols failed to achieve satisfactory yields[36]), which was prepared by methods reported in the literature.[13,22] Each of the halide precursors (**4-9**, **16-20[X]**) was combined with a 10% excess of $AgN(CN)_2$ in deionized water and heated at 50 ^oC for 1 h. At the end of the metathesis reaction, the silver halide by-product was filtered, and subsequent evaporation of water from the filtrate using an air stream resulted in the 11 dicyanamide salts in fair to good yields (75-92%). One of these compounds, **6[$N(CN)_2$]**, has been previously reported,[20] and the published data is discussed below in the comparison of all compounds.

To check purity at each stage of the synthesis, ^1H NMR analysis confirmed the structure of all cations (**4-20**) and served as a check for the presence of organic starting materials in **4-7**, **10-15[NO_3]** and **4-9, 16-20[$N(CN)_2$]**, which were found to be below detection limits (< 1 mol%).[37] FT-IR spectroscopy was used to identify the characteristic intense absorption band for the free nitrate anion (ν_{max}(N-O) = 1350-1360 cm^{-1})[38] in **4-7**, **10-15[NO_3]**, as well as absorption for the dicyanamide anion (ν_{max}(C≡N) region around 2250 (m), 2220 (m), and 2150 (s) cm^{-1}).[39] Spot-testing the eluted nitrate salt fractions with 1.0 M silver nitrate solution served to

qualitatively confirm the absence of halide in the final product with the complete anion exchange of halide for nitrate (< 100 ppm).[40] Determination of halide impurity in the dicyanamide samples was attempted following a literature method[41,42] that used silver nitrate titration in the presence of a potassium chromate indicator; however, this did not conclusively indicate halide in the samples obtained.

Single Crystal Structures by X-ray Diffraction

Crystallographic analyses were performed on the halide salts **5[Br]** and **10[Br]**, the nitrate salt **4[NO_3]**, and the dicyanamide salt **4[$N(CN)_2$]**. Single crystals were obtained by recrystallization from methanol solutions with slow-vapor diffusion using diethyl ether. The asymmetric units for each of the solved structures are shown in Figure 2.1, where each structure is oriented perpendicular with respect to the plane of the imidazolium ring. The bond lengths and angles are all typical for the imidazolium ring, although the bonds involving C2 in **4[$N(CN)_2$]** (Figure 2.1D) are significantly shorter than the others, and there is variability of the C-CN bond among the structures. All imidazolium rings are fairly planar, although **10[Br]** (Figure 2.1B) has the least planar ring.

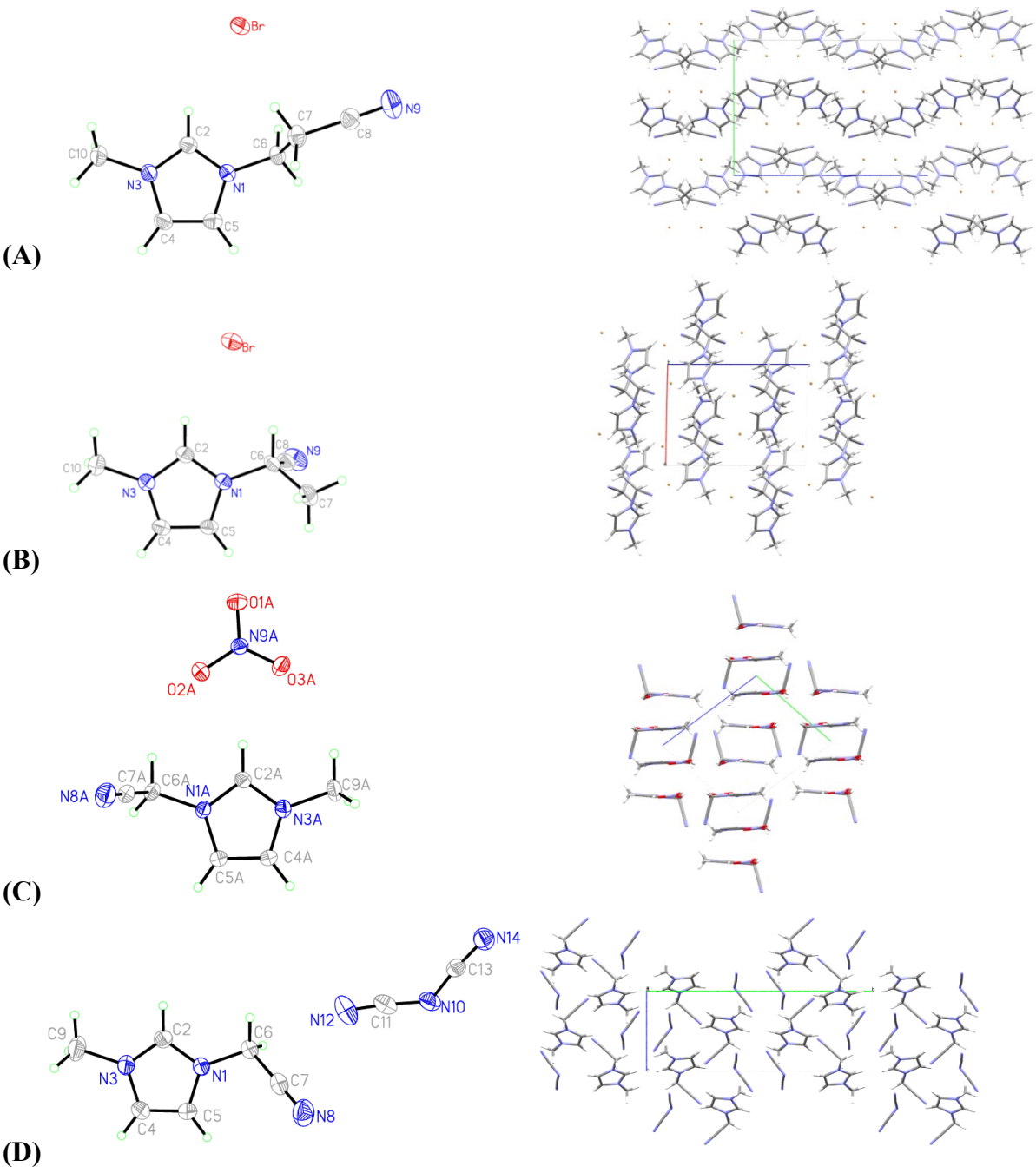

Figure 2.1. ORTEP illustrations (50% probability ellipsoids) of the formula units (illustrating the closest cation-anion approach) and packing diagrams for **5[Br]**, (A), **10[Br]**, (B), **4[NO_3]**, (C), and **4[$N(CN)_2$]**, (D).

The overall packing in **5[Br]** is salt-like (Figure 2.1A), but the nitrile groups do not participate in short contacts. Crystal structures of 1-(2-cyanoethyl)-3-methylimidazolium salts

have not yet been reported in the literature but, in two similar salts reported by Zhao *et al.*, the nitrile groups are oriented parallel to and make short contacts with the imidazolium rings.[19] Nitrile-imidazolium short contacts are observed in the other 3 structures reported here (Figure 2.1B, 2.1C, and 2.1D), and together these observations imply that it is unusual that the nitrile groups in **5[Br]** do not participate in short contacts. The cations do interact *via* edge-to-edge pi-pi stacking between the C4 and C5 positions (C4•••C5 = 3.413(2) Å). The anions interact through hydrogen bonds to hydrogen atoms at the C2 and C4 positions, but do not appear to reside in the coloumbically favorable positions above and below the imidazolium ring.[13]

10[Br] also shows salt-like packing with alternating anion and cation layers. There are short contacts between cations involving the nitrile group and hydrogen atoms, as well as pi-stacked cation dimers with C4 on one ring approaching C5 on another at a distance of 3.559(3) Å, with the rings parallel. The anions participate in three different interactions with cations: a hydrogen bond to the hydrogen at the C2 position, a hydrogen bond to a hydrogen atom at the C5 position, and an out-of-plane interaction with the C2 carbon atom from one side of the ring.

4[NO_3] has two symmetry-independent formula units, however, the environment and packing is nearly the same for both of them. Packing seems to be dominated by cation-anion interactions with the side-chains oriented to maximize hydrogen bonding to the nitrile group, where all anions and imidazolium rings are roughly parallel. Cation-cation short contacts occur between the hydrogen atom at C4 and nitrile groups on two cations (a bifurcated contact). The anion makes three in-plane hydrogen bonds: a very short, bifurcated contact between the oxygen atoms and the hydrogen atom on C2, a bifurcated hydrogen bond to the hydrogen atom at C5, and short contacts to the methylene hydrogen atoms and C7. There is also an out-of-plane interaction between the anion and C2.

4[N(CN)$_2$] also shows efficient salt-like packing with separate anion and cation layers. This structure has only one cation-cation short contact, which is between the nitrile group and the methylene hydrogen atoms. The anion exhibits several types of interactions, with each atom participating differently. One of the terminal nitrogen atoms, N14, makes a hydrogen bond to H2A on one cation, a short contact to the methyl group on a second cation, and is situated above the C2 position of a third cation. N10 makes a hydrogen bond to a ring hydrogen atom at C5. C11 makes short contacts to a methyl group on one cation and C2 on another cation. The carbon atoms in the dicyanamide anion behave as hydrogen bond acceptors as was reported for other related crystal structures.[13,39,43]

Thermal and Sensitivity Investigations

Most of the 41 compounds synthesized and reported here are ILs by definition (i.e., mp < 100 ^{o}C), with the exception of **4[Cl]**, **5[Br]**, **6[Cl]**, **4[NO$_3$]**, **5[NO$_3$]**, and **4[N(CN)$_2$]** which are all higher melting crystalline solids. Phase transition temperatures were obtained by DSC (Table 2.1) and include crystallization and melting transition temperatures ($\boldsymbol{T}_{cryst}$ and $\boldsymbol{T}_{m}$, respectively), as well as glass and liquid-liquid transition temperatures ($\boldsymbol{T}_{g}$ and $\boldsymbol{T}_{l\text{-}l}$, respectively). $\boldsymbol{T}_{g}$ and $\boldsymbol{T}_{l\text{-}l}$ were determined from the second heating cycle after initially heating the material from ambient temperature to an upper limit based upon the thermal stability of the compound as determined by TGA. Phase transitions determined after the first heating cycle were considered to be generally more accurate, where there is evidence for improved surface contact between the sample and the DSC sample pan in subsequent heating cycles.[44]

Crystallization was taken as the onset for an exothermic peak in the second heating cycle (with the exception of **4[NO$_3$]**, which showed $\boldsymbol{T}_{cryst}$ = 43 ^{o}C as an exothermic peak during each cooling cycle), and these are typical for transformations of super-cooled liquids to crystalline

solids.[45] T_m values were measured from the onset of a sharp, endothermic peak on heating, and T_g values were identified from the onset of small shifts in heat flow arising from the transition between amorphous glassy to liquid states when heating.

The thermal stabilities (by TGA) for all prepared compounds are presented in Table 2.1 as the onset of thermal decomposition for the first 5% weight loss ($T_{5\%onset}$). The value for $T_{5\%onset}$ was considered a more accurate assessment of thermal stability than the onset of thermal decomposition (T_{onset}, included for comparison in parentheses in Table 2.1) that is more commonly reported in the literature.[46] All compounds were heated to 600 ^{o}C at a rate of 5 $^{o}C \cdot min^{-1}$ with an isothermal hold at 75 ^{o}C for 30 min.

Sensitivity testing for all dicyanamide salts **4-9**, **16-20[N(CN)$_2$]** was conducted using an Olin-Mathieson drop weight tester, and the values obtained are reported in the last column of Table 2.1. In addition, the same compounds were tested for sensitivity to friction using a Julius Peters apparatus, as well as sensitivity to electrostatic discharge (ESD) using an Air Force Research Laboratory ESD test apparatus with initial sample test level at 5000 V with capacitance set to deliver 0.25 J.

Table 2.1. Thermal and sensitivity characterization of halide, nitrate, and dicyanamide salts with cations **4-20.**

Cation	Cation#	R_2CN	$[X]^-$				$[NO_3]^-$			$[N(CN)_2]^-$			
			[X]	T_g ($T_{l\text{-}l}$) (°C)[a]	T_m (T_{cryst}) (°C)[a]	$T_{5\%onset}$ (T_{onset}) (°C)[b]	T_g ($T_{l\text{-}l}$) (°C)	T_m (T_{cryst}) (°C)	$T_{5\%onset}$ (T_{onset}) (°C)	T_g ($T_{l\text{-}l}$) (°C)	T_m (T_{cryst}) (°C)	$T_{5\%onset}$ (T_{onset}) (°C)	Impact (kg·cm)[c]
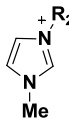	**4**	**CH_2CN**	**Cl^-**	36	174 Lit. 170[34] (114)	206 (251) (Lit. 221[27])	**---**	103 (43)	183 (195)	**-60**	**67** **(12)**	210 (234)	>200
	5	**$(CH_2)_2CN$**	**Br^-**	-21	143	205 (241)	**-47**	**62** **(1.9)**	166 (198)	**-67**	**12**	161 (173)	172
	6	**$(CH_2)_3CN$**	**Cl^-**	**-35** Lit. -34[19]	**96** Lit. 90[19] **(21)** (Lit. 26[19])	258 (290) (Lit. T_d = 255[19])	**-56** **(38)**	**---**	223 (270)	**-80** Lit. -72[20] **(50)**	**---**	244 (260) (Lit. T_d = 278[20])	170
	7	**$(CH_2)_4CN$**	**Cl^-**	**-51** **(45)**	Lit. 32[19]	224 (262)	**-56** **(52)**	**---**	266 (294)	**-74** **(47)**	**---**	247 (273)	170
	8	**$(CH_2)_5CN$**	**Br^-**	**-44** **(50)**	**---**	248 (284)	n.s.	n.s.	n.s.	**-78** **(59)**	**---**	264 (287)	170
	9	**$(CH_2)_6CN$**	**Br^-**	**-48** **(49)**	**---**	257 (280)	n.s.	n.s.	n.s.	**-77** **(46)**	**---**	266 (289)	170
	10	**$CH(CH_3)CN$**	**Br^-**	-3.1	131 (76)	219 (254)	**-58**	**42** **(-9.7)**	168 (209)	n.s.	n.s.	n.s.	n.s.
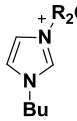	**11**	**CH_2CN**	**Cl^-**	**-22** **(114)**	**---**	186 (213)	**-43** **(46)**	**---**	168 (179)	n.s.	n.s.	n.s.	n.s.
	12	**$(CH_2)_2CN$**	**Br^-**	**-31** **(52)**	**86**	227 (259)	**-52** **(63)**	**---**	180 (202)	n.s.	n.s.	n.s.	n.s.
	13	**$(CH_2)_3CN$**	**Cl^-**	**-36** **(40)**	**---**	243 (279)	**-59** **(48)**	**---**	258 (292)	n.s.	n.s.	n.s.	n.s.
	14	**$(CH_2)_4CN$**	**Cl^-**	**-39** **(50)**	**---**	240 (278)	**-59** **(42)**	**---**	263 (291)	n.s.	n.s.	n.s.	n.s.
	15	**$CH(CH_3)CN$**	**Br^-**	**-12** **(132)**		211 (246)	**-50** **(50)**	**---**	157 (214)	n.s.	n.s.	n.s.	n.s.
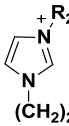	**16**	**CH_2CN**	**Cl^-**	0.26 (49)	120	196 (222)	n.s.	n.s.	n.s.	**-43** **(50)**	**---**	148 (162)	176
	17	**$(CH_2)_3CN$**	**Cl^-**	**-27** **(95)**	**---**	196 (210)	n.s.	n.s.	n.s.	**-62** **(72)**	**---**	164 (182)	176
	18	**$(CH_2)_4CN$**	**Cl^-**	**-36** **(51)**	**---**	190 (221)	n.s.	n.s.	n.s.	**-61** **(51)**	**---**	170 (178)	174
	19	**$(CH_2)_5CN$**	**Br^-**	**-42** **(52)**	**---**	202 (241)	n.s.	n.s.	n.s.	**-66** **(53)**	**---**	165 (192)	174
	20	**$(CH_2)_6CN$**	**Br^-**	**-42** **(58)**	**---**	161 (221)	n.s.	n.s.	n.s.	**-66** **(58)**	**---**	157 (192)	170

[a] Melting point (T_m) and/or glass transition temperatures (T_g) were measured as onset of transition by DSC from the second heating cycle at a ramp rate of 5 °C·min^{-1} after initially melting then cooling to -100 °C, unless otherwise indicated. Salts meeting the definition of ionic liquids (mp < 100 °C) are in **bold**. [b] Reported decomposition temperatures were obtained by TGA, heating at 5 °C·min^{-1} under dried air atmosphere and are reported as (i) onset to 5 weight % loss of mass ($T_{5\%onset}$) and (ii) onset to total mass loss (T_{onset}) (parentheses). [c] Impact sensitivity analysis was carried out on an Olin-Mathieson drop weight tester where a small sample (20 mg) was placed in a standard sample cup (liquid or solid cell employed as appropriate), and a multi-kilogram mass was dropped vertically from measured heights upon the closed sample. [d] n.s. = not synthesized.

Differential Scanning Calorimetry. The observed thermal behavior of the *N*-cyanoalkyl-functionalized salts was often complex, and phase transitions were classified according to one of four different observations. Figure 2.2 compares the first and second heating cycles were for representative compounds **16[N(CN)$_2$]**, Class I; **6[Cl]**, Class II; **12[Br]**, Class III; and **4[NO$_3$]**, Class IV.

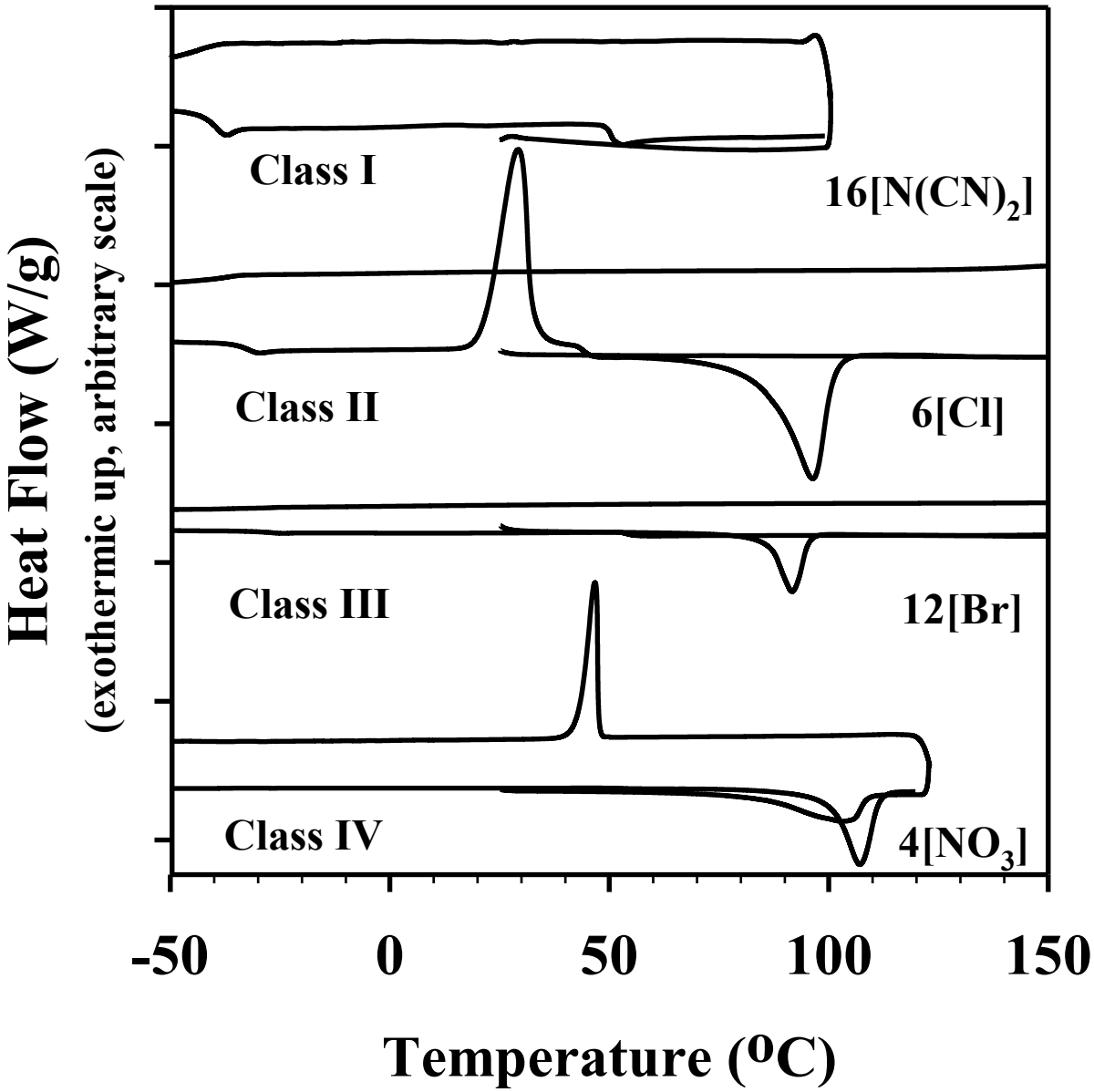

Figure 2.2. Comparison of first and second heating cycle DSC data exemplifying different classes of thermal behavior: **16[N(CN)$_2$]**, (Class I), **6[Cl]**, (Class II), **12[Br]**, (Class III), and **4[NO$_3$]**, (Class IV).

The most common trend in the DSC data (Figure 2.2, Class I) featured a reversible glass transition followed by an additional liquid-liquid transition during the second and third consecutive heating cycles. Compounds of this type include **7[Cl]**, **8[Br]**, **9[Br]**, **11[Cl]**, **13[Cl]**, **14[Cl]**, **15[Br]**, **17[Cl]**, **18[Cl]**, **19[Br]**, **20[Br]; 6**, **7**, **11-15[NO$_3$]**; and **5-9**, **16-20[N(CN)$_2$]**.

Structural features common to this class include the *N*-butyl-substituted nitrate salts, most of the dicyanamide ILs (Class II **4[N(CN)$_2$]** is an exception), and the halide salts featuring longer *N*-cyanoalkyl functional groups.

Those compounds in Class II did not show melting on the first heating cycle but, rather, featured a reversible, low-temperature glass transition, crystallization on heating from a super-cooled phase, and a subsequent melting transition. This class of thermal behavior was observed for compounds **4[Cl]**, **6[Cl]**, **10[Br]**, **5[NO$_3$]**, **10[NO$_3$]**, and **4[N(CN)$_2$]** (Figure 2.2, Class II), which featured short *N*-cyanoalkyl chain lengths (e.g., *N*-cyanomethyl, *N*-(1-cyanoethyl), and *N*-(2-cyanoethyl)), with the exception of **6[Cl]** that was functionalized with the *N*-(3-cyanopropyl) group.

There were also a few examples for which the thermal behavior differed significantly from the above. For example, in three cases melting occurred in the first heating cycle, but only a reversible glass transition prior to a liquid-liquid transition was observed for the next consecutive heating cycles. This small class of compounds consists of all halide salts featuring the *N*-(2-cyanoethyl) functional group (Figure 2.2, Class III, compounds **5[Br]** **12[Br]**, and **16[Cl]**).

Finally, in a single case melting was observed for each heating cycle, as well as crystallization for each cooling cycle (Figure 2.2, Class IV, **4[NO$_3$]**). For this compound, there was no glass transition observed. The melting point for **4[NO$_3$]** (T_m = 103 ^oC) was the highest observed for all nitrates and dicyanamide salts, presumably from the more efficient packing of the smallest cation (**4**) of the nitrate salt. However, several halides with short *N*-cyanoalkyl groups were observed to have significantly higher melting points (T_m = 174 ^oC, **4[Cl]**; 143 ^oC,

5[Br]; 131 ^{o}C, **10[Br]**, 120 ^{o}C, **16[Cl]**), which resulted from the small size of both cation and anion.

Class I compounds did not exhibit well-defined melting temperatures, which is consistent with the suggestion that the relatively high viscosity of ILs (compared to molecular liquids) can inhibit crystallization during the timeframe of the DSC experiment.[1] Our group has observed similar thermal behavior previously for a series of protonated ILs,[2] and it was proposed that the varying degree of inclination in the onset of the $\boldsymbol{T}_{l\text{-}l}$ signal might indicate variation of crystallization attempts for the ILs. Figure 2.3 compares the second heating cycles for four of the Class I compounds, where the variation in slope of the $\boldsymbol{T}_{l\text{-}l}$ onset varies significantly in both the exothermic rise as well as the endothermic trough.

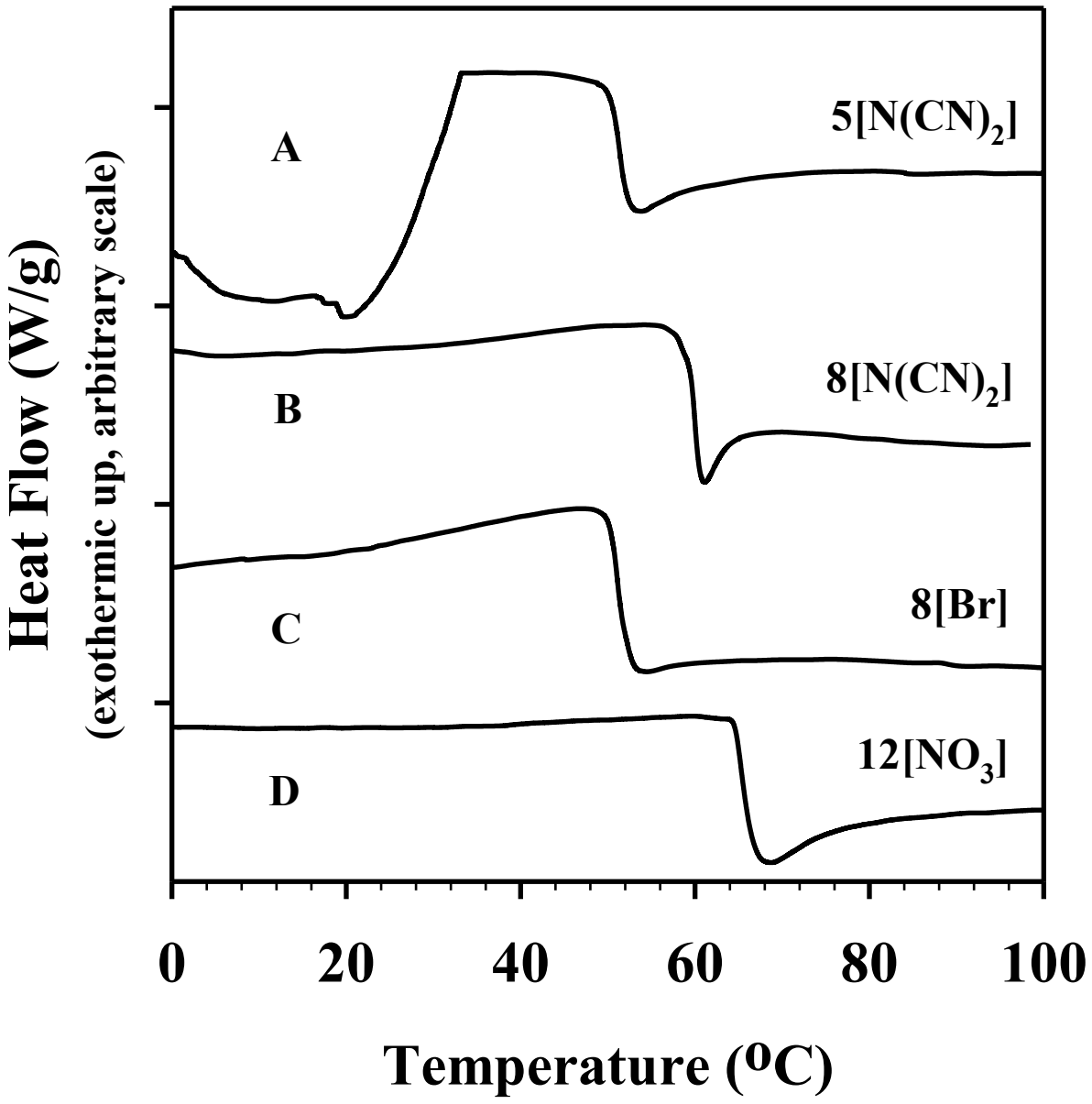

Figure 2.3. Selected DSC traces showing varying degrees of curvature in $T_{l\text{-}l}$ transition from a super-cooled liquid state on the second heating cycle.

For the example **5[N(CN)$_2$]** (Figure 2.3**A**), the observed sharp exothermic increase might signify the start of crystallization. However, the plateau of the signal maxima and broad

endothermic trough are not characteristic of typical crystallization/melt curves as found, for example, in Class II compounds. The other compounds shown in Figure 2.3 also indicated increasingly glass-like transitions from a super-cooled phase (compare Figure 2.3**B-C**), where changing heat flow both in the onset and offset of the signal differed from the characteristic shift of glass transitions. Further DSC study of these materials at slower DSC scan rates may provide a greater understanding of this complex thermal behavior, where others have interpreted similar thermal behavior as a result of conformational disorder,[44,3,4] or plastic crystalline behavior as extensively reported by MacFarlane and co-workers.[5-6]

Without exception, the $\boldsymbol{T}_g$ for salts of the same cation structure decreased in the order of $[X]^- > [NO_3]^- > [N(CN)_2]^-$. In addition, compounds that showed melting behavior also followed this trend (*N*-cyanomethyl-functionalized: $\boldsymbol{T}_m$ = 174 °C, **4[Cl]**; 103 °C, **4[NO$_3$]**; 67 °C, **4[N(CN)$_2$]**; *N*-(2-cyanoethyl)-functionalized: $\boldsymbol{T}_m$ = 143 °C, **5[Br]**; 62 °C, **5[NO$_3$]**; 12 °C, **5[N(CN)$_2$]**). Increasing proton affinity and diffusivity of the negative charge in the anion, in part, may explain the lower $\boldsymbol{T}_g$ observed for nitrate and dicyanamide salts, respectively.[7,8] These factors can also affect the hydrogen-bonding interactions of the anion and, thus, influence the molecular packing and the observed melting points for the compounds.[9] Differences in anion size ($[X]^- < [NO_3]^- < [N(CN)_2]^-$) have also been correlated with decreasing melting points.[10]

Shorter *N*-cyanoalkyl-substituted halide salts with the *N*-methyl group showed high temperature melting transitions ($\boldsymbol{T}_m$ = 174 °C, **4[Cl]**; 143 °C, **5[Br]**, 96 °C, **6[Cl]**), where only one case of an *N*-butyl-substituted halide salt was found to have a melting transition ($\boldsymbol{T}_m$ = 86 °C, **12[Br]**). This behavior has been attributed to the less efficient packing of ions for longer *N*-alkyl and *N*-cyanoalkyl substituents, resulting in liquid-state properties at lower temperatures.[26] In

Figure 2.4, the observed trends in thermal behavior with changing *N*-cyanoalkyl and *N*-alkyl substituent lengths are illustrated for a selection of the chloride salts reported here.

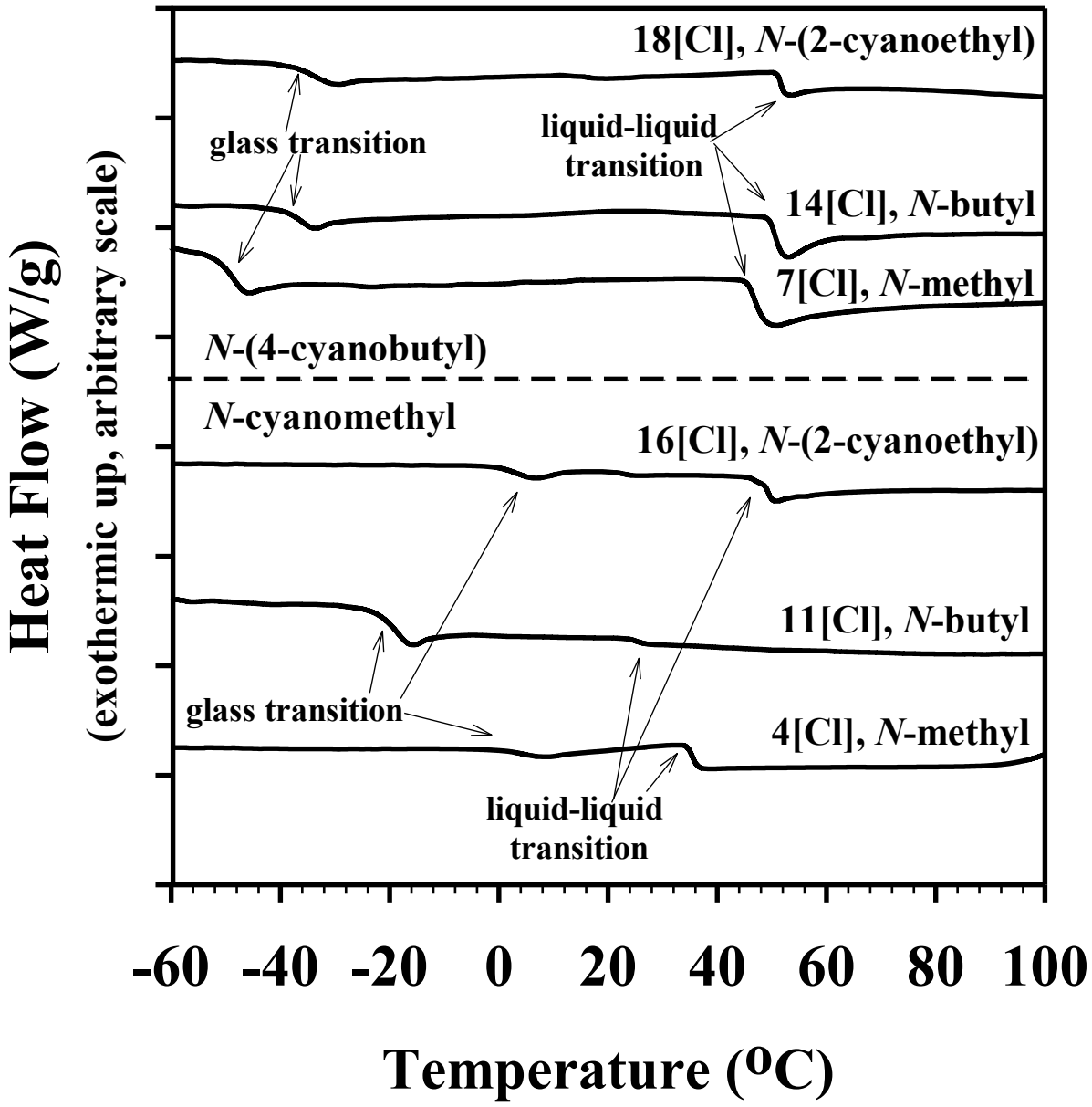

Figure 2.4. Comparison of glass transition (T_g) and liquid-liquid transition ($T_{l\text{-}l}$) trends in DSC data for *N*-cyanomethyl- (bottom) and *N*-(4-cyanobutyl)-functionalized (top) chloride salts with different *N*-alkyl substituents (*N*-methyl, *N*-butyl, and *N*-(2-cyanoethyl)).

A higher T_g was observed for *N*-methyl-substituted **4[Cl]** compared to analogous *N*-butyl **11[Cl]** (Figure 2.4, bottom), where less efficient packing of *N*-butyl- *vs.* *N*-methyl-substituted cations has been reported to promote the liquid state at lower temperatures.[2] Higher T_g values were observed for *N*-(2-cyanoethyl)-substituted imidazolium halides (**16[Cl]** and **18[Cl]**, Figure 2.4), and it has been suggested that the lone-pair- and π-electrons of the nitrile functional group are capable of inter-ion interactions (as seen in the crystal structures of **10[Br]**, **4[NO_3]**, and **4[$N(CN)_2$]**) which may contribute to higher T_g values.[11] The cation-cation contacts observed in the crystal structure of *N*-cyanoethyl-substituted **5[Br]** reinforces this claim, where organization of the IL structure though hydrogen bonding can result in elevated T_g values. Finally, T_g values are generally lower for longer *N*-cyanoalkyl-functionalized salts (e.g., *N*-(4-cyanobutyl), Figure 2.4, top) in comparison with shorter analogs (e.g., *N*-cyanomethyl, Figure 2.4, bottom), similar to the *N*-alkyl chain-length effect previously described.[2]

As with the halide series, several *N*-methyl-substituted nitrate salts with shorter *N*-cyanoalkyl chains showed melting transitions (T_m = 103 °C, **4[NO_3]**; 62 °C **5[NO_3]**; 42 °C, **10[NO_3]**), again, presumably due to the more efficient packing of *N*-methyl- *vs.* *N*-butyl-substituted cations.[12] Also similar to the halide series, the glass transitions for nitrate salts were found to decrease with increasing *N*-cyanoalkyl chain length (considering nitrates, *N*-methyl: T_g = -47 °C, **5[NO_3]** *vs.* -56 °C, **6[NO_3]**; *N*-butyl: T_g = -43 °C, **11[NO_3]**; -52 °C, **12[NO_3]**; -59 °C, **13[NO_3]**). However, in contrast to halides, no significant differences were found for changes in chain length for longer *N*-cyanoalkyl-functionalized nitrate salts (T_g = -56 °C, **6[NO_3]**, -56 °C, **7[NO_3]**, and T_g = -59 °C, **13[NO_3]**, -59 °C, **14[NO_3]**), and only small differences were observed in glass transitions with variation between *N*-methyl- and *N*-butyl-substituted compounds.

One of the most visible trends in the DSC data resulted from a variation of the anion, where there was a high coincidence of low-temperature T_g values for all *N*-(2-cyanoalkyl)-functionalized imidazolium dicyanamide salts (T_g = -67 °C, **5[N(CN)$_2$]**; -62 °C, **17[N(CN)$_2$]**; -61 °C, **18[N(CN)$_2$]**; -66 °C, **19[N(CN)$_2$]**; -66 °C, **20[N(CN)$_2$]**). Interestingly, the *N*-methyl-substituted compounds **4-9[N(CN)$_2$]** showed much lower T_g values when compared with analogous *N*-(2-cyanoethyl)-substituted products **16-20[N(CN)$_2$]**. It seems that the introduction of a second *N*-cyanoalkyl substituent in combination with the cyano groups present on the dicyanamide anion may have a synergistic effect for increasing T_g, possibly by increasing the interactions between ions through available π and lone-pair electrons from a total of four cyano groups per ion pair. In comparison to analogous halide and nitrate salts, however, ILs featuring the dicyanamide anion show the lowest T_g values reported here. This is in agreement with the literature, where dicyanamide-based ILs exhibit some of the lowest glass transition temperatures and broadest liquid ranges to date.[26]

Thermal Gravimetric Analysis. In agreement with previous reports,[23,24] there was not a significant difference observed for the thermal stabilities of halides or nitrates when comparing *N*-methyl and *N*-butyl-substituted compounds within each series (**4-7**, **10-15[X]** and **4-7**, **10-15[NO$_3$]**, respectively). To illustrate this, the TGA traces for *N*-methyl and *N*-butyl-substituted salts are compared in Figures 2.5 and 2.6.

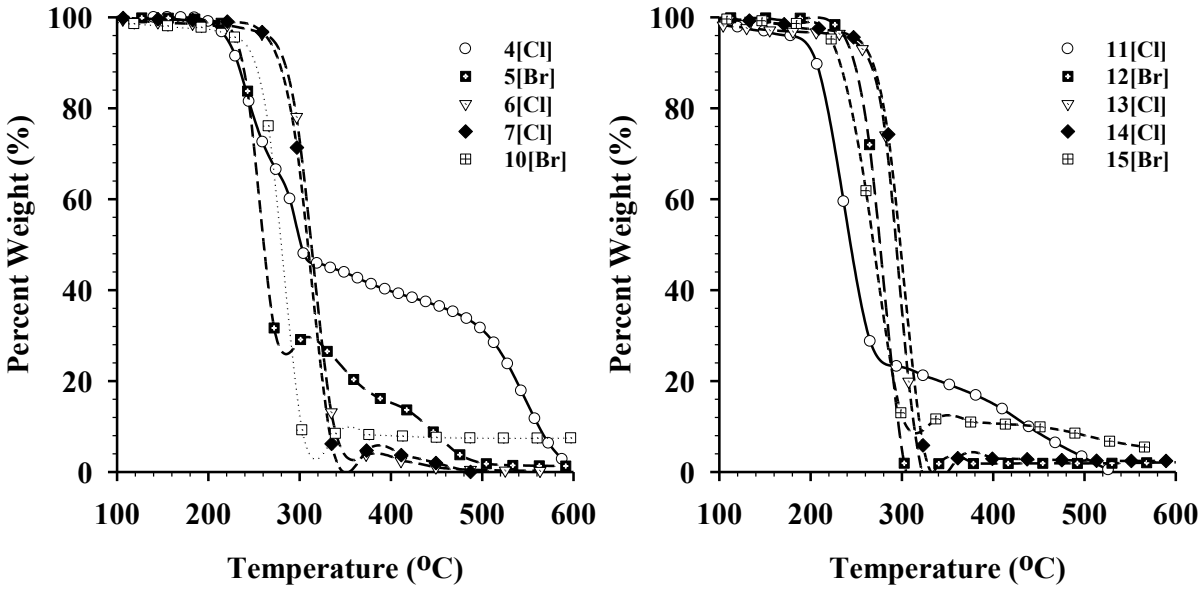

Figure 2.5. Comparison of TGA data for *N*-methyl- (**4-7**, **10[X]**, left) *vs. N*-butyl-substituted (**11-15[X]**, right) halide salts.

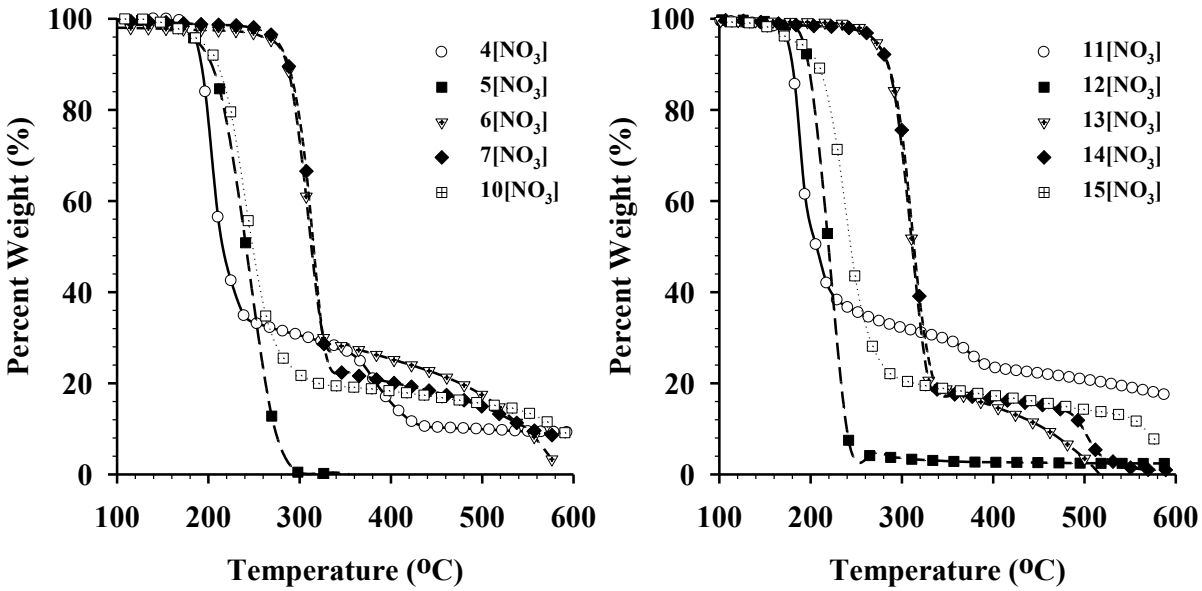

Figure 2.6. Comparison of TGA data for *N*-methyl- (**4-7**, **10[NO_3]**, left) *vs. N*-butyl-substituted (**11-15[NO_3]**, right) nitrate salts.

From analysis of the data in Figures 2.5 and 2.6 above, the thermal stability for both *N*-methyl and *N*-butyl-substituted salts were found to be similar for halide and nitrate analogs with

longer *N*-cyanoalkyl chains; compare **6**, **7**, **13**, **14[NO$_3$]** and **[X]**, where all $\boldsymbol{T}_{5\%onset}$ temperatures are *ca.* 250 ^{o}C as reported in Table 2.1. However, as the *N*-cyanoalkyl chain is shortened, there is a significant decrease in thermal stability observed for the nitrate salts (e.g., compare $\boldsymbol{T}_{5\%onset}$ = 183 ^{o}C, **4[NO$_3$]**; 166 ^{o}C, **5[NO$_3$]** (*N*-methyl) and $\boldsymbol{T}_{5\%onset}$ = 168 ^{o}C, **11[NO$_3$]**; 180 ^{o}C, **12[NO$_3$]** (*N*-butyl)). Additionally, the *N*-(1-cyanoethyl)-substituted nitrate salts also showed reduced thermal stability (e.g., $\boldsymbol{T}_{5\%onset}$ = 168 ^{o}C, **10[NO$_3$]**; 157 ^{o}C, **15[NO$_3$]**) in comparison with *N*-cyanoalkyl-functionalized cations in the same series with longer chain lengths. Thus, *N*-cyanoalkyl-functionalized salts appear to be less stable in the nitrate form compared with analogous halides for shorter *N*-cyanoalkyl-functional groups. It is postulated that the proximity of the nitrile group to the formal charge of the imidazolium ring may have an activating effect for the decomposition pathway involving the nitrate anion that is not observed for halides. Increasing the proximity of the electron-withdrawing nitrile group to the imidazolium core may result in destabilization similar to that observed when nitrile groups are directly appended to the imidazolium core.[16]

N-(2-cyanoethyl)-substituted imidazolium halides **16-20[N(CN)$_2$]** were generally more stable than their *N*-methyl and *N*-butyl analogs (compare $\boldsymbol{T}_{5\%onset}$ = 196 ^{o}C, **16[Cl]**; 206 ^{o}C, **4[Cl]**; 186 ^{o}C, **11[Cl]**). However, thermal stability is greatly reduced for *N*-methyl *vs.* *N*-(2-cyanoethyl)-functionalized dicyanamide salts (> 100 ^{o}C difference, see Figure 2.7).

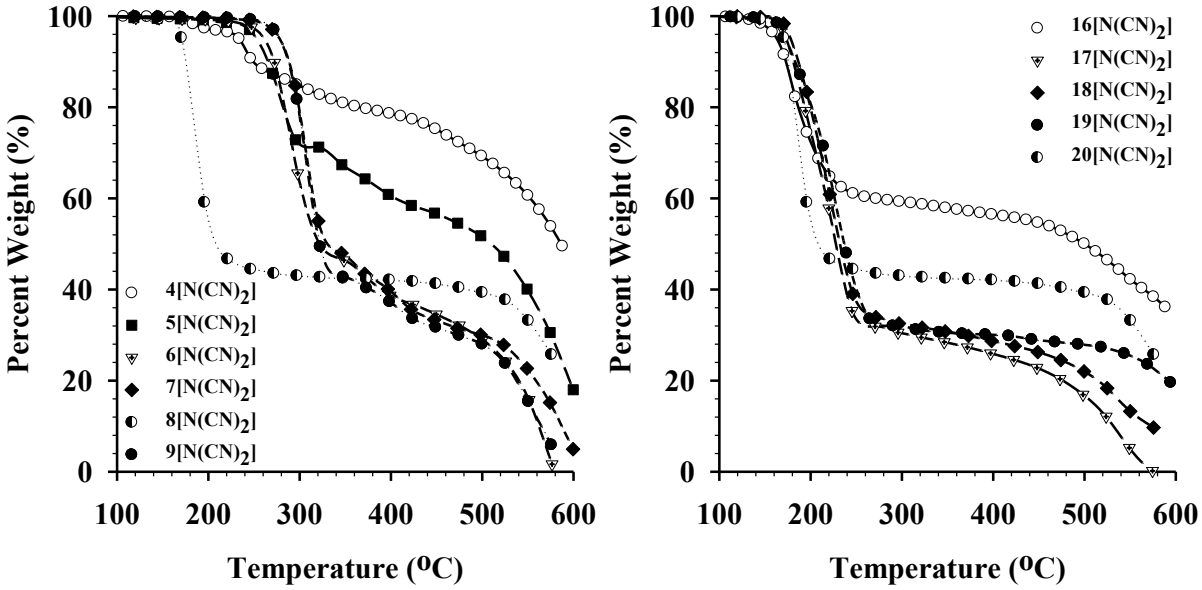

Figure 2.7. Comparison of TGA plots for *N*-methyl- (**4-9[N(CN)$_2$]**, left) *vs.* *N*-(2-cyanoethyl)-substituted (**16-20[N(CN)$_2$]**, right) dicyanamide salts.

Considering the similarity of the $T_{5\%onset}$ values for the *N*-(2-cyanoethyl) salts **16-20[N(CN)$_2$]** (Figure 2.7, right) with the 1-(2-cyanoethyl)-3-methylimidazolium dicyanamide salt, **5[N(CN)$_2$]** (Figure 2.7, left), we can then consider the possibility that the 2-cyanoethyl substituent has a key role in the thermal degradation of the material. This same functional group is known as a facile leaving group in the deprotection step for the synthesis of 1-cyanoalkylimidazoles using heat under basic conditions,[28] and all *N*-(2-cyanoethyl)-*N*-cyanoalkyl-substituted dicyanamide salt thermal stabilities coincide with that found for *N*-(2-cyanoethyl)-functionalized **5[N(CN)$_2$]** ($T_{5\%onset}$ = 161 °C). Thus, without the *N*-(2-cyanoethyl) substituent (e.g., *N*-methyl analogs), a more thermally-stable material results that shows initial mass loss at much higher temperatures. Halides featuring the *N*-(2-cyanoethyl) functionality showed low, uniform decomposition temperatures across the series. This observed uniformity is also found for the *N*-(2-cyanoethyl)-functionalized dicyanamide compounds, however, the

$T_{5\%onset}$ values are much lower when compared with analogous halides ($T_{5\%onset}$ (range): 148-170 ^{o}C, see Table 2.1).

As can be noted from the comparative TGA plots provided here (Figures 2.5-2.7), there are some ILs that did not completely decompose under the conditions of the TGA experiment. For the halide salts, those featuring short *N*-cyanoalkyl-functionalized cations (e.g., **4**, **5**, **10**, **11**, **15[X]**) all showed a two-step decomposition pattern. Upon initial onset (as reported in Table 2.1), decomposition continued gradually from about 300 ^{o}C until reaching nearly 10-40% of original mass near 500 ^{o}C. For nitrate salts, all but the *N*-(2-cyanoethyl)-functionalized compounds (**5**, **12[NO_3]**) showed this trend, with around 10-30% of initial mass remaining. Char formation was especially pronounced for *N*-cyanomethyl (**4**, **11[NO_3]**) and *N*-(1-cyanoethyl)-functionalized (**10**, **15[NO_3]**) nitrate salts. Finally, the highest production of thermally stable material is evident for the dicyanamide salts, where all salts were found to result in char formation (30-80% mass). Upon visual inspection of the material in the TGA pan, the material appears as a light-weight foam with a dark gray, metallic sheen.

There have been reports in the literature for similar formation of carbonaceous char from nitrile-functionalized imidazolium salts in the temperature ranges reported above, where cyclization of nitrile into carbonitride or nitrogen-doped graphene have found utility as microporous and mesoporous materials for catalyst support or chemical separation membranes.[13,14] The absence of char formation for **5[NO_3]** and **12[NO_3]** implies that, under the temperature and atmosphere of the TGA experiment, these nitrate salts preferentially undergo complete thermal decomposition rather than forming carbonaceous matter. Schnick[15,16] and MacFarlane[46] have indicated similar cyclization and polymerization of cyanamide and dicyanamide anions. The high productivity for char in all dicyanamide salts seems to be

additive, where the nitrile groups from both *N*-cyanoalkyl, as well as the dicyanamide anion are available for reaction. As the weight percent of the carbonaceous material is variable depending on the type of cation, as well as the identity of the anion, there is potential application for these findings as a modular system for the design of porous materials for numerous applications.

Impact, Friction, and Electrostatic Discharge Sensitivity. All dicyanamide salts (**4-9**, **16-20[N(CN)$_2$]**) were found to be very insensitive (Table 2.1, last column). Drop-hammer testing results indicated a range of 170-200 kg·cm and, when compared to impact sensitivity values of other known energetic materials such as TNT (98 kg·cm), RDX (28 kg·cm), and DNB (28 kg·cm),[17] the salts reported here are considered to be insensitive to impact.

The results from both friction testing (no response at greater than 211 Newtons for the Julius Peters test) and electrostatic discharge testing (negative response at 1 Joule determined from use of Air Force Research Laboratory ESD apparatus) also provide evidence that these dicyanamide salt structures exhibit low sensitivities. These properties would be appreciated in applications where non-sensitive liquids are desired (e.g., fuels and lubricants).

Conclusions

The focus for this work was to explore the synthesis of new 1-alkyl-3-cyanoalkylimidazolium ILs and to examine the effects of different cation substituent lengths (*N*-alkyl, *N*-cyanoalkyl), as well as energetic anions (nitrate and dicyanamide) on the observed thermal properties for each salt reported. Most of the 41 compounds prepared were ILs by definition (melting point below 100 ^{o}C). DSC analyses indicated several distinct classes of thermal behavior, including liquid-liquid transitions from failed attempts for the salt to crystallize from a super-cooled phase within the timeframe of the DSC experiment. This thermal

behavior was most frequently observed for compounds with long *N*-alkyl and *N*-cyanoalkyl chain lengths, as well as for most dicyanamide salts.

Melting transitions were observed mainly for short-chain *N*-cyanoalkyl-functionalized cations, and the trends for $\boldsymbol{T}_g$ were generally the same with changing *N*-cyanoalkyl chain lengths. Nonetheless, the effects of *N*-alkyl chain length on $\boldsymbol{T}_g$ in general often depended on the type of anion present, where halides often showed a greater decrease in glass transition temperature than nitrates when comparing *N*-methyl versus *N*-butyl analogs. The dicyanamide salts had uniformly lower $\boldsymbol{T}_g$ values than analogous halides and nitrates, and the *N*-methyl-substituted dicyanamide ILs exhibited lower $\boldsymbol{T}_g$ values than *N*-(2-cyanoethyl)-functionalized salts.

There appeared to be considerably different trends in the observed $\boldsymbol{T}_{5\%onset}$ values obtained by TGA with respect to changes in the *N*-alkyl substituent, the *N*-cyanoalkyl chain length, and the class of anion present. Halide salts with short *N*-cyanoalkyl substituents were less stable than the *N*-butyl analogs. Although the difference between *N*-methyl and *N*-butyl analogs of nitrate salts did not differ significantly, there was a much lower stability in short *N*-cyanoalkyl-functionalized nitrates in comparison with longer chain analogs.

For the dicyanamide-based ILs, all *N*-methyl substituted salts seemed to be very thermally stable in comparison with halides and nitrates. However, an exception to this was **5[N(CN)$_2$]** which showed a $\boldsymbol{T}_{5\%onset}$ much lower than the others in the series. Recognizing the similarity in thermal decomposition behavior of **5[N(CN)$_2$]** with other *N*-(2-cyanoethyl)-functionalized compounds (**16-20[N(CN)$_2$]**), it is concluded that the cyanoethyl functionality may have a profound influence on the thermal decomposition pathway observed in the TGA experiment for these compounds. Furthermore, the prevalence of carbonaceous char for all compounds seemed to follow the anion trend $[X]^- < [NO_3]^- < [N(CN)_2]^-$, where all shorter *N*-

cyanoalkyl-functionalized ILs for halides and nitrates exhibited a characteristic 2-step decomposition pattern. The exception to this was for *N*-(2-cyanoethyl)-functionalized nitrate salts (**5[NO_3]** and **12[NO_3]**), which showed complete decomposition without any residual material remaining.

Finally, in the case of the dicyanamide salts, the most char production was clearly evident, where up to 80% of the original weight was found to remain up to nearly 500 ^{o}C. As such, the *N*-cyanoalkyl-substituted imidazolium salts studied here suggest potential use as building blocks for porous mesoscale materials that can be further functionalized to provide a versatile scaffold for numerous applications (e.g., heterogeneous catalysis, chemical separations, *etc.*).

Experimental

Materials and Methods

Reagents were used as obtained from commercial sources (Sigma-Aldrich, Milwaukee, WI) unless otherwise noted. All solvents were 'solvent grade' and used as received without additional purification.

The ^{1}H and ^{13}C NMR spectra were recorded using a Bruker AV-500 (Karlsruhe, Germany) spectrometer operating at 500 MHz and 125 MHz, respectively. Infrared (IR) analyses were obtained by direct measurement of the neat samples by utilizing a Perkin-Elmer 100 FT-IR instrument, Perkin-Elmer (Shelton, CT), featuring an attenuated total reflection (ATR) force gauge, and spectra were obtained in the range of ν_{max} = 650 – 4000 cm^{-1}.

Thermogravimetric analyses (TGA) were performed using a TGA 2950, TA Instruments, Inc. (New Castle, DE). These experiments were conducted under air atmosphere and measured in the dynamic heating regime. Samples between 5-15 mg were heated from 30-600 ^{o}C under

constant heating ramp of 5 ^{o}C min^{-1} with a 30 min isotherm at 75 ^{o}C. Temperatures reported for the decomposition profiles for all materials were established as the onset temperature for decomposition of the first 5% of the sample ($\boldsymbol{T}_{5\%onset}$).

Melting point/glass transition analyses were performed by differential scanning calorimetry (DSC) using a DSC 2920 Modulated DSC, TA Instruments, Inc. (New Castle, DE) cooled with a liquid nitrogen cryostat. The calorimeter was calibrated for temperature and cell constants using indium ($\boldsymbol{T}_{m}$ = 156.61 ^{o}C; $\boldsymbol{C}$ = 28.71 J·g^{-1}). Data were collected at atmospheric pressure, where samples were initially heated at a rate of 5 ^{o}C·min^{-1} to a temperature not to exceed 50 ^{o}C below the measured $\boldsymbol{T}_{5\%onset}$ (obtained from TGA). The sample was then held for a 5 min isotherm prior to two cycles of cooling and heating (back to upper temperature limit from first heating) at a rate of 5 ^{o}C·min^{-1} spaced by 5 min isothermal holding at lower ($\boldsymbol{T}$ = -100 ^{o}C, unless otherwise stated) and upper (as indicated above) endpoint temperatures. Samples between 5-15 mg were used in aluminum sample pans (sealed, then perforated with a pin-hole to equilibrate pressure resulting from potential expansion of evolved gases). The DSC was adjusted so that zero heat flow was between 0 and -0.5 mW, and the baseline drift was less than 0.1 mW over the temperature range of 0-180 ^{o}C. An empty sample pan served as the reference. Temperatures reported for the glass transition ($\boldsymbol{T}_{g}$) and melting ($\boldsymbol{T}_{m}$) were established as the onset temperature for the endothermic change in heat flow measured through the material and as the onset temperature for the exothermic change in heat flow measured in the case of observed crystallization ($\boldsymbol{T}_{cryst}$).

Impact sensitivity testing was performed at the Air Force Research Laboratory (Edwards Air Force Base, CA). Analysis was carried out on an Olin-Mathieson drop weight tester, where a small sample (20 mg) was placed in a standard sample cup (liquid or solid cell employed as

appropriate), and a multi-kilogram mass was dropped vertically from measured heights upon the closed sample.[18-19] The drop height in centimeters was recorded, and the point was determined at which 50% of impacts were positive. A sample of water was used as a standard calibration for liquid samples, and 1,3,5-trinitroperhydro-1,3,5-triazine was used for calibration for solid samples.

For friction testing, a Julius-Peters friction tester was employed whereby a small amount of sample (20 mg) was placed on a small ceramic square plate and a steel pin was pushed across the sample under a known load. Any evidence of discoloration, odor, smoke, or spark was considered a positive test. All samples tested were insensitive to friction, showing negative response at greater than 211 Newton. Sensitivity to electrostatic discharge (ESD) was determined using the AFRL ESD test apparatus with initial sample test level at 5000 V with capacitance set to deliver 0.25 J. Each of the samples was determined to be insensitive to ESD, as they all showed negative response under 1 Joule when tested.

Single-crystal X-ray diffraction data were collected for compounds **5[Br]**, **10[Br]**, **4[NO_3]**, and **4[$N(CN)_2$]** on a Bruker SMART diffractometer equipped with a CCD area detector using graphite-monochromated Mo-*K*α (λ = 0.71073 Å) radiation. Crystals were cooled to -100 °C during data collection. The structures were solved using the SHELXTL software package,[20] and the absorption corrections were made with SADABS.[21] The structures were refined by full-matrix least-squares on F^2. Non-hydrogen atoms were located from the difference map and refined anisotropically. Hydrogen atoms were constrained to idealized positions, except methyl hydrogen atoms which were refined using a riding rotating model.

Synthetic Protocols

<u>*N*-Cyanoalkyl-functionalized imidazolium halides (**4-20[X]**)</u>:

***General procedure to prepare 4[Cl] and 11[Cl]*:** Compounds **4[Cl]** and **11[Cl]** were each prepared based on a previous method.[31] Yields and reaction times were not optimized, and the following serves as a general procedure. In a 50 mL round-bottom flask with a magnetic stirbar, chloroacetonitrile (10% molar excess) was slowly added to 1-alkylimidazole (**1** or **2**, respectively). The mixture was stirred at room temperature overnight, and the resulting product was washed with ethyl acetate (4 x 5 mL) and dried by rotary evaporation prior to final removal of residual solvent by high vacuum at room temperature for 24 h.

***1-Cyanomethyl-3-methylimidazolium chloride* (4[Cl]):** Compound **4[Cl]** was prepared from **1** (2.870 g, 35 mmol). White solid, water soluble (90%); ^{1}H NMR (500 MHz, DMSO-d_6) δ ppm 9.56 (s, 1H), 8.00 (t, 1H), 7.87 (t, 1H), 5.82 (s, 2H), 3.92 (s, 3H); ^{13}C NMR (125 MHz, DMSO-d_6) δ ppm 138.3, 124.8, 123.0, 115.3, 37.2, 36.6; FT-IR (ν_{max} in cm^{-1}): 3392 (w), 3032 (s), 2977 (s), 2906 (s), 1575 (s), 1565 (s), 1439 (m), 1337 (m), 1254 (s), 1168 (s), 915 (m).

***1-Butyl-3-cyanomethylimidazolium chloride* (11[Cl]):** Compound **11[Cl]** was prepared from **2** (2.612 g, 20 mmol). Amber liquid (57%); ^{1}H NMR (500 MHz, DMSO-d_6) δ ppm 9.70 (s, 1H), 8.04 (d, 1H), 7.99 (d, 1H), 5.83 (s, 2H), 4.27 (t, 2H), 1.75 (pent, 2H), 1.23 (m, 2H), 0.88 (t, 3H); ^{13}C NMR (125 MHz, DMSO-d_6) δ ppm 137.2, 123.0, 122.6, 114.7, 48.8, 36.7, 31.1, 18.6, 13.1; FT-IR (ν_{max} in cm^{-1}): 3370 (b), 3135 (w), 3064 (m), 2960 (s) 2934 (s), 2874 (m), 1638 (w), 1558 (s), 1463 (m), 1420 (w), 1337 (w), 1251 (w), 1209 (w), 1163 (s), 1115 (w), 1030 (m), 926 (w), 872 (w), 755 (s), 708 (w), 662 (w).

General procedure to prepare 5-10, 12-15[X]: Compounds **5-10, 12-15[X]** were obtained under solvent-free conditions as with **4[Cl]** and **11[Cl]**, but with the addition of heat during the reaction. Yields and reaction times were not optimized, and the following serves as a general procedure. To a 20 mL Ace Glass high temperature vial fitted with a Teflon screw-cap,

the appropriate haloalkylnitrile (10% molar excess) was added to 1-alkylimidazole (**1** or **2**). Upon fastening the screw-cap on the vial, the mixture was stored in a furnace set to 70 ^{o}C for 48 h. As exceptions to this procedure, compound **5[Br]** was inadvertently left for 20 days in the furnace at 70 ^{o}C, and compound **12[Br]** was obtained from first preparing 1-(2-cyanoethyl)imidazole, **3**, by literature methods (see **3**, below),[28] which was then alkylated with 1-bromobutane in 10% molar excess. After each reaction was finished, the reaction mixtures were washed with ethyl acetate or acetone (4 x 5 mL) prior to drying first by rotary evaporation followed by removal of residual solvent by high vacuum for 24 h at room temperature.

1-(2-Cyanoethyl)imidazole **(3):** Compound **3** was prepared by combining imidazole (5.301 g, 100 mmol) with acrylonitrile (6.799 g, 110 mmol) in toluene (20 mL) and then adding triethylamine (1 mL). With the addition of a magnetic Teflon stir bar, the reaction mixture was stirred and heated to 50 ^{o}C and maintained at this temperature for 30 h, when the product separated as a lower liquid phase from the toluene solution. Purification of **3** was achieved by removing the solvent from the lower product phase by first decanting and then washing the product phase of residual solvent and starting materials with 3 x 10 mL with acetone. After removal of residual solvent by rotary evaporation, final purification involved further drying under high vacuum at room temperature for 24 h prior to use. Amber liquid (71%); ^{1}H NMR (500 MHz, DMSO-d_6) $\boldsymbol{\delta}$ ppm 7.69 (s, 1H), 7.23 (t, 1H), 6.92 (t, 1H), 4.26 (t, 2H), 3.04 (t, 2H); ^{13}C NMR (125 MHz, DMSO-d_6) $\boldsymbol{\delta}$ ppm 137.3, 128.7, 119.2, 118.5, 41.6, 19.5; FT-IR ($\boldsymbol{\nu}_{max}$ in cm^{-1}): 3551 (m), 3473(m), 3413 (w), 3240 (m), 3078 (w), 2966 (w), 2252 (w), 1616 (s), 1538 (m), 1410 (m), 1374 (m), 1376 (m), 1275 (m), 1231 (m), 1181 (m), 1116 (w), 1034 (w), 907 (m), 758 (m), 705 (m).

Caution: Acrylonitrile is a very hazardous irritant and permeator for skin and eyes, and requires protective clothing and a properly ventilated workspace when handling. Prolonged exposure should be avoided, as there may be carcinogenic/tetratogenic/mutagenic effects, as well as toxicity related to target organs including blood, liver, central nervous system, and kidneys. Additionally, explosive mixtures can be formed when vapors are allowed to mix with air, and accumulation of evaporated material is to be avoided. Please refer to Material Safety Data Sheet (MSDS) for further precautionary details (CAS #107-13-1).

***1-(2-Cyanoethyl)-3-methylimidazolium bromide* (5[Br]):** Compound **5[Br]** was prepared from **1** (4.621 g, 38 mmol). Yellow solid (86%); ^{1}H NMR (500 MHz, DMSO-d_6) $\boldsymbol{\delta}$ ppm 9.31 (s, 1H), 7.88 (s, 1H), 7.80 (s, 1H), 4.53 (t, 2H), 3.90 (s, 3H), 3.25 (t, 2H); ^{13}C NMR (125 MHz, DMSO-d_6) $\boldsymbol{\delta}$ ppm 137.5, 124.4, 122.8, 118.2, 44.9, 36.5, 19.2; FT-IR ($\boldsymbol{\nu}_{max}$ in cm^{-1}): 3139 (w), 3082 (s), 3042 (s), 2958 (w), 2845 (w), 2250 (w), 1780 (w), 1761 (w), 1727 (w), 1676 (w), 1575 (m), 1559 (w), 1448 (w), 1426 (w), 1401 (w), 1359 (w), 1341 (w), 1280 (w), 1199 (w), 1160 (s), 1092 (w), 1022 (w), 892 (w), 864 (s), 789 (s), 741 (s), 652 (m).

***1-(3-Cyanopropyl)-3-methylimidazolium chloride* (6[Cl]):** Compound **6[Cl]** was prepared from **1** (3.610 g, 44 mmol). Yellow solid (92%); ^{1}H NMR (500 MHz, DMSO-d_6) $\boldsymbol{\delta}$ ppm 9.42 (s, 1H), 7.87 (t, 1H), 7.78 (t, 1H), 4.28 (t, 2H), 3.86 (s, 3H), 2.61 (t, 2H), 2.14 (pent, 2H); ^{13}C NMR (125 MHz, DMSO-d_6) $\boldsymbol{\delta}$ ppm 136.9, 123.5, 122.2, 119.5, 47.4, 35.6, 25.2, 13.4; FT-IR ($\boldsymbol{\nu}_{max}$ in cm^{-1}): 3435 (s), 3371 (s), 3244 (w), 3126 (w), 3109 (w), 3063 (m), 2971 (w), 2938 (w), 2915 (w), 2839 (w), 2244 (m), 2186 (w), 2111 (w), 1731 (w), 1655 (w), 1619 (m), 1574 (s), 1562 (s), 1453 (m), 1425 (m), 1391 (w), 1344 (w), 1334 (w), 1325 (w), 1266 (w), 1160 (s), 1092 (s), 1017 (m), 867 (s), 850 (w), 774 (s), 723 (w), 665 (m).

***1-(4-Cyanobutyl)-3-methylimidazolium chloride* (7[Cl]):** Compound **7[Cl]** was prepared from **1** (1.232 g, 15 mmol). Amber liquid (95%); ^{1}H NMR (500 MHz, DMSO-d_6) $\boldsymbol{\delta}$ ppm = 9.24 (s, 1H), 7.82 (t, 1H), 7.75 (t, 1H), 4.24 (t, 2H), 3.86 (s, 3H), 2.57 (t, 2H), 1.87 (pent, 2H), 1.53 (pent, 2H); ^{13}C NMR (125 MHz, DMSO-d_6) $\boldsymbol{\delta}$ ppm = 137.1, 124.1, 122.7, 120.9, 48.3, 36.3, 29.0, 22.0, 16.2; FT-IR ($\boldsymbol{\nu}_{max}$ in cm^{-1}): 3372 (b), 3143 (w), 3058 (m), 2952 (w), 2869 (w), 2242 (w), 1637 (w), 1571 (s), 1458 (m), 1427 (w), 1385 (w), 1335 (w), 1293 (w), 1161 (s), 1091 (w), 1020 (w), 843 (w), 760 (m), 697 (w).

***1-(5-Cyanopentyl)-3-methylimidazolium bromide* (8[Br]):** Compound **8[Br]** was prepared from **1** (1.724 g, 21 mmol). Amber liquid (94%); ^{1}H NMR (500 MHz, DMSO-d_6) $\boldsymbol{\delta}$ ppm = 9.31 (s, 1H), 7.85 (s, 1H), 7.77 (s, 1H), 4.21 (t, 2H), 3.87 (s, 3H), 2.52 (t, 2H), 1.83 (pent, 2H), 1.59 (pent, 2H), 1.33 (pent, 2H); ^{13}C NMR (125 MHz, DMSO-d_6) $\boldsymbol{\delta}$ ppm = 136.8, 123.8, 122.5, 120.8, 48.6, 36.0, 28.8, 24.7, 24.3, 16.3; FT-IR ($\boldsymbol{\nu}_{max}$ in cm^{-1}): 3381 (b), 3141 (w), 3060 (m), 2936 (m), 2864 (w), 2242 (w), 1571 (s), 1459 (m), 1426 (m), 1362 (w), 1336 (w), 1167 (s), 1094 (w), 1029 (w), 835 (w), 755 (m), 697 (w).

***1-(6-Cyanohexyl)-3-methylimidazolium bromide* (9[Br]):** Compound **9[Br]** was prepared from **1** (1.483 g, 18 mmol). Amber liquid (92%); ^{1}H NMR (500 MHz, DMSO-d_6) $\boldsymbol{\delta}$ ppm = 9.23 (s, 1H), 7.82 (s, 1H), 7.74 (s, 1H), 4.18 (t, 2H), 3.87 (s, 3H), 2.50 (t, 2H), 1.80 (pent, 2H), 1.55 (pent, 2H), 1.37 (pent, 2H), 1.27 (pent, 2H); ^{13}C NMR (125 MHz, DMSO-d_6) $\boldsymbol{\delta}$ ppm = 137.0, 124.1, 122.7, 121.1, 49.1, 36.2, 29.5, 27.8, 25.1, 24.9, 16.5; FT-IR ($\boldsymbol{\nu}_{max}$ in cm^{-1}): 3417 (b), 3141 (w), 3059 (m), 2934 (m), 2861 (w), 2242 (w), 1731 (w), 1570 (s), 1459 (m), 1426 (m), 1365 (w), 1337 (w), 1297 (w), 1246 (w), 1164 (s), 1088 (w), 1046 (w), 1020 (w), 829 (m), 756 (m), 697 (w).

***1-(1-Cyanoethyl)-3-methylimidazolium bromide* (10[Br]):** Compound **10[Br]** was prepared from **1** (0.615 g, 7.4 mmol). Yellow powder (85%); ^{1}H NMR (500 MHz, DMSO-d_6) $\boldsymbol{\delta}$ ppm 9.53 (s, 1H), 8.12 (s, 1H), 7.79 (s, 1H), 6.17 (q, 1H), 3.90 (s, 3H), 1.90 (d, 3H); ^{13}C NMR (125 MHz, DMSO-d_6) $\boldsymbol{\delta}$ ppm 137.5, 125.1, 121.4, 117.5, 45.7, 36.7, 19.5; FT-IR ($\boldsymbol{\nu}_{max}$ in cm^{-1}): 3172 (w), 3150 (w), 3170 (w), 3043 (s), 3012 (s), 2882 (m), 2847 (w), 2618 (w), 2556 (w), 2249 (w), 1776 (w), 1735 (w), 1654 (w), 1580 (m), 1552 (s), 1448 (m), 1419 (m), 1381 (w), 1324 (w), 1302 (m), 1260 (w), 1182 (s), 1168 (s), 1100 (s), 1020 (m), 989 (w), 892 (w), 863 (s), 843 (m), 768 (s), 717 (m), 674 (w).

***1-Butyl-3-(2-cyanoethyl)imidazolium bromide* (12[Br]):** Compound **12[Br]** was prepared by alkylation of **3** (1.521 g, 12 mmol) with 1-bromobutane (2.125 g, 15 mmol). Yellow solid (86%); ^{1}H NMR (500 MHz, DMSO-d_6) $\boldsymbol{\delta}$ ppm 9.43 (s, 1H), 7.92 (d, 1H), 7.91 (d, 1H), 4.53 (t, 2H), 4.23 (t, 2H), 3.28 (t, 2H), 1.78 (pent, 2H), 1.24 (m, 2H), 0.89 (t, 3H); ^{13}C NMR (125 MHz, DMSO-d_6) $\boldsymbol{\delta}$ ppm 136.4, 122.6, 122.3, 117.5, 48.6, 44.3, 31.1, 18.5, 18.5, 13.1; FT-IR ($\boldsymbol{\nu}_{max}$ in cm^{-1}): 3378 (b), 3134 (w), 3055 (m), 2960 (m), 2935 (m), 2875 (w), 1707 (m), 1640 (w), 1557 (s), 1463 (w), 1421 (w), 1362 (m), 1223 (w), 1160 (s), 1115 (w), 1020 (w), 925 (w), 871 (w), 754 (s), 708 (w).

***1-(3-Cyanopropyl)-3-butylimidazolium chloride* (13[Cl]):** Compound **13[Cl]** was prepared from **2** (4.969 g, 40 mmol). Amber liquid (45%); ^{1}H NMR (500 MHz, DMSO-d_6) $\boldsymbol{\delta}$ ppm 9.44 (s, 1H), 7.87 (s, 1H), 7.85 (s, 1H), 4.28 (t, 2H), 4.17 (t, 2H), 2.61 (t, 2H), 2.15 (pent, 2H), 1.78 (pent, 2H), 1.28 (m, 2H), 0.90 (t, 3H); ^{13}C NMR (125 MHz, DMSO-d_6) $\boldsymbol{\delta}$ ppm 136.3, 122.4, 122.3, 119.5, 48.5, 47.6, 31.1, 25.0, 18.7, 13.4, 13.2; FT-IR ($\boldsymbol{\nu}_{max}$ in cm^{-1}): 3372 (b), 3134 (w), 3049 (m), 2959 (m), 2935 (m), 2873 (w), 2245 (s), 1639 (w), 1561 (s), 1370 (w), 1335 (w), 1163 (s), 1115 (w), 1054 (w), 1021 (w), 949 (w), 852 (m), 753 (m).

***1-(4-Cyanobutyl)-3-butylimidazolium chloride* (14[Cl]):** Compound **14[Cl]** was prepared from **2** (1.870 g, 15 mmol). Amber liquid (97%); ^{1}H NMR (500 MHz, DMSO-d_6) $\boldsymbol{\delta}$ ppm 9.62 (s, 1H), 7.91 (d, 1H), 7.90 (d, 1H), 4.27 (t, 2H), 4.20 (t, 2H), 2.59 (t, 2H), 1.89 (pent, 2H), 1.78 (pent, 2H), 1.53 (pent, 2H), 1.24 (m, 2H), 0.89 (t, 3H); ^{13}C NMR (125 MHz, DMSO-d_6) $\boldsymbol{\delta}$ ppm 136.2, 122.4, 122.3, 120.2, 48.7, 31.1, 28.3, 21.4, 18.6, 15.5, 13.1; FT-IR ($\boldsymbol{\nu}_{max}$ in cm^{-1}): 3372 (b), 3131 (w), 3046 (m), 2957 (s), 2934 (s), 2872 (m), 2242 (w), 1638 (w), 1561 (s), 1458 (s), 1370 (w), 1333 (w), 1259 (w), 1160 (s), 1116 (w), 1050 (w), 1022 (w), 949 (w), 879 (m), 753 (s).

***1-Butyl-3-(1-cyanoethyl)imidazolium bromide* (15[Br]):** Compound **15[Br]** was prepared from **2** (2.755 g, 22 mmol). Amber liquid (87%); ^{1}H NMR (500 MHz, DMSO-d_6) $\boldsymbol{\delta}$ ppm 9.71 (s, 1H), 8.19 (s, 1H), 8.04 (s, 1H), 6.27 (q, 1H), 4.24 (t, 2H), 1.90 (d, 3H), 1.79 (pent, 2H), 1.27 (m, 2H), 0.88 (t, 3H); ^{13}C NMR (125 MHz, DMSO-d_6) $\boldsymbol{\delta}$ ppm 136.4, 123.3, 121.0, 117.0, 48.9, 46.2, 31.0, 18.7, 13.2; FT-IR ($\boldsymbol{\nu}_{max}$ in cm^{-1}): 3126 (w), 3046 (s), 2959 (s), 2934 (s), 2873 (m), 2251 (w), 1691 (w), 1569 (m), 1551 (m), 1458 (m), 1381 (w), 1337 (w), 1315 (w), 1260 (w), 1210 (w), 1165 (s), 1115 (w), 1088 (w), 1021 (w), 983 (w), 948 (w), 842 (w), 752 (m).

***1-(2-Cyanoethyl)-3-cyanomethylimidazolium chloride* (16[Cl]):** Compound **16[Cl]** was obtained from **3** (2.423 g, 20 mmol). White solid (87%); ^{1}H NMR (500 MHz, DMSO-d_6) $\boldsymbol{\delta}$ ppm 7.82 (s, 1H), 4.51 (t, 2H), 3.14 (t, 2H), 2.74 (s, 2H); ^{13}C NMR (125 MHz, DMSO-d_6) $\boldsymbol{\delta}$ ppm 146.0, 122.2, 118.3, 43.6, 18.6, 10.0; FT-IR ($\boldsymbol{\nu}_{max}$ in cm^{-1}): 3327 (s), 3276 (s), 3167 (w), 3140 (w), 3126 (w), 3068 (m), 3036 (s), 2986 (m), 2954 (w), 2855 (w), 2254 (m), 1808 (w), 1693 (w), 1678 (w), 1651 (m), 1574 (w), 1561 (s), 1511 (w), 1449 (m), 1418 (m), 1404 (m), 1367 (w), 1349 (m), 1289 (m), 1238 (w), 1161 (s), 1113 (m), 1051 (w), 1020 (w), 1000 (w), 952 (w), 925 (m), 914 (m), 907 (m), 863 (s), 797 (s), 750 (m), 661 (s).

***1-(3-Cyanopropyl)-3-(2-cyanoethyl)imidazolium chloride* (17[Cl]):** Compound **17[Cl]** was prepared from **3** (1.824 g, 15 mmol). Amber liquid (91%); ^{1}H NMR (500 MHz, DMSO-d_6) $\boldsymbol{\delta}$ ppm 9.59 (s, 1H), 7.97 (s, 1H), 7.95 (s, 1H), 4.55 (t, 2H), 4.33 (t, 2H), 3.28 (t, 2H), 2.62 (t, 2H), 2.16 (pent, 2H); ^{13}C NMR (125 MHz, DMSO-d_6) $\boldsymbol{\delta}$ ppm 137.5, 123.2, 123.1, 120.1, 118.2, 48.3, 44.9, 25.7, 19.1, 14.0; FT-IR ($\boldsymbol{\nu}_{max}$ in cm^{-1}): 3370 (b), 3140 (w), 3058 (m), 2963 (w), 2906 (w), 2845 (w), 2248 (w), 1705 (w), 1638 (w), 1563 (s), 1450 (m), 1420 (m), 1358 (w), 1342 (w), 1229 (w), 1163 (s), 1109 (w), 1076 (w), 1050 (w), 1021 (w), 910 (w), 847 (w), 826 (w), 762 (s).

***1-(4-Cyanobutyl)-3-(2-cyanoethyl)imidazolium chloride* (18[Cl]):** Compound **18[Cl]** was prepared from **3** (2.445 g, 20 mmol). Amber liquid (61%); ^{1}H NMR (500 MHz, DMSO-d_6) $\boldsymbol{\delta}$ ppm 9.20 (s, 1H), 7.81 (s, 1H), 7.73 (s, 1H), 4.17 (t, 2H), 2.51 (t, 2H), 1.80 (pent, 2H), 1.55 (pent, 2H), 1.37 (pent, 2H), 1.27 (pent, 2H); ^{13}C NMR (125 MHz, DMSO-d_6) $\boldsymbol{\delta}$ ppm 137.0, 124.1, 122.7, 121.1, 49.1, 36.2, 29.5, 27.8, 25.1, 16.5; FT-IR ($\boldsymbol{\nu}_{max}$ in cm^{-1}): 3376 (b), 3137 (w), 3054 (m), 2958 (s), 2246 (w), 1639 (w), 1561 (s), 1455 (m), 1423 (m), 1363 (w), 1340 (w), 1236 (w), 1161 (s), 1052 (w), 1033 (w), 914 (w), 871 (w), 828 (w), 759 (s), 660 (w).

***1-(5-Cyanopentyl)-3-(2-cyanoethyl)imidazolium bromide* (19[Br]):** Compound **19[Br]** was prepared from **3** (1.273 g, 10 mmol). Amber liquid (97%); ^{1}H NMR (500 MHz, DMSO-d_6) $\boldsymbol{\delta}$ ppm 9.39 (s, 1H), 7.91 (d, 2H), 4.53 (t, 2H), 4.25 (t, 2H), 3.26 (t, 2H), 2.51 (t, 2H), 1.84 (pent, 2H), 1.59 (pent, 2H), 1.34 (pent, 2H); ^{13}C NMR (125 MHz, DMSO-d_6) $\boldsymbol{\delta}$ ppm 137.0, 123.3, 123.0, 121.0, 118.2, 49.1, 45.0, 28.9, 24.5, 19.2, 16.5; FT-IR ($\boldsymbol{\nu}_{max}$ in cm^{-1}): 3401 (s), 3140 (w), 3078 (m), 2940 (m), 2867 (w), 2246 (w), 1628 (m), 1561 (s), 1509 (w), 1458 (m), 1421 (m), 1363 (w), 1340 (w), 1290 (w), 1234 (w), 1158 (s), 1108 (w), 1083 (w), 1051 (w), 1033 (w), 915 (w), 826 (m), 754 (m), 660 (w).

***1-(6-Cyanohexyl)-3-(2-cyanoethyl)imidazolium bromide* (20[Br]):** Compound **20[Br]** was prepared from **3** (1.067 g, 8.8 mmol). Amber liquid (86%); ^{1}H NMR (500 MHz, DMSO-d_6) $\boldsymbol{\delta}$ ppm 9.36 (s, 1H), 7.89 (d, 2H), 4.52 (t, 2H), 4.23 (t, 2H), 3.25 (t, 2H), 2.51 (t, 2H), 1.81 (pent, 2H), 1.54 (pent, 2H), 1.35 (pent, 2H), 1.26 (pent, 2H); ^{13}C NMR (125 MHz, DMSO-d_6) $\boldsymbol{\delta}$ ppm 137.0, 123.3, 123.0, 121.1, 118.2, 49.4, 44.9, 29.4, 27.8, 25.0, 24.9, 19.2, 16.5; FT-IR ($\boldsymbol{\nu}_{max}$ in cm^{-1}): 3409 (b), 3135 (w), 3058 (m), 2838 (s), 2863 (m), 2244 (w), 1628 (w), 1561 (s), 1455 (s), 1422 (m), 1358 (w), 1340 (w), 1234 (w), 1161 (s), 1107 (w), 1052 (w), 1033 (w), 914 (w), 824 (w), 757 (s), 659 (w).

N-Cyanoalkyl-functionalized imidazolium nitrates (**4-7**, **9-15[NO$_3$]**): ***Preparation of nitrate-form of anion exchange resin:*** Strongly basic anion exchange resin (BioRad AG 1-X8, chloride form) was converted to nitrate form by successive washes of a loaded column (~ 8 cm^3 bed volume) with 1 N sodium nitrate solution. Each eluted fraction was spot-tested with 0.1 M silver nitrate solution to visually indicate when the resin had been fully exchanged (e.g., no silver chloride precipitate formed). Final conditioning of the nitrate resin column included washing with 2 bed volumes of deionized water.

General procedure for the exchange of halides for nitrate anion and product isolation, 4-7, 9-15[NO$_3$]: A solution of *N*-cyanoalkyl imidazolium halide salt (**4-7**, **9-15[X]**) was prepared based upon the calculated 'dry weight' capacity of the resin being used (2.6 meq/g dry resin). All halide salts were eluted as solutions in 100 mL of water though a prepared column of the nitrate anion exchange resin. All collected fractions were spot-tested with 0.1 M silver nitrate solution to confirm the absence of halide (e.g., no precipitate shown) prior to combining and removing water, first by evaporation under air stream and then further drying under high vacuum overnight.

***1-Cyanomethyl-3-methylimidazolium nitrate* (4[NO_3]):** Compound **4[NO_3]** was prepared from **4[Cl]** (1.063 g, 6.5 mmol). White solid (81%); ^{1}H NMR (500 MHz, DMSO-d_6) δ ppm 9.26 (s, 1H), 7.89 (t, 1H), 7.79 (t, 1H), 5.59 (s, 2H), 3.89 (s, 3H); ^{13}C NMR (125 MHz, DMSO-d_6) δ ppm 137.7, 124.3, 122.4, 114.6, 36.7, 36.0; FT-IR (ν_{max} in cm^{-1}): 3431 (b), 3154 (w), 3130 (w), 3088 (m), 3035 (m), 3011 (m), 2966 (w), 1789 (w), 1748 (w), 1662 (w) 1581 (m), 1561 (m), 1472 (w), 1457 (w), 1425 (m), 1413 (m), 1387 (m), 1328 (s), 1275 (s), 1166 (s), 11087 (w), 1090 (w), 1041 (w), 1020 (w), 953 (w), 921 (w), 900 (s), 827 (m), 783 (m), 775 (m), 749 (m), 725 (w) 708 (w), 673 (w).

***1-(2-Cyanoethyl)-3-methylimidazolium nitrate* (5[NO_3]):** Compound **5[NO_3]** was prepared from **5[Br]** (1.281 g, 5.9 mmol). Yellow solid (84%); ^{1}H NMR (500 MHz, DMSO-d_6) δ ppm 9.28 (s, 1H), 7.82 (t, 1H), 7.76 (t, 1H), 3.89 (s, 3H), 3.21 (t, 2H); ^{13}C NMR (125 MHz, DMSO-d_6) δ ppm 137.0, 123.9, 122.2, 117.6, 44.3, 35.8, 18.5; FT-IR (ν_{max} in cm^{-1}): 3156 (w), 3126 (w), 3088 (m), 3040 (m), 2258 (m), 1746 (w), 1664 (w), 1579 (m), 1566 (m), 1450 (w), 1426 (w), 1363 (m), 1332 (s), 1301 (m), 1176 (s), 1084 (w), 1042 (w), 1029 (w), 1016 (w), 943 (w), 888 (m), 877 (m), 827 (m), 775 (s), 748 (m), 706 (w), 657 (m).

***1-(3-Cyanopropyl)-3-methylimidazolium nitrate* (6[NO_3]):** Compound **6[NO_3]** was prepared from **6[Cl]** (1.062 g, 5.7 mmol). Amber liquid (76%); ^{1}H NMR (500 MHz, DMSO-d_6) δ ppm 9.18 (s, 1H), 7.80 (t, 1H), 7.73 (t, 1H), 4.24 (t, 2H), 3.84 (s, 3H), 2.58 (t, 2H), 2.13 (pent, 2H); ^{13}C NMR (125 MHz, DMSO-d_6) δ ppm 136.8, 123.6, 122.2, 119.5, 47.5, 35.6, 25.1, 13.3; FT-IR (ν_{max} in cm^{-1}): 3151 (w), 3101 (m), 2960 (w), 2247 (w), 1745 (w), 1633 (w), 1576 (m), 1566 (m), 1451 (w), 1425 (w), 1327 (s), 1166 (s), 1084 (w), 1024 (w), 847 (w), 830 (m), 756 (m), 699 (w).

***1-(4-Cyanobutyl)-3-methylimidazolium nitrate* (7[NO_3]):** Compound **7[NO_3]** was prepared from **7[Cl]** (0.644 g, 3.2 mmol). Amber liquid (83%); ^{1}H NMR (500 MHz, DMSO-d_6) $\boldsymbol{\delta}$ ppm 9.17 (s, 1H), 7.78 (t, 1H), 7.72 (t, 1H), 4.21 (t, 2H), 3.85 (s, 3H), 2.54 (t, 2H), 1.87 (dt, 2H), 1.54 (dt, 2H); ^{13}C NMR (125 MHz, DMSO-d_6) $\boldsymbol{\delta}$ ppm 136.6, 123.6, 122.1, 120.2, 47.8, 35.6, 28.4, 21.4, 15.5; FT-IR ($\boldsymbol{\nu}_{max}$ in cm^{-1}): 3147 (w), 3100 (w), 2955 (w), 2244 (w), 1744 (w), 1574 (s), 1458 (w), 1426 (w), 1330 (s), 1216 (w), 1163 (w), 1084 (w), 1039 (w), 1024 (w), 854 (w), 830 (m), 754 (m), 698 (w).

***1-(1-Cyanoethyl)-3-methylimidazolium nitrate* (10[NO_3]):** Compound **10[NO_3]** was prepared from **10[Br]** (1.314 g, 6.1 mmol). Yellow solid (95%); ^{1}H NMR (500 MHz, DMSO-d_6) $\boldsymbol{\delta}$ ppm 9.44 (s, 1H), 8.09 (s, 1H), 7.85 (s, 1H), 6.05 (q, 1H), 3.89 (s, 3H), 1.89 (d, 3H); ^{13}C NMR (125 MHz, DMSO-d_6) $\boldsymbol{\delta}$ ppm 137.0, 124.5, 120.8, 116.9, 45.1, 36.0, 18.8; FT-IR ($\boldsymbol{\nu}_{max}$ in cm^{-1}): 3149 (w), 3097 (w), 2951 (w), 1747 (w), 1631 (w), 1581 (m), 1557 (m), 1452 (w), 1330 (s), 1261 (w), 1170 (s), 1090 (m), 1041 (w), 1021 (w), 984 (w), 842 (w), 829 (m) 755 (m), 718 (w).

***1-Butyl-3-cyanomethylimidazolium nitrate* (11[NO_3]):** Compound **11[NO_3]** was prepared from **11[Cl]** (1.336 g, 6.5 mmol). Amber liquid (76%); ^{1}H NMR (500 MHz, DMSO-d_6) $\boldsymbol{\delta}$ ppm 9.39 (s, 1H), 7.93 (t, 1H), 7.91 (t, 1H), 5.61 (s, 2H), 4.22 (t, 2H), 1.77 (pent, 2H), 1.26 (m, 2H), 0.89 (t, 3H); ^{13}C NMR (125 MHz, DMSO-d_6) $\boldsymbol{\delta}$ ppm 137.3, 123.1, 122.7, 114.6, 48.9, 36.8, 31.1, 18.7, 13.2; FT-IR ($\boldsymbol{\nu}_{max}$ in cm^{-1}): 3142 (w), 3100 (w), 2963 (w), 2937 (w), 2875 (w), 2430 (w), 1789 (w), 1560 (w), 1325 (s), 1163 (s), 1115 (m), 1041 (w), 1033 (w), 1021 (w), 926 (w), 832 (s), 754 (m), 708 (w).

***1-Butyl-3-(2-cyanoethyl)imidazolium nitrate* (12[NO_3]):** Compound **12[NO_3]** was prepared from **12[Br]** (1.544 g, 6.0 mmol). Amber liquid (94%); ^{1}H NMR (500 MHz, DMSO-d_6) $\boldsymbol{\delta}$ ppm 9.34 (s, 1H), 7.88 (t, 1H), 7.86 (t, 1H), 4.51 (t, 2H), 4.22 (t, 2H), 3.23 (t, 2H), 1.77

(pent, 2H), 1.26 (m, 2H), 0.88 (t, 3H); ^{13}C NMR (125 MHz, DMSO-d_6) $\boldsymbol{\delta}$ ppm 136.5, 122.8, 122.4, 117.7, 48.7, 44.4, 31.2, 18.6, 18.5, 13.2; FT-IR ($\boldsymbol{\nu}_{max}$ in cm^{-1}): 3140 (w), 3096 (w), 3038 (w), 2962 (w), 2935 (w), 2875 (w), 2252 (w), 1745 (w), 1631 (w), 1563 (m), 1459 (m), 1335 (s), 1163 (s), 1113 (w), 1041 (w), 1023 (w), 949 (w), 914 (w), 854 (w), 829 (w), 754 (w).

1-(3-Cyanopropyl)-3-butylimidazolium nitrate **(13[NO$_3$]):** Compound **13[NO$_3$]** was prepared from **13[Cl]** (1.305, 5.8 mmol). Amber liquid (83%); ^{1}H NMR (500 MHz, DMSO-d_6) $\boldsymbol{\delta}$ ppm 9.28 (s, 1H), 7.83 (s, 1H), 7.82 (s, 1H), 4.26 (t, 2H), 4.17 (t, 2H), 2.59 (t, 2H), 2.15 (pent, 2H), 1.78 (pent, 2H), 1.26 (m, 2H), 0.90 (t, 3H); ^{13}C NMR (125 MHz, DMSO-d_6) $\boldsymbol{\delta}$ ppm 136.3, 122.5, 122.3, 119.5, 48.5, 47.7, 31.1, 25.0, 18.7, 13.3, 13.1; FT-IR ($\boldsymbol{\nu}_{max}$ in cm^{-1}): 3140 (w), 3096 (w), 2961 (w), 2934 (w), 2875 (w), 2246 (w), 1744 (w), 1564 (m), 1459 (w), 1330 (s), 1162 (s), 1114 (w), 1084 (w), 1040 (w), 1026 (w), 949 (w), 852 (w), 830 (w), 753 (m), 708 (w).

1-(4-Cyanobutyl)-3-butylimidazolium nitrate **(14[NO$_3$]):** Compound **14[NO$_3$]** was prepared from **14[Cl]** (1.298 g, 5.4 mmol). Amber liquid (79%); ^{1}H NMR (500 MHz, DMSO-d_6) $\boldsymbol{\delta}$ ppm 9.25 (s, 1H), 7.82 (d, 1H), 7.81 (d, 1H), 4.21 (t, 2H), 4.17 (t, 2H), 2.56 (t, 2H), 1.88 (dt, 2H), 1.79 (dt, 2H), 1.54 (dt, 2H), 1.26 (dt, 2H), 0.90 (t, 3H); ^{13}C NMR (125 MHz, DMSO-d_6) $\boldsymbol{\delta}$ ppm 136.0, 122.4, 122.3, 120.2, 48.5, 47.9, 31.1, 28.3, 21.5, 18.7, 15.5, 13.1; FT-IR ($\boldsymbol{\nu}_{max}$ in cm^{-1}): 3139 (w), 3093 (w), 2961 (w), 2934 (w), 2874 (w), 2244 (w), 1744 (w), 1564 (s), 1459 (m), 1330 (s), 1217 (w), 1160 (s), 1114 (w), 1084 (w), 1039 (w), 1026 (w), 949 (w), 857 (w), 830 (w), 753 (m), 707 (w).

1-Butyl-(1-cyanoethyl)imidazolium nitrate **(15[NO$_3$]):** Compound **15[NO$_3$]** was prepared from **15[Br]** (1.673 g, 6.5 mmol). Amber liquid (89%); ^{1}H NMR (500 MHz, DMSO-d_6) $\boldsymbol{\delta}$ ppm 9.49 (s, 1H), 8.12 (t, 1H), 7.95 (t, 1H), 6.01 (q, 1H), 4.21 (t, 2H), 1.90 (d, 3H), 1.79 (pent, 2H), 1.28 (m, 2H), 0.90 (t, 3H); ^{13}C NMR (125 MHz, DMSO-d_6) $\boldsymbol{\delta}$ ppm 136.4, 123.3,

121.0, 116.9, 49.0, 42.2, 31.0, 18.8, 18.7, 13.1; FT-IR (ν_{max} in cm^{-1}): 3253 (s), 3156 (m), 3118 (m), 3083 (m), 2878 (w), 1754 (w), 1587 (m), 1550 (m), 1470 (s), 1335 (m), 1309 (m), 1280 (m), 1162 (w), 1007 (s), 933 (m), 855 (w), 828 (w), 754 (w), 715 (w), 666 (w).

N-Cyanoalkyl-functionalized imidazolium dicyanamide salts (**4-9**, **16-20[N(CN)$_2$]**): ***General procedure to prepare 4-9, 16-20[N(CN)$_2$]:*** To a tared 100 mL round-bottom flask, halide precursor salts **4-9**, **16-20[X]** (2.8 to 18.7 mmol) were each dissolved in 40 mL deionized water. Silver dicyanamide was prepared by a literature method,[22] where sodium dicyanamide (15.290 g, 161 mmol) was added to an aqueous solution of silver nitrate (24.937 g, 147 mmol) at room temperature, and the mixture was stirred overnight in darkness. The solids were filtered, washed several times with water, and then combined with the filtrate prior to concentrating under air stream overnight and further dried under high vacuum for 24 h. The prepared silver dicyanamide (1.1 eq.) was added at room temperature to an aqueous solution of **4-9**, **16-20[X]** and homogenized using a magnetic Teflon stirbar prior to being brought to 50 ^{o}C in darkness and stirred for 1 h. The resulting yellowish/white solids were filtered and washed several times with water, and then the aqueous filtrate was concentrated under an air stream prior to final drying on high vacuum for 48 h at 60 ^{o}C. In addition to the routine characterization by NMR, FT-IR, TGA, and DSC, all dicyanamide samples were tested for impact and friction sensitivity.

1-Cyanomethyl-3-methylimidazolium dicyanamide **(4[N(CN)$_2$]):** Compound **4[N(CN)$_2$]** was prepared from **4[Cl]** (2.510 g, 16 mmol). White solid (87%); ^{1}H NMR (500 MHz, DMSO-d_6) δ ppm 9.24 (s, 1H), 7.88 (t, 1H), 7.78 (t, 1H), 5.58 (s, 2H), 3.98 (s, 3H); ^{13}C NMR (125 MHz, DMSO-d_6) δ ppm 137.6, 124.2, 122.5, 119.0, 114.6, 36.7, 36.0; FT-IR (ν_{max} in cm^{-1}): 3681 (m), 3493 (w), 3149 (m), 3088 (m), 2953 (s), 2867 (w), 2230 (s), 2195 (m), 2125 (s), 1712 (w), 1612

(w), 1577 (w), 1558 (m) 1419 (w), 1410 (w), 1305 (s), 1218 (w), 1170 (s), 1111 (w), 1055 (m), 1033 (m), 933 (w), 906 (w), 857 (m), 745 (s); Impact sensitivity: > 200 kg·cm.

***1-(2-Cyanoethyl)-3-methylimidazolium dicyanamide* (5[N(CN)$_2$]):** Compound **5[N(CN)$_2$]** was prepared from **5[Br]** (3.591 g, 15 mmol). Amber liquid (74%); ^{1}H NMR (500 MHz, DMSO-d_6) $\boldsymbol{\delta}$ ppm 9.11 (s, 1H), 7.80 (t, 1H), 7.48 (t, 1H), 4.50 (t, 2H), 3.89 (s, 3H) 3.19 (s, 2H); ^{13}C NMR (125 MHz, DMSO-d_6) $\boldsymbol{\delta}$ ppm 136.9, 123.9, 122.2, 119.0, 117.6, 43.3, 35.8, 18.5; FT-IR ($\boldsymbol{\nu}_{max}$ in cm^{-1}): 3681 (m), 3494 (w), 3150 (w), 3108 (m), 2967 (m), 2865 (w), 2229 (s), 2192 (m), 2119 (s), 1577 (m), 1562 (m) 1455 (w), 1420 (w), 1306 (s), 1165 (s), 1108 (w), 1053 (m), 1033 (m), 904 (w), 844 (m), 750 (m); Impact sensitivity: 172 kg·cm.

***1-(3-Cyanopropyl)-3-methylimidazolium dicyanamide* (6[N(CN)$_2$]):** Compound **6[N(CN)$_2$]** was prepared from **6[Cl]** (1.560 g, 7.2 mmol). Amber liquid (93%); ^{1}H NMR (500 MHz, DMSO-d_6) $\boldsymbol{\delta}$ ppm 9.11 (s, 1H), 7.76 (s, 1H), 7.70 (s, 1H), 4.23 (t, 2H), 3.84 (s, 3H), 2.57 (t, 2H), 2.13 (m, 2H); ^{13}C NMR (125 MHz, DMSO-d_6) $\boldsymbol{\delta}$ ppm 136.7, 123.6, 122.2, 119.5, 47.6, 35.7, 25.1, 13.4; FT-IR ($\boldsymbol{\nu}_{max}$ in cm^{-1}): 3681 (m), 3428 (m), 3152 (w), 3108 (w), 3010 (w), 2966 (m), 2866 (w), 2233 (s), 2196 (m), 2125 (s), 1632 (w), 1575 (m), 1565 (m) 1454 (w), 1425 (w), 1309 (s), 1166 (s), 1054 (m), 1033 (m), 1015 (w), 905 (w), 843 (w), 751 (m); Impact sensitivity: 170 kg·cm.

***1-(4-Cyanobutyl)-3-methylimidazolium dicyanamide* (7[N(CN)$_2$]):** Compound **7[N(CN)$_2$]** was prepared from **7[Cl]** (0.563 g, 2.8 mmol). Amber liquid (83%); ^{1}H NMR (500 MHz, DMSO-d_6) $\boldsymbol{\delta}$ ppm 9.10 (s, 1H), 7.76 (t, 1H), 7.71 (t, 1H), 4.20 (t, 2H), 3.85 (s, 3H), 2.55 (q, 2H), 1.87 (m, 2H), 1.55 (m, 2H); ^{13}C NMR (125 MHz, DMSO-d_6) $\boldsymbol{\delta}$ ppm 136.5, 123.6, 122.1, 120.2, 119.0, 47.8, 35.7, 28.4, 21.4, 15.6; FT-IR ($\boldsymbol{\nu}_{max}$ in cm^{-1}): 3681 (m), 3489 (w), 3149 (w), 3104 (w), 3011 (w), 2950 (m), 2867 (w), 2227 (s), 2192 (m), 2125 (s), 1623 (w), 1574 (m), 1456

(w), 1425 (w), 1305 (s), 1163 (s), 1055 (m), 1033 (w), 1017 (w), 903 (w), 842 (w), 749 (m); Impact sensitivity: 170 kg·cm.

***1-(5-Cyanopentyl)-3-methylimidazolium dicyanamide* (8[N(CN)$_2$]):** Compound **8[N(CN)$_2$]** was prepared from **8[Br]** (2.299 g, 8.9 mmol). Amber liquid (84%); ^{1}H NMR (500 MHz, DMSO-d_6) $\boldsymbol{\delta}$ ppm 9.11 (s, 1H), 7.77 (t, 1H), 7.71 (t, 1H), 4.18 (t, 2H), 3.86 (s, 3H), 2.51 (t, 2H), 1.82 (m, 2H), 1.60 (m, 2H), 1.34 (m, 2H); ^{13}C NMR (125 MHz, DMSO-d_6) $\boldsymbol{\delta}$ ppm 136.4, 123.5, 122.1, 120.4, 119.0, 48.3, 35.6, 28.4, 24.4, 23.9, 15.8; FT-IR ($\boldsymbol{\nu}_{max}$ in cm^{-1}): 3681 (w), 3491 (w), 3149 (w), 3104 (w), 3011 (w), 2941 (m), 2866 (w), 2227 (s), 2192 (m), 2125 (s), 1624 (w), 1574 (m), 1460 (w), 1425 (w), 1304 (s), 1168 (s), 1055 (m), 1033 (w), 1017 (w), 903 (w), 841 (w), 751 (m); Impact sensitivity: 170 kg·cm.

***1-(6-Cyanohexyl)-3-methylimidazolium dicyanamide* (9[N(CN)$_2$]):** Compound **9[N(CN)$_2$]** was prepared from **9[Br]** (1.973 g, 7.2 mmol). Amber liquid (87%); ^{1}H NMR (500 MHz, DMSO-d_6) $\boldsymbol{\delta}$ ppm 9.10 (s, 1H), 7.76 (s, 1H), 7.69 (s, 1H), 4.16 (t, 2H), 3.85 (s, 3H), 2.48 (t, 2H), 1.80 (m, 2H), 1.56 (m, 2H), 1.40 (m, 2H), 1.34 (m, 2H); ^{13}C NMR (125 MHz, DMSO-d_6) $\boldsymbol{\delta}$ ppm 136.4, 123.5, 122.1, 120.5, 190.0, 48.6, 35.6, 29.0, 27.3, 24.6, 24.4, 15.9; FT-IR ($\boldsymbol{\nu}_{max}$ in cm^{-1}): 3667 (w), 3490 (w), 3149 (w), 3104 (w), 2938 (m), 2865 (w), 2230 (s), 2194 (m), 2125 (s), 1625 (w), 1573 (m), 1460 (w), 1425 (w), 1308 (s), 1167 (s), 1055 (m), 1033 (w), 903 (w), 842 (w), 753 (m); Impact sensitivity: 170 kg·cm.

***1-(2-Cyanoethyl)-3-cyanomethylimidazolium dicyanamide* (16[N(CN)$_2$]):** Compound **16[N(CN)$_2$]** was prepared from **16[Cl]** (1.487 g, 7.5 mmol). Amber liquid (88%); ^{1}H NMR (500 MHz, DMSO-d_6) $\boldsymbol{\delta}$ ppm 9.38 (s, 1H), 7.96 (t, 1H), 7.91 (t, 1H), 5.63 (s, 2H), 4.56 (t, 2H), 3.21 (s, 2H); ^{13}C NMR (125 MHz, DMSO-d_6) $\boldsymbol{\delta}$ ppm 138.3, 123.7, 123.6, 119.6, 118.1, 115.1, 45.3, 37.6, 19.0; FT-IR ($\boldsymbol{\nu}_{max}$ in cm^{-1}): 3427 (w), 3145 (w), 3114 (w), 3015 (w), 2981 (w), 2233 (s),

2195 (m), 2125 (s), 1692 (w), 1623 (w), 1562 (m), 1457 (w), 1418 (w), 1310 (s), 1233 (w), 1164 (s), 1107 (w), 1080 (w), 1027 (w), 909 (w), 846 (w), 747 (m); Impact sensitivity: 176 kg·cm.

***1-(3-Cyanopropyl)-3-(2-cyanoethyl)imidazolium dicyanamide* (17[N(CN)$_2$]):** Compound **17[N(CN)$_2$]** was prepared from **17[Cl]** (4.823 g, 18 mmol). Amber liquid (92%); ^{1}H NMR (500 MHz, DMSO-d_6) $\boldsymbol{\delta}$ ppm 9.26 (s, 1H), 7.85 (t, 1H), 7.84 (t, 1H), 4.50 (t, 2H), 4.29 (t, 2H), 3.19 (t, 2H), 2.58 (t, 2H), 2.15 (m, 2H); ^{13}C NMR (125 MHz, DMSO-d_6) $\boldsymbol{\delta}$ ppm 136.7, 122.7, 122.5, 119.4, 119.0, 117.6, 47.8, 44.4, 25.1, 18.5, 13.4; FT-IR ($\boldsymbol{\nu}_{max}$ in cm^{-1}): 3491 (w), 3144 (w), 3108 (w), 3015 (w), 2967 (w), 2229 (s), 2193 (m), 2125 (s), 1624 (w), 1564 (m), 1504 (w), 1452 (w), 1420 (w), 1306 (s), 1233 (w), 1161 (s), 1108 (w), 1079 (w), 1047 (w), 1023 (w), 906 (w), 844 (w), 750 (m); Impact sensitivity: 176 kg·cm.

***1-(4-Cyanobutyl)-3-(2-cyanoethyl)imidazolium dicyanamide* (18[N(CN)$_2$]):** Compound **18[N(CN)$_2$]** was prepared from **18[Cl]** (1.541 g, 6.0 mmol). Amber liquid (91%); ^{1}H NMR (500 MHz, DMSO-d_6) $\boldsymbol{\delta}$ ppm 9.25 (s, 1H), 7.84 (s, 2H), 4.50 (t, 2H), 4.26 (t, 2H), 3.20 (t, 2H), 2.55 (t, 2H), 1.89 (m, 2H), 1.55 (m, 2H); ^{13}C NMR (125 MHz, DMSO-d_6) $\boldsymbol{\delta}$ ppm 136.5, 122.7, 122.5, 120.2. 119.0, 117.6, 48.1, 44.4, 28.4, 21.4, 18.5, 15.6; FT-IR ($\boldsymbol{\nu}_{max}$ in cm^{-1}): 3697 (w), 3665 (w), 3488 (w), 3144 (w), 2981 (m), 2939 (m), 2923 (m), 2866 (m), 2844 (m), 2233 (s), 2195 (m), 2125 (s), 1631 (w), 1563 (m), 1509 (w), 1455 (w), 1420 (w), 1310 (s), 1239 (w), 1159 (s), 1107 (w), 1055 (s), 1033 (s), 1016 (s), 908 (w), 827 (w), 748 (m); Impact sensitivity: 174 kg·cm.

***1-(5-Cyanopentyl)-3-(2-cyanoethyl)imidazolium dicyanamide* (19[N(CN)$_2$]):** Compound **19[N(CN)$_2$]** was prepared from **19[Br]** (2.247 g, 7.6 mmol). Amber liquid (85%); ^{1}H NMR (500 MHz, DMSO-d_6) $\boldsymbol{\delta}$ ppm 9.26 (s, 1H), 7.85(s, 2H), 4.50 (t, 2H), 4.24 (t, 2H), 3.21 (t, 2H), 2.49 (t, 2H), 1.84 (m, 2H), 1.60 (m, 2H), 1.36 (m, 2H); ^{13}C NMR (125 MHz, DMSO-d_6) $\boldsymbol{\delta}$ ppm 136.4, 122.7, 122.4, 120.4, 119.0, 117.6, 48.5, 28.4, 24.4, 23.9, 18.6, 15.9; FT-IR ($\boldsymbol{\nu}_{max}$ in cm^{-1}): 3707

(w), 3681 (w), 3488 (w), 3144 (w), 2981 (m), 2967 (m), 2939 (m), 2866 (m), 2844 (m), 2229 (s), 2193 (m), 2125 (s), 1563 (m), 1509 (w), 1455 (w), 1420 (w), 1345 (m), 1308 (s), 1160 (s), 1055 (s), 1033 (s), 1016 (s), 906 (w), 826 (w), 749 (m); Impact sensitivity: 174 kg·cm.

1-(6-Cyanohexyl)-3-(2-cyanoethyl)imidazolium dicyanamide **(20[N(CN)$_2$]):** Compound **20[N(CN)$_2$]** was prepared from **20[Br]** (1.401 g, 4.5 mmol). Amber liquid (85%); ^{1}H NMR (500 MHz, DMSO-d_6) $\boldsymbol{\delta}$ ppm 9.25 (s, 1H), 7.85(q, 2H), 4.49 (t, 2H), 4.21 (t, 2H), 3.21 (t, 2H), 2.49 (t, 2H), 1.80 (m, 2H), 1.54 (m, 2H), 1.36 (m, 2H), 1.22 (m, 2H); ^{13}C NMR (125 MHz, DMSO-d_6) $\boldsymbol{\delta}$ ppm 136.4, 122.7, 122.4, 120.5, 119.0, 117.6, 48.8, 44.4, 28.9, 27.2, 24.5, 24.3, 18.6, 15.9; FT-IR ($\boldsymbol{\nu}_{max}$ in cm^{-1}): 3697 (w), 3681 (w), 3489 (w), 3144 (w), 2966 (m), 2939 (m), 2866 (m), 2844 (m), 2231 (s), 2194 (m), 2125 (s), 1624 (w), 1563 (m), 1508 (w), 1455 (w), 1421 (w), 1308 (s), 1162 (s), 1055 (s), 1033 (s), 1017 (s), 906 (w), 825 (w), 752 (m); Impact sensitivity: 170 kg·cm.

Acknowledgements

This research was supported by the Air Force Office of Scientific Research (Grant FA9550-10-1-0521).

References

1 Klapötke, T. M.; Holl, G. *Green Chem.* **2001**, *3*, G75.

2 Wasserscheid, P.; Keim, W. *Angew. Chem., Int. Ed.* **2000**, *39*, 3772.

3 Tishkoff, J. M.; Berman, M. R. *40th AIAA Aerospace Sciences Meeting & Exhibit*, Reno, NV, 2002.

4 Drake, G. W.; Hawkins, T.; Brand, A.; Hall, L.; Mckay, M.; Vij, A.; Ismail, I. *Propellants, Explos., Pyrotech.* **2003**, *28*, 174.

5 Singh, R. P.; Verma, R. D.; Meshri, D. T.; Shreeve, J. M. *Angew. Chem., Int. Ed.* **2006**, *45*, 3584.

6 Steinhauser. G.; Klapötke, T. M. *Angew. Chem., Int. Ed.* **2008**, *47*, 3330.

7 Trohalaki, S.; Pachter, R.; Drake, G. W.; Hawkins, T. *Energy Fuels* **2005**, *19*, 279.

8 Ye, C.; Shreeve, J. M. *J. Phys. Chem. A* **2007**, *111*, 1456.

9 Galvez-Ruiz, J. C.; Holl, G.; Karaghiosoff, K.; Klapötke, T. M.; Loehnwitz, K.; Mayer, P.; Noeth, H.; Polborn, K.; Rohbogner, C. J.; Suter, M.; Weigand, J. J. *Inorg. Chem.* **2005**, *44*, 4237.

10 Schmidt, M. W.; Gordon, M. S.; Boatz, J. A. *J. Phys. Chem. A* **2005**, *109*, 7285.

11 Pagoria, P. F.; Lee, G. S.; Mitchell, A. R.; Schmidt, R. D. *Thermochim. Acta* **2002**, *384*, 187.

12 Date, S.; Itadzu, N.; Sugiyama, T.; Miyata, Y.; Iwakuma, K.; Abe, M.; Yoshitake, K.; Nishi, S.; Hasue, K. *Sci. Technol. Ener. Mater.* **2009**, *70*, 152.

13 Schneider, S.; Hawkins, T.; Rosander, M.; Vaghjiani, G.; Chambreau, S.; Drake, G. *Energy Fuels* **2008**, *22*, 2871.

14 Zhang, Y.; Gao, H.; Guo, Y.; Joo, Y. –H.; Shreeve, J. M. *Chem. –Eur. J.* **2010**, *16*, 3114.

15 Katritzky, A. R.; Singh, S.; Kirichenko, K.; Holbrey, J. D.; Smiglak, M.; Reichert, W. M.; Rogers, R. D. *Chem. Commun.* **2005**, 868.

16 Katritzky, A. R.; Yang, H.; Zhang, D.; Kirichenko, K.; Smiglak, M.; Holbrey, J. D.; Reichert, W. M.; Rogers, R. D. *New J. Chem.* **2006**, *3*, 349.

17 Smiglak, M.; Bridges, N. J.; Dilip, M.; Rogers, R. D. *Chem. –Eur. J.* **2008**, *36*, 11314.

18 Gao, Y.; Gao, H.; Piekarski, C.; Shreeve, J. M. *Eur. J. Inorg. Chem.* **2007**, 4965.

19 Zhao, D. B.; Fei, Z. F.; Scopelliti, R.; Dyson, P. J. *Inorg. Chem.* **2004**, *43,* 2197.

20 Zhang, Q.; Li, Z.; Zhang, J.; Zhang, S.; Zhu, L.; Yang, J.; Zhang, X.; Deng, Y. *J. Phys. Chem. B* **2007**, *111,* 2864.

21 Fu, S. –K.; Liu, S. –T. *Synth. Commun.* **2006**, *36*, 2059.

22 Mazille, F.; Fei, Z.; Kuang, D.; Zhao, D.; Zakeeruddin, S. M.; Grätzel, M.; Dyson, P. J. *Inorg. Chem.* **2006**, *45*, 1585.

23 Huddleston, J. G.; Visser, A. E.; Reichert, W. M.; Willauer, H. D.; Broker, G. A.; Rogers, R. D. *Green Chem.* **2001**, *3*, 156.

24 Holbrey, J. D.; Seddon, K. R. *J. Chem. Soc., Dalton Trans.* **1999**, 2133.

25 Oommen, C.; Jain, S. R. *J. Haz. Mater.* **1999**, *67*, 253.

26 MacFarlane, D. R.; Golding, J.; Forsyth, S.; Forsyth, M.; Deacon, G. B. *Chem. Commun.* **2001**, 1430.

27 Drab, D. M.; Shamshina, J. L.; Smiglak, M.; Hines, C. C.; Cordes, D. B.; Rogers, R. D. *Chem. Commun.* **2010**, *46*, 3544.

28 Horvath, A. *Synthesis* **1994**, *1*, 102.

29 Olivier-Bourbigou, H.; Favre, F. In *Ionic Liquids in Synthesis,* P. Wasserscheid, T. Welton, Eds.; Wiley-VCH: New York, 2008; 2nd edn., pp 490-491.

30 Hitchcock, P. B.; Seddon, K. R.; Welton, T. *J. Chem. Soc., Dalton Trans.* **1993**, 2639.

31 Herrmann, W. A.; Goossen, L. J.; Spiegler, M. *Organometallics* **1998**, *17*, 2162.

32 Tao, G.; Zou, M.; Wang, X.; Chen, Z.; Evans, D. G.; Kou, Y. *Aust. J. Chem.* **2005**, *58*, 327.

33 Gong, S. –M.; Ma, H. –Y.; Wan, X. –H.; Zhao, Y. –F.; He, J. –Y.; Zhou, Q. –F. *Gaodeng Xuexiao Huaxue Xuebao* **2006**, *27*, 761.

34 *AG 1, AG MP-1, and AG 2 Strong Anion Exchange Resin: Instruction Manual*, BioRad Laboratories: Hercules, CA (LIT212 Rev C; accessed online August 17, 2010; http://www.biorad.com/webroot/web/pdf/lsr/literature/ 9114_AG_1.pdf).

35 Dinares, I.; Garcia de Miguel, C.; Ibanez, A.; Mesquida, N.; Alcalde, E. *Green Chem.* **2009**, *11*, 1507.

36 Gathergood, N.; Garcia, M. T.; Scammells, P. J. *Green Chem.* **2004**, *6*, 166.

37 Clare, B.; Sirwardana, A.; MacFarlane, D. R. *Top. Curr. Chem.* **2009**, *290*, 1.

38 Drake, G. W.; Tollison, K.; Hall, L.; Hawkins, T. In *Ionic Liquids III: Fundamentals, Progress, Challenges, and Opportunities*, R. D. Rogers, K. R. Seddon, Eds.; American Chemical Society: Washington, DC, 2005.

39 Lotsch, B. V.; Schnick, W. *Chem. Mater.* **2005**, *17*, 3976.

40 Svehla, G. *Vogel's Qualitative Inorganic Analysis (6th edition)*; Longman Scientific & Technical: Essex, UK, 1987; pp 174-178.

41 Toral, A. R.; de los Ríos, A. P.; Hernández, F. J.; Janssen, M. H. A.; Schoevaart, R.; van Rantwijk, F.; Sheldon, R. A. *Enzyme Microb. Technol.* **2007,** *40*, 1095.

42 Zhao, H.; Baker, G. A.; Song, Z.; Olubajo, O.; Zanders, L.; Campbell, S. M. *J. Mol. Catal., B* **2009**, *57*, 149.

43 Seeber, A. J.; Forsyth, M.; Forsyth, C. M.; Forsyth, S. A.; Annat, G.; MacFarlane, D. R. *Phys. Chem. Chem. Phys.* **2003**, *5*, 2692.

44 Endo, T.; Nishikawa, K. *J. Phys. Chem. A* **2008**, *112*, 7543.

45 Fredlake, C. P.; Crosthwaite, J. M.; Hert, D. G.; Aki, S. N. V. K.; Brennecke, J. F. *J. Chem. Eng. Data* **2004**, *49,* 954.

46 Wooster, T. J.; Johanson, K. M.; Fraser, K. J.; MacFarlane, D. R.; Scott, J. L. *Green Chem.* **2006**, *8*, 691.

47 Krossing, I.; Slattery, J. M.; Daguenet, C.; Dyson, P. J.; Oleinikova, A.; Weingartner, H. *J. Am. Chem. Soc.* **2006**, *128*, 13427.

48 Smiglak, M. Ph.D. Dissertation, The University of Alabama, 2007.

49 Jayaraman, S.; Maginn, E. J. *J. Chem. Phys.* **2007**, *127*, 214504.

50 Nishikawa, K.; Wang, S.; Katayanagi, H.; Hayashi, S.; Hamaguchi, H.; Koga, Y.; Tozaki, K. *J. Phys. Chem. B* **2007**, *111*, 4894.

51 MacFarlane, D. R.; Huang, J.; Forsyth, M. *Nature* **1999**, *402*, 792.

52 Pringle, J. M.; Adebahr, J.; MacFarlane, D. R.; Forsyth, M. *Phys. Chem. Chem. Phys.* **2010**, *12*, 7234.

53 Lungwitz, R.; Spange, S. *New J. Chem.* **2008**, *32*, 392.

54 Izgorodia, E. I.; Forsyth, M.; MacFarlane, D. R. *Aust. J. Chem.* **2007**, *60*, 15.

55 Kun, D.; Suojiang, Z.; Daxi, W.; Xiaoqian, Y. *J. Phys. Chem. A* **2006**, *110,* 9775.

56 Endres, F.; Abedinw, S. Z. *Phys. Chem. Chem. Phys.* **2006**, *8*, 2101.

57 Chambreau, S. D.; Schneider, S.; Rosander, M.; Hawkins, T.; Gallegos, C. J.; Pastewait, M. F.; Vaghjiani, G. L. *J. Phys. Chem. A* **2008**, *112*, 7816.

58 Klapötke, T. M.; Stierstorfer, J. *Dalton Trans.* **2009**, 643.

59 Kuhn, P.; Forget, A.; Su, D.; Thomas, A.; Antonietti, M. *J. Am. Chem. Soc.* **2008**, *130*, 13333.

60 Lee, J. S.; Wang, X.; Luo, H.; Baker, G. A.; Dai, S. *J. Am. Chem. Soc.* **2009**, *131*, 4596.

61 Irran, E.; Jürgens, B. J.; Schnick, W. *Chem.– Eur. J.* **2001**, *7*, 5372.

62 Schnick, W. *J. Am. Chem. Soc.* **2003**, *125*, 10288.

63 Keshavarz, M. H.; Pouretedal, H. R. *J. Haz. Mater.* **2005**, *A124*, 27.

64 Test methods according to the *UN Recommendations on the Transport of Dangerous Goods*, Test 3, 3rd Edn., United Nations, New York and Geneva, 1999.

65 Data Bulletin # 61770: *Technoproducts Drop-Weight Tester Procedure for Testing Solids*, Technoproducts, Inc., Saratoga, CA.

66 Sheldrick, G. M. In *SHELXTL* version 5.05, Siemens Analytical X-ray Instruments, Inc., 1996.

67 Sheldrick, G. M. In *Program for Semiempirical Absorption Correction of Area Detector Data*, University of Göttingen, Germany, 1996.

68 MacFarlane, D. R.; Forsyth, S. A.; Golding, J.; Deacon, G. B. *Green Chem.* **2002**, *4*, 444.

CHAPTER 3

A GENERAL DESIGN PLATFORM FOR IONIC LIQUID IONS BASED ON BRIDGED MULTI-HETEROCYCLES WITH FLEXIBLE SYMMETRY AND CHARGE

Taken in part from a published manuscript: Drab, D. M.; Shamshina, J. L.; Smiglak, M.; Hines, C. C.; Cordes, D. B.; Rogers, R. D. *Chem. Commun.* **2010**, *46*, 3544.

Acknowledgements: J. L. Shamshina and M. Smiglak (The University of Alabama, Tuscloosa, AL) assisted with data collection and synthesis of tri-heterocyclic MHILs. C. C. Hines (The University of Alabama, Tuscaloosa, AL) collected and refined the X-ray diffraction data reported here.

Abstract

A conceptual design platform for new ionic liquids with variable heterocycles, bridges, symmetry, and charge was developed using simple alkylation, click, and ionic liquid chemistries and demonstrated with 1-(2-(5-tetrazolidyl)ethyl)-3-(5-1*H*-tetrazolyl)methylimidazolium and its conversion into room-temperature cationic or anionic ionic liquids.

Ionic Liquids (ILs, salts that exhibit melting points at or below 100 ^{o}C[1]) have been identified as attractive candidates for new and improved propellants[2,3] and explosives[4,5] due to several features ideal for energetic materials (EMs) such as low vapor pressures, broad liquid ranges, low melting points, reduced sensitivities to impact, and frequently high heats of formation and temperatures of decomposition. Perhaps more importantly, the unique dual-functional nature of ILs permits the independent modification of structure of either ion, allowing

both targeting of optimal performance and reduction of materials hazards in the final product with minimal or no covalent modifications.[6]

While others have been pursuing new examples of ILs that are energetic,[4,5,7] where the primary driver for the synthesis of these materials has been to include energetic ions with targeted physical properties, it has been our interest to understand the underlying science behind how proper combinations of performance and physicochemical characteristics might be incorporated into energetic ILs.[8-11] We have not tried to make energetic materials *per se*, but to understand the influence of added energetic components on IL behavior, and thus we have investigated structural modifications that afford predictable changes in both the properties and reactivity of the final materials,[12] while at the same time exploring new ion platforms and improved synthetic routes to them.[13]

The relationships between materials properties and structure of ILs have been extensively researched and reviewed,[14,15] and for nitrogen heterocycles includes changes in the length of alkyl substituent on azolium ions to result in predictable viscosity, melting point, hydrophilicity-hydrophobicity, and density;[16,17] variations in the size and shape of the ions; total ion charge; and charge distribution.[18,19] Several "rules-of-thumb" have been imported from more generalized IL research, resulting in the push to include ions with low, delocalized charge and asymmetry.

Nonetheless, the research to-date in introducing *multi-heterocyclic ions* has primarily focused on the synthesis of 'bolo'-type ILs that featured <u>symmetric</u> heterocycles bridged by either alkyl or ether linkages and with a formal charge on each head group.[20-22] Shreeve and coworkers, however, have reported both non-bridged[23] and bridged tetrazole-functionalized bi-heterocycles from *in situ* generation and reaction of cyanogenazide,[24] and Armstrong, *et al.* have also reported the synthesis of asymmetric alkyl-bridged ammonium-heterocyclic dications.[25] In

most cases, the introduction of an additional heterocycle resulted in an increase in the overall charge as well as increased melting points and viscosity.

We were interested in developing a generalized synthetic platform that would allow us to construct *singly-charged* multi-heterocycle cations and anions with design flexibility in (i) the identity and/or number of incorporated heterocycles, (ii) their charges, (iii) bridging units (e.g., alkylene, alkylene ethers, *etc.*), and (iv) type and length of substituents appended to each heterocyclic core. Such a degree of synthetic flexibility would provide a systematic approach to control symmetry, charge, and structure in the final product, while at the same time increasing the number of energetic azole cores per cation or anion. Such a strategy might be considered as intermediate between the well-studied single-azole ion ILs[5] and solid state energetic polymers that utilize azole building blocks;[26] thus allowing multiple azole design while retaining the properties of a liquid.

To address this challenge, we propose a systematic and versatile multi-heterocyclic synthetic platform combining a) classic alkylation reactions, b) click chemistry, and c) IL strategies (Figure 3.1) to obtain highly variable anions, cations, and zwitterions for potential application as novel energetic ILs. Such a generalized approach allows (i) simple formation of functionalized azoles capable of further cyclization, (ii) facile cyclization of functionalized azoles to form bridged multi-heterocyclic compounds, and (iii) utilization of IL-based strategies to access zwitterions, neutral molecules, anions, and cations from common multi-heterocyclic precursors. Here we illustrate the utility of this approach with the synthesis and characterization of bicyclic and tricyclic precursors and their use in the formation of ILs.

The overall design strategy begins (Step A, Figure 3.1) with selection of a starting azole core (Az) which is alkylated one or more times with one or more alkylating agents containing a

"clickable" unit (RX and/or R′X, where X = cyano, azo, *etc.*). Although the core heterocycle could itself be formed *via* click chemistry – a general class of 3+2 dipolar cycloaddition reactions that occur with fast reaction times, mild conditions, and good to excellent yields[27] – we have chosen to start the discussion of our platform approach from the point where most IL researchers entered the field; by alkylation of an azole core. The number of alkylations corresponds to the number of desired heterocycles to be appended to the core. The alkyl group (R) in the alkylating agent determines the length and nature of the bridges between the heterocycles, and the clickable reagent (X) determines the identity of the appended heterocyles after 'clicking' (Step B Figure 3.1).

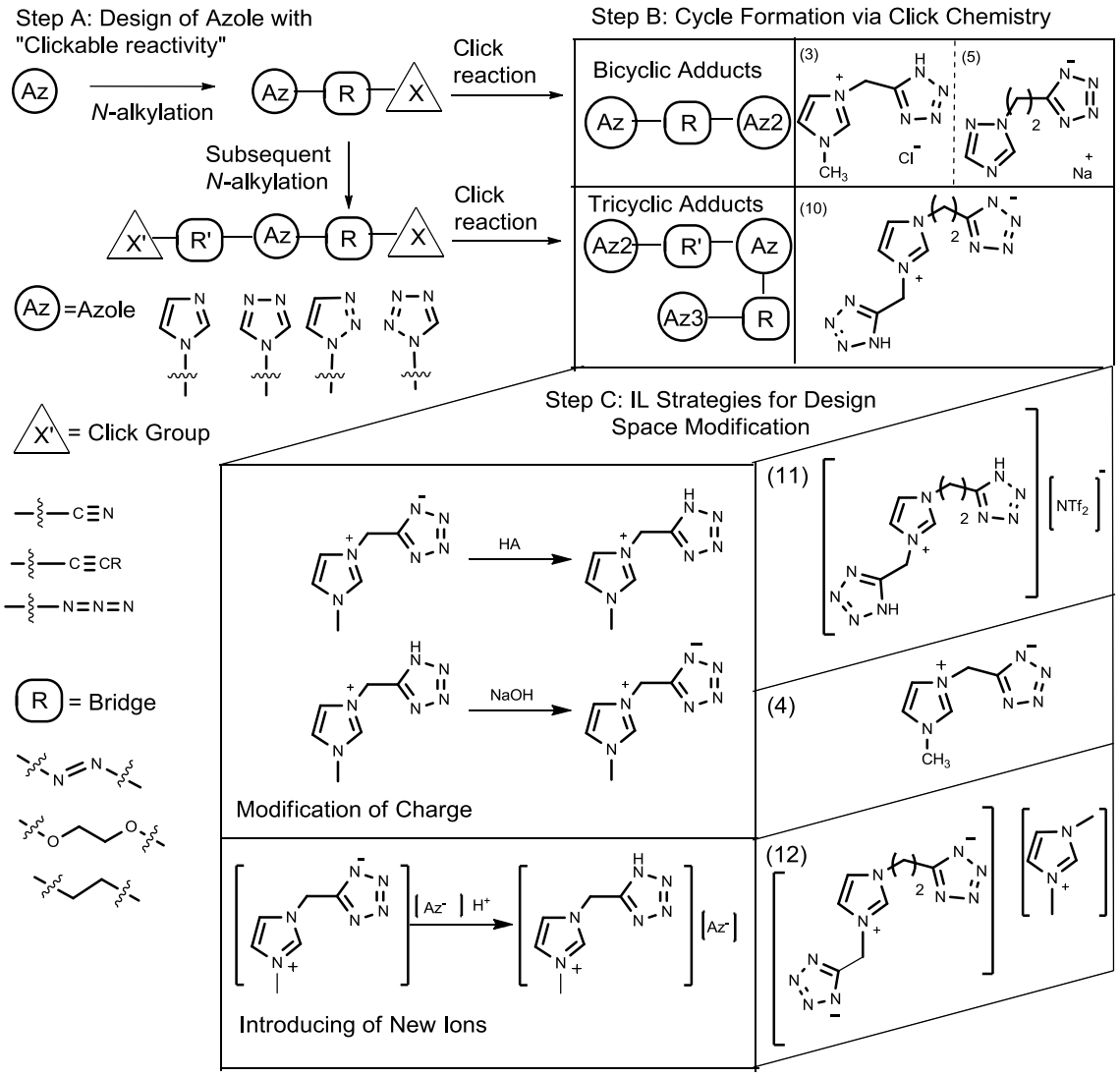

Figure 3.1. A flexible platform for the synthesis of multi-heterocyclic targets and their utilization within IL-based design strategies. Numbered compounds have been prepared in this study.

Step C implements IL-based strategies to obtain the final products. For example, the overall *charge* may be altered through simple protonation/deprotonation, alkylation, *etc.*, resulting in anionic, cationic, zwitterionic, or even neutral products. Additional modification (e.g., alkylation/acylation) of the new heterocyclic cores can introduce new functionalities to tune the final properties of the product or introduce new reactive sites for additional synthetic (e.g., click) operations.

We began our investigations with the simplest example of the design approach, a bicyclic system prepared as in Scheme 3.1. 1-Methylimidazole was alkylated neat with a slight excess of chloroacetonitrile using a literature protocol to prepare 1-cyanomethyl-3-methylimidazolium chloride (**1**).[28] Reaction of **1** with sodium azide and zinc bromide provided the desired bicyclic core in the form of the Zn-coordinated 1-(5-tetrazolidyl)methyl-3-methylimidazolium•(ZnBrCl) (**2**).[27] Fast formation of **2** (greater than 85% conversion within 2 h, estimated by ^{1}H NMR data) was achieved under mild aqueous conditions at room temperature, suggesting preferable conditions for scale-up, as the solid product **2** readily precipitated from the reaction mixture and was characterized by single-crystal X-ray diffraction.

Removal of Zn metal was achieved by a preparatory-scale adaptation of a literature procedure[29] utilizing a strongly basic anion exchange resin (Bio-Rad AG1-X8 in Cl^- form) under high chloride concentration (9 N HCl) to afford the protonated chloride salt **3** (crystallographically confirmed) in 71% yield. Final treatment of **3** with the OH^- form of the same exchange resin resulted in the free zwitterion **4** that was isolated in 75% yield upon filtration of the resin and removal of water.

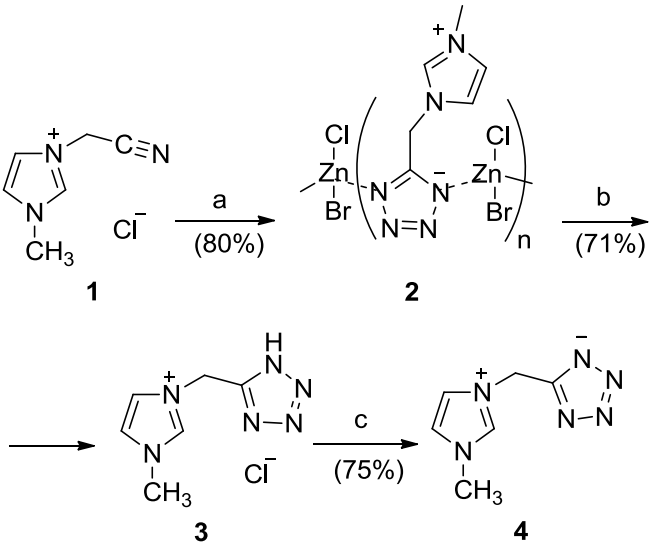

Scheme 3.1. Synthesis of imidazole-tetrazole bicyclic targets: (a) NaN_3 (1.1 eq.), $ZnBr_2$, water (24 h, RT); (b) BioRad AG 1-X8 (Cl^- form) in 9 N HCl; (c) BioRad AG 1-X8 (OH^- form). **1** was prepared by a solvent-free, RT modification of a literature procedure.[30]

To demonstrate the anionic case proposed in Scheme 3.2, we started with 1,2,4-triazole (**5**) and prepared 1-(2-cyanoethyl)-1,2,4-triazole (**6**) by reaction with acrylonitrile with heating in toluene at 70 ^oC. Treatment of **6** with NaN_3, in the presence of AcOH offered colorless crystals of sodium 5-(2-(1,2,4-triazol-1-yl)ethyl)tetrazolate (**7**) in a single step. The structure of **7** was confirmed crystallographically.

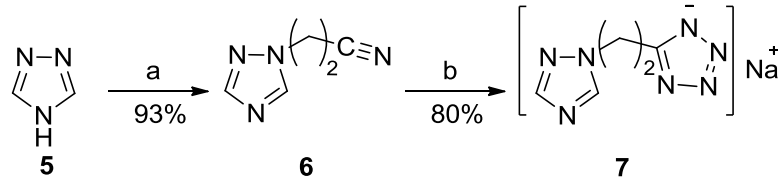

Scheme 3.2. Synthesis of sodium 5-(2-(1,2,4-triazol-1-yl)ethyl)tetrazolate, **7**, from neutral 1-(2-cyanoethyl)-1,2,4-triazole, **6**: (a) acrylonitrile (1 eq.), Et_3N (cat.), toluene, reflux, 30 h; (b) NaN_3 (1.1 eq.), AcOH, 60-70 ^oC, 24 h.

In order to more fully demonstrate the scope and versatility of the proposed platform, we designed and prepared the triheterocyclic system (Scheme 3.3) to demonstrate possible incorporation of (i) asymmetric alkyl units bridging each heterocycle and (ii) tunable charge from cationic, zwitterionic, to anionic in the same molecule. The cationic 1-(2-cyanoethyl)-3-(1-

cyanomethyl)imidazolium chloride (**9**) was prepared by a sequence of alkylation reactions including reaction of 1*H*-imidazole (**8**) with acrylonitrile under base-catalyzed conditions to result in the *in situ* formation of 1-(2-cyanoethyl)imidazole and further alkylation with chloroacetonitrile to form **9**. Next, reaction of **9** with 2.2 eq. of NaN_3 under weakly acidic conditions (AcOH) afforded the tricyclic zwitterionic 1-(2-(5-tetrazolidyl)ethyl)-3-(5-1*H*-tetrazolyl)methylimidazolium (**10)**, in a single step.

The ready isolation of zwitterion **10** in good yield and purity *via* crystallization allowed us to easily prepare two ILs from this precursor with synthetic operations we normally use to prepare ILs. The protonation of **10** with hydrogen bis(trifluoromethanylsulfonyl)amide resulted in quantitative formation of 1-(2-(5-1*H*-tetrazolyl)ethyl)-3-(5-1*H*-tetrazolyl)methylimidazolium bis(trifluoromethanylsulfonyl)amide (**11**). Deprotonation of **10** was realized by reaction with l,3-dimethylimidazolium-2-carboxylate (as described in procedures published by our group[13]) leading to 1,3-dimethylimidazolium 1-(2-(5-tetrazolidyl)ethyl)-3-(5-tetrazolidyl)methylimidazolium (**12**) in quantitative yield in a single step. Each of the salts derived from the parent zwitterion were liquid at RT ($\boldsymbol{T}_m$ = 10.5 ^oC and -25.4 ^oC for **11** and **12**, respectively), thereby demonstrating how one may selectively obtain either cationic or anionic ILs from a common zwitterionic precursor utilizing known IL-based strategies.

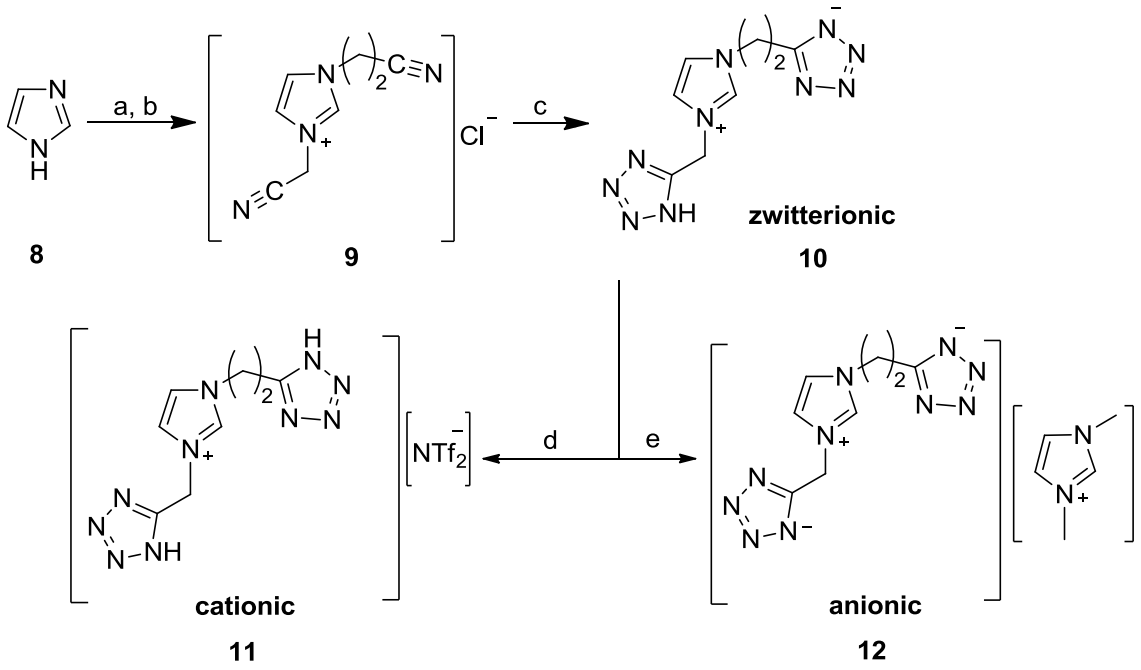

Scheme 3.3. Top: Synthesis of zwitterionic **10** from **8**: (a) acrylonitrile (1 eq.), Et_3N (cat.), toluene, reflux, 30 h; (b) chloroacetonitrile, 70 °C, (c) NaN_3 (2.2 eq.), AcOH, 70 °C, 24 h. Bottom: Synthesis of **11** and **12** from zwitterionic **10**: (d) hydrogen bis(trifluoromethanylsulfonyl)amide ($HNTf_2$), MeOH/water 1/1, RT; (e) 1,3-dimethylimidazolium-2-carboxylate, MeOH/water 1/1, DMSO (cat.), RT, 6 h.

Conclusions

The design strategy for a systematic and versatile multi-heterocyclic synthetic platform allows for the formation of highly variable anions, cations, and zwitterions for potential application as novel IL components or precursors. We believe that the ability to extend the number, identity, and bridging of heterocycles, especially to *asymmetric, singly-charged molecular ions* will be a more useful strategy to make ILs than any of the known oligomeric approaches to multi-heterocyclic IL ions. We have demonstrated this here with low-valent bridged bi- and tricyclic compounds, including the synthesis of the crystalline zwitterion 1-(2-(5-tetrazolidyl)ethyl)-3-(5-1*H*-tetrazolyl)methylimidazolium and its conversion into room temperature ionic liquids as either the cation or the anion. Given the richness of this design space – from available multi-heterocyclic precursors to the diversity enabled by IL-based

modifications – we foresee this platform as a powerful tool that may be utilized towards new multi-heterocyclic IL targets of yet unlimited scope.

Experimental Section

Materials and Methods:

Commercial reagents were used directly as obtained from commercial sources (Aldrich) unless otherwise noted. All solvents were 'solvent grade' and were used as received without additional purification. BioRad AG 1-X8 strongly basic anion exchange resin was prepared according to manufacturer's specifications.

Single-crystal X-ray diffraction data were collected on a Bruker CCD area detector-equipped diffractometer (Madison, WI) with graphite-monochromated Mo-*K*α radiation (λ = 0.71073 Å). The crystals of **2**, **3**, **7**, and **8** were cooled to -100 ^{o}C with a stream of nitrogen gas, whereas the crystal of **4** was air stable and analysis was performed at room temperature. SHELXTL-5 software was used for structure solution and refinement.[31] Each structure was refined by using full-matrix least-squares methods on F^2. All atoms were readily located and the positions of all non-hydrogen atoms were refined anisotropically, where all hydrogens were located in calculated positions riding on the bonded atom.

Melting point/glass transition analyses were performed by Differential Scanning Calorimetry (DSC) using a DSC 2920 Modulated DSC, TA Instruments, Inc. (New Castle, DE) cooled with a liquid nitrogen cryostat. The calorimeter was calibrated for temperature and cell constants using indium (melting point 156.61 ^{o}C; C = 28.71 J g^{-1}). Data were collected at constant atmospheric pressure, with heating at a rate of 5 ^{o}C min^{-1} using samples between 5-15 mg in aluminum sample pans (sealed then perforated with a pin-hole to equilibrate pressure from

potential expansion of evolved gases). The DSC was adjusted so that zero heat flow was between 0 and -0.5 mW, and the baseline drift was less than 0.1 mW over the temperature range of 0-180 ^{o}C. An empty sample pan served as the reference.

Thermogravimetric analysis (TGA) was performed using a TGA 2950, TA Instruments, Inc. (New Castle, DE). These experiments were conducted under air atmosphere and measured in the dynamic heating regime. Samples between 5-15 mg were heated from 30-600 ^{o}C under constant heating ramp of 5 ^{o}C min^{-1} with a 30 minute isotherm at 75 ^{o}C.

The ^{1}H and ^{13}C NMR spectra were recorded using a Bruker spectrometer operating at 500 or 360 MHz and 90 or 125 MHz, respectively. Infrared (IR) analyses were obtained by direct measurement of the neat samples by utilizing a Perkin-Elmer 100 FT-IR instrument featuring an ATR force gauge, and spectra were obtained in the range of ν_{max} = 650 – 4000 cm^{-1}.

Synthetic Protocols for the formation of Reported Major products:

Preparation of 1-cyanomethyl-3-methylimidazolium chloride precursor salt* (1)*: Compound **1** was prepared by a solvent-free adaptation of a previously reported method.[30] Yields and reaction times are not optimized. The following serves as general procedure. In a 50 mL round bottom flask with magnetic stirbar, chloroacetonitrile (2.867 g, 37.9 mmol) was slowly added to 1-methylimidazole (2.87 g, 35 mmol). The mixture was stirred at room temperature overnight, and the resulting white solid precipitate washed with ethyl acetate (4 x 10 mL) and dried by rotary evaporation then high vacuum at room temperature for 24 h. White solid, water soluble, 90% yield, (DSC) $\boldsymbol{T}_{m}$ = 179 ^{o}C, $\boldsymbol{T}_{5\%onset}$ = 221 ^{o}C; ^{1}H NMR (500 MHz, DMSO-d_6) $\boldsymbol{\delta}$ ppm 9.56 (s, 1H), 8.00 (t, J = 1.73 Hz, 1H), 7.87 (t, J = 1.64 Hz, 1H), 5.82 (s, 2H), 3.92 (s, 3H); ^{13}C NMR (125 MHz, DMSO-d_6) $\boldsymbol{\delta}$ ppm 138.2, 124.8, 123.0, 115.3, 37.2, 36.6; FT-

IR (ν_{max}): 3392 (w), 3032 (s), 2977 (s), 2906 (s), 1575 (s), 1565 (s), 1439 (m), 1337 (m), 1254 (s), 1168 (s), 915 (m) cm^{-1}.

***Preparation of 1-(5-tetrazolidyl)methyl-3-methylimidazolium•($ZnBr_{0.8}Cl_{1.2}$) and recrystallization as* catena*-poly[(bromochlorozinc)-μ-[1-(5-tetrazolato)methyl-3-methylimidazolium]-N^1:N^4] coordination polymer* (2):** Compound **2** was prepared by modifying the methods of Sharpless and co-workers[27] for the halide salt precursor 1-cyanomethyl-3-methylimidazolium chloride (**1**). Yields and reaction times are not optimized. The following serves as a general procedure. Subsequent monitoring of the reaction by way of ^{1}H-NMR spectroscopy resulted in ~ 85% conversion of **1** to product **2** under room temperature conditions with all other factors the same.

1-Cyanomethyl-3-methylimidazolium chloride (**1**) (2.81 g, 17.2 mmol) was combined with NaN_3 (1.30 g, 20 mmol) in a 100 mL round-bottom flask with 50 mL water and stirred to dissolve with a magnetic stir bar. Zinc bromide was added (4.49 g, 20 mmol), and the mixture stirred to reflux overnight. The resultant white solid was rinsed with water and filtered. The final product was dried at 60 ^oC for 24 h in an oven. White powder, 80% yield, $\boldsymbol{T}_g$ = none observed; $\boldsymbol{T}_{5\%onset}$ = 306 ^oC; ^{1}H NMR (360 MHz, DMSO-d_6) $\boldsymbol{\delta}$ ppm 9.18 (s, 1H), 7.75 (t, J = 1.72 Hz, 1H), 7.68 (t, J = 1.74 Hz, 1H), 5.57 (s, 2H); 3.87 (3H, s); ^{13}C NMR (125 MHz, DMSO-d_6) $\boldsymbol{\delta}$ ppm 154.171, 138.060, 124.442, 123.563, 42.915, 36.557. FT-IR (ν_{max}): 3498 (w), 3103 (s), 3078 (s), 2076 (s), 16128 (w), 1572 (s), 1446 (s), 1433 (s), 1421 (s), 1340 (m), 1171 (s), 1072 (m), 839 (s), 816 (s), 776 (s), 692 (s) cm^{-1}. **2** was crystallized for X-ray diffraction analysis by dissolution in a minimum amount of concentrated HNO_3, evaporating the resulting mixture to near dryness, washing the residual with dry acetone, and then slow evaporation in air.

Isolation and recrystallization of 1-(5-1H-tetrazolyl)methyl-3-methylimidazolium chloride as zinc-free salt* (3)*: Compound **3** was obtained from the Zn-coordination polymer (**2**) *via* a preparatory adaptation of an anion exchange resin technique reported to remove trace Zn selectively from water and industrial waste samples[32]. Yields and reaction times are not optimized.

Conditioning of anion exchange resin: To 15.167 g of BioRad AG 1-X8 strongly basic anion exchange resin (100-200 mesh), 40 mL D.I. water was added and the resin stirred in a 125 mL flask to slurry for 20 min. The slurry was then introduced into a glass column (~ 0.5 cm ID, 40 cm length; prewashed with 9 N HCl and rinsed several times with D.I. water) with a sand and glass wool plug. 9 N HCl was then eluted through the column (2 x 30 mL) and discarded upon neutralization.

Sample preparation for anion exchange: The Zn-coordination polymer **2** was added to a 50 mL Erlenmeyer flask (0.508 g, 1.473 mmol) and 15 mL of 9 N HCl was added and stirred to dissolve the solid material. The solution was sonicated briefly to break up residual solids suspended in the acidic solution, and an additional 10 mL 9 N HCl was added to completely dissolve the material.

Zn separation from 2 by anion exchange resin: 10 mL collection vials were numbered and arranged to collect eluted fractions from the column, and **2** dissolved in minimal 9 N HCl was introduced by 3 mL increments to the top of the resin bed and eluted at a rate of ~ 1 drop/s (controlled by positive pressure introduced to top of column). When sample introduction was complete, 9 N HCl was eluted for complete removal of the salt **3**. After this step, the column was eluted with 0.005 M HCl followed by eluting the column with enough water until elution

had tested negative for chloride by silver nitrate spot test (~1:1 v/v ratio of eluted fraction to 0.1 M $AgNO_3$). In all, 24 vials were collected from the exchange resin, where each vial contained approximated 5-10 mL of eluted material.

Qualitative analysis of Zn removal by pH measurement and $K_2[Hg[CNS)_4]$ spot test: Determination of Zn in eluted fractions was estimated by two methods. First, the approximate pH of the elution in each collected tube could be obtained by pH indicator paper (Tubes 1-19, pH < 1; Tube 20, pH ~ 3-5; Tubes 21-24, pH ~ 5). As the $[ZnCl_4]^{2-}$ anion is present at high chloride concentrations, the zinc should remain supported on the resin and it may be assumed that the earlier elution volumes were relatively Zn-free. Next, a solution of $K_2[Hg(CNS)_4]$ (prepared the previous day by established methods,[33] 2.7% $HgCl_2$ and 3.9% in D.I. water) was used to test each of the eluted fractions for Zn by spot test (1:1 ratio of 0.5 mL each, sample to test solution; concentration limit = 1/10,000). A white precipitate indicating the presence of Zn formed quickly (less than 1 min) for elution tubes #14-22, where 14-16 only had a slight precipitate. To ensure the quality of the samples, only tubes 2-5 and 7-11 were included for sample collection. Tubes #1 and #6 seemed to visually contain column impurity (yellow coloring) and were stored separately. Tubes 12 and 13, although not obviously precipitating, were kept separate as well to increase the window between the eluted sample and Zn-containing eluted solution.

Isolation of 1-(5-1H-tetrazolyl)methyl-3-methylimidazolium chloride (3): Each of the eluted fractions of **3** was heated (~ 60 ^{o}C, 24 h) to remove water and excess HCl, and the residual solids were triturated with dry ethanol. From the reserved ethanol, the product was obtained as a white solid upon evaporation. White solid, 71% yield, $\boldsymbol{T}_{m}$ = 155 ^{o}C; $\boldsymbol{T}_{5\%onset}$ = 213 ^{o}C, ^{1}H NMR (500 MHz, DMSO-d_6) $\boldsymbol{\delta}$ ppm 9.35 (s, 1H), 7.86 (t, J = 1.65 Hz, 1H), 7.77 (t, J = 1.61 Hz, 1H),

5.89 (s, 2H), 3.89 (s, 3H); ^{13}C NMR (125 MHz, DMSO-d_6) $\boldsymbol{\delta}$ ppm 153.3, 137.5, 123.8, 122.9, 42.2, 36.9; FT-IR (ν_{max}): 3107 (m), 3001 (s), 2468 (w), 2395 (s), 1801 (m), 1668 (w), 1584 (m), 1552 (s), 1424 (w), 1178 (m), 1084 (s), 1027 (s), 1015 (s); 790 (s), 785 (s), 740 (s) cm^{-1}. Separately, a crystal was obtained from 1:1 MeOH/CH_3CN by slow diffusion of diethyl ether and submitted for single crystal X-ray diffraction analysis.

***Isolation and recrystallization of 1-(5-tetrazolidyl)methyl-3-methylimidazolium zwitterion* (4):** Compound **4** was obtained from the 1-(5-1*H*-tetrazolyl)methyl-3-methylimidazolium chloride salt (**3**) *via* neutralization reaction using hydroxide-exchanged anion exchange resin as solid-supported base. Yields and reaction times were not optimized.

Conditioning of anion exchange resin (OH$^-$): Approximately 5 g of BioRad AG 1-X8 strongly basic anion exchange resin in chloride form was eluted with ~20 bed volumes (~1 L) of 1 N NaOH and each eluted volume was tested for Cl^- anion by using the silver nitrate test. The column was then washed with 2 bed volumes of D.I. water, filtered, and rinsed dry with ethanol before storing under high vacuum for 48 h.

Neutralization of 3 by OH$^-$ form of anion exchange resin: The required volume of dry resin needed to convert **3** to the zwitterion **4** was added to a 125 mL Erlenmeyer flask, washed three times with 25 mL of D.I. water and decanted to remove fines from ruptured resin beads, and then **3** (0.240 g, 1.20 mmol) was added to the flask as a solution in 25 mL of water.

The mixture was gently stirred by rotating the flask for 20 min prior to spot checking the solution for Cl^- anion by silver nitrate test (0.1 M $AgNO_3$), the resin was filtered and washed with 3 x 10 mL D.I. water, and the resulting aqueous filtrates combined and evaporated to dryness at room temperature in an open beaker.

***Isolation of 1-(5-tetrazolidyl)methyl-3-methylimidazolium* (4):** Neutralized fractions were combined and allowed to evaporate at room temperature to remove water. Additional recrystallization of isolated **4** from slow evaporation from hot methanol resulted in the final product. A crystal from this batch was submitted for single crystal X-ray diffraction analysis. White solid, 75% yield, $\boldsymbol{T}_m$ = 124 ^oC ; $\boldsymbol{T}_{5\%onset}$ = 241 ^oC, ^1H NMR (500 MHz, DMSO-d_6) **δ** ppm 9.15 (s, 1H), 7.72 (t, J = 1.50 Hz, 1H), 7.65 (t, J = 1.51 Hz, 1H), 5.52 (s, 2H), 3.84 (s, 3H); ^{13}C NMR (125 MHz, DMSO-d_6) **δ** ppm 155.5, 136.4, 123.2, 122.6, 44.6, 35.6; FT-IR (ν_{max}): 3146 (m), 3094 (s), 3074 (s), 1575 (m), 1560 (m), 1402 (w), 1331 (s), 1193 (w), 1150 (s), 1122 (m), 1080 (w), 862 (s), 815 (s), 780 (s), 751 (s), 698 (s) cm^{-1}.

***Preparation of 1-(2-cyanoethyl)-1,2,4-triazole* (6):** Compound **6** was prepared from the 1,2,4-triazole, **5**. Yields and reaction times are not optimized. The following serves as a general procedure. A sample of 1,2,4-triazole (1.724 g, 25 mmol) was dissolved in toluene (10 mL) and placed into a 50 mL round bottom flask to which a Teflon stirbar was added. Acrylonitrile (1.3562 g, 25 mmol) was added to the flask drop-wise as a solution in toluene (2 mL) followed by addition of triethylamine (0.5 mL) directly to the reaction mixture. The reaction mixture was fit with a condenser and heated to reflux. The reaction mixture was then refluxed for an additional 30 h.

At the end of the reaction time, **6** separated from the toluene as a second amber liquid phase and isolated by decanting the toluene from the mixture and washing the residue with additional toluene. Residual solvent was then removed by rotary evaporation. White solid (93%), $\boldsymbol{T}_m$ = 31 ^oC ; $\boldsymbol{T}_{5\%onset}$ = 120 ^oC; ^1H NMR (360 MHz, DMSO-d_6) **δ** ppm 8.62 (s, 1H), 8.07 (s, 1H), 4.51 (d, J = 6.38 Hz, 2H), 3.13 (t, J = 6.38 Hz, 2H); ^{13}C NMR (90 MHz, DMSO-d_6) **δ**

ppm 152.4, 144.9, 118.6, 44.7, 18.; FT-IR (ν_{max}): 3406 (br m), 3120 (m), 2253 (m), 1508 (s), 1450 (m), 1418 (m), 1274 (s) 1206 (m), 1135 (s), 1040 (m), 1022 (m), 1003 (s), 919 (m), 872 (m), 679 (s) cm^{-1}.

Preparation of 5-(2-(1,2,4-triazol-1-yl)ethyl)tetrazolate as sodium coordination polymer* (7)*: Compound **7** was prepared from 1-(2-cyanoethyl)-1,2,4-triazole (**6**). Yields and reaction times are not optimized. The following serves as a general procedure. In an Ace Glass high-pressure glass vial with a Teflon screw-cap, 1-(2-cyanoethyl)-1,2,4-triazole (1.195 g, 9.8 mmol) was combined with sodium azide (0.6437 g, 9.8 mmol) in glacial acetic acid (0.6 mL, 10 mmol). A Teflon magnetic stir bar was added, the vial sealed, and the mixture stirred on an oil bath at 60-70 ^{o}C for 24 h. At the end of the reaction period, the vial was set on a rotary evaporator at 70-80 ^{o}C for 4 h to remove residual acetic acid followed by dissolving the white solids with dry ethanol. Single crystals were obtained from slow evaporation of ethanol from the crude reaction mixture, and the final product, **6**, was obtained from removal of residual solvent by high vacuum. White solid (48%); $\boldsymbol{T}_m$ = none observed ^{o}C ; $\boldsymbol{T}_{5\%onset}$ = 313 ^{o}C, ^{1}H NMR (360 MHz, DMSO-d_6) $\boldsymbol{\delta}$ ppm 8.42 (s, 1H), 7.92 (s, 1H), 4.47 (t, J = 7.62 Hz, 2H), 3.15 (t, J = 7.59 Hz, 2H); ^{13}C NMR (90 MHz, DMSO-d_6) $\boldsymbol{\delta}$ ppm 157.8, 151.5, 144.3, 48.8, 26.9; FT-IR (ν_{max}): 3322 (s), 3219 (s), 3144 (s), 1687 (m), 1571 (s), 1516 (s), 1468 (m), 1435 (m), 1380 (s), 1277 (s), 1205 (s), 1139 (s), 1104 (w), 1043 (w), 1014 (s), 970 (w), 923 (w), 858 (m), 673 (m) cm^{-1}.

1-(2-(5-tetrazolidyl)ethyl)-3-(5-1*H*-tetrazolyl)methylimidazolium zwitterion* (10)*: Azolium zwitterion, **10**, was obtained by reacting **9** (3.037 g, 20 mmol) with sodium azide (2.880 g, 44 mmol) in 10 mL of glacial acetic acid in a heated oil bath (60-70 ^{o}C) for 48 h. The mixture resulted in a suspended white solid in amber liquid, and the solid product was washed several

times with dry ethanol. Final drying at high vacuum resulted in final product. White solid (78%); $\boldsymbol{T}_m$ = 49 °C; $\boldsymbol{T}_{5\%onset}$ = 237 °C; ^{1}H NMR (500 MHz, DMSO- d_6) $\boldsymbol{\delta}$ ppm 9.27 (s, 1H), 7.75 (dd, J = 10.47 Hz, 2H), 5.55 (s, 2H), 4.64 (t, J = 6.95 Hz, 2H), 3.50 (t, J = 6.97 Hz, 2H); ^{13}C NMR (500 MHz, DMSO- d_6) $\boldsymbol{\delta}$ ppm 155.9, 154.1, 137.0, 123.3, 122.8, 46.8, 45.1, 24.7; FTIR (ν_{max}): 3143 (m), 3113 (m), 3043 (m), 2344 (br m), 1945 (br m), 1567 (s), 1459 (m), 1434 (m), 1234 (m), 1211 (m), 1170 (s), 1099 (s), 1045 (m), 950 (m), 872 (m), 860 (m), 802 (s), 761 (s), 744 (s), 690 (s), 665 (s) cm^{-1}.

***1-(2-(5-1H-tetrazolyl)ethyl)-3-(5-1H-tetrazolyl)methylimidazolium bis(trifluoro-methanylsulfonyl)amide* (11):** The synthesis of **11** was carried out in the hood by reacting 123 mg (0.5 mmol) of zwitterion **10** and 140 mg (0.5 mmol) of hydrogen bis(trifluoromethanylsulfonlyl)amide ($HNTf_2$) in 10 mL of 1:1 methanol/water at RT for about 72 h in a 20 mL borosilicate glass vial. The mixture was kept at ambient conditions in order to allow the volatile solvent to evaporate and then water was removed by air stream. The product **11** was kept under high vacuum to afford clear, viscous oil. Colorless oil (80%); $\boldsymbol{T}_g$ = 10 °C, $\boldsymbol{T}_m$ = 50 °C; $\boldsymbol{T}_{5\%onset}$ = 245 °C, ^{1}H NMR (500 MHz, DMSO- d_6) $\boldsymbol{\delta}$ ppm 9.35 (s, 1H), 7.87 (dt, J = 24.61 Hz, 2H), 5.91 (s, 2H), 4.71 (t, J = 6.81 Hz, 2H), 3.54 (t, J = 6.82 Hz, 2H); ^{13}C NMR (500 MHz, DMSO- d_6) $\boldsymbol{\delta}$ ppm 138.0, 123.8, 123.4, 121.4, 121.2, 118.6, 46.8, 43.0, 24,3; FTIR (ν_{max}): 3531 (w), 3245 (w), 3153 (m), 3090 (m), 1562 (s), 1442 (m), 1345 (s), 1183 (s), 1134 (s), 1054 (s), 791 (m), 741 (s) cm^{-1}.

***1,3-dimethylimidazolium 1-(2-(5-tetrazolidyl)ethyl)-3-(5-tetrazolidyl)methylimidazolium* (12):** The synthesis of **12** was carried out in the hood by reacting 123 mg (0.5 mmol) of zwitterion **10** and 70 mg (0.5 mmol) of 1,3-dimethylimidazolium-2-carboxylate in 10 mL of a

1:1 solution of methanol/water (and 2 drops of DMSO) at RT for about 72 h in a 20 mL borosilicate glass vial. The mixture was kept at ambient conditions in order to allow the volatile solvent to evaporate and then water was removed by air stream. The compound was kept under high vacuum to afford clear, viscous oil. Colorless oil (78%). The NMR spectrum revealed the presence of 33% 1,3-dimethylimidazolium-2-carboxylate, which was removed by slow dissolution in hot acetone (6 x 2 mL). Yield of **12** after purification, 52%; $\boldsymbol{T}_g$ = -24; $\boldsymbol{T}_m$ = 44 ^oC; $\boldsymbol{T}_{5\%onset}$ = 161 ^oC, ^1H NMR (500 MHz, DMSO- d_6) $\boldsymbol{\delta}$ ppm 9.21 (d, J = 78.05 Hz, 2H), 7.69 (dt, J = 15.80, 15.54, 1.47 Hz, 4H), 5.51 (s, 2H), 4.52 (t, J = 7.23 Hz, 2H), 3.84 (s, 1H), 3.21 (t, J = 7.24 Hz, 2H); ^{13}C NMR (500 MHz, DMSO- d_6) $\boldsymbol{\delta}$ ppm 157.2, 156.1, 137.5, 136.7, 123.9, 122.9, 122.9, 48.6, 45.1, 36.1, 26.9; FTIR (ν_{max}): 3372 (w), 3149 (w), 3096 (m), 2956 (w), 2858 (w) 2602 (w), 2338 (w), 1727 (w), 1701 (w), 1656 (m), 1567 (s), 1516 (w), 1439 (m), 1397 (m), 1326 (m), 1229 (m), 1170 (s), 1111 (w), 1083 (w), 1051 (w), 1019 (w), 990 (w), 836 (w), 742 (s), 693 (w), 662 (w) cm^{-1}.

Acknowledgements

This research was supported by the Air Force Office of Scientific Research (Grant F49620-03-1-0357)

References

1 Chan, B. K. M.; Chang, N. –H.; Grimmett, M. R. *Aust. J. Chem.* **1977**, *30*, 2005.

2 Drake, G.; Hawkins, T.; Brand, A.; Hall, L.; McKay, M.; Vij, A.; Ismail, I. *Propellants, Explos., Pyrotech.* **2003**, *28*, 174.

3 Jones, C. B.; Haiges, R.; Schroer, T.; Christe, K. O. *Angew. Chem., Int. Ed.* **2006**, *45*, 4981.

4 Steinhauser, G.; Klapötke, T. M. *Angew. Chem., Int. Ed.* **2008**, *47*, 2.

5 Singh, R. P.; Verma, R. D.; Meshri, D. T.; Shreeve, J. M. *Angew. Chem., Int. Ed.* **2006**, *45*, 3584.

6 Forsyth, S. A.; Pringle, J. M.; MacFarlane, D. R. *Aust. J. Chem.* **2004**, *57*, 113.

7 Petrie, M. A.; Sheehy, J. A.; Boatz, J. A.; Rasul, G.; Prakash, G. K. S.; Olah, G. A.; Christie, K. O. *J. Am. Chem. Soc.* **1997**, *119*, 8802.

8 Katritzky, A. R.; Yang, H.; Zhang, D.; Kirichenko, K.; Holbrey, J. D.; Reichert, W. M.; Smiglak, M.; Rogers, R. D. *New J. Chem.* **2006**, *30*, 349.

9 Katritzky, A. R.; Singh, S.; Kirichenko, K.; Holbrey, J. D.; Smiglak, M.; Reichert, W. M.; Rogers, R. D. *Chem. Commun.* **2005**, 868.

10 Katritzky, A. R.; Singh, S.; Kirichenko, K.; Smiglak, M.; Holbrey, J. D.; Reichert, W. M.; Spear, S. K.; Rogers, R. D. *Chem. Eur. J.* **2006**, *12*, 4630.

11 Smiglak, M.; Reichert, W. M.; Holbrey, J. D.; Wilkes, J. S.; Sun, L.; Thrasher, J. S.; Kirichenko, K.; Singh, S.; Katritzky, A. R.; Rogers, R. D. *Chem. Commun.* **2006**, 2554.

12 Huddleston, J. G.; Visser, A. E.; Reichert, W. M.; Willauer, H. D.; Broker, G. A.; Rogers, R. D. *Green Chem.* **2001**, *3*, 156.

13 Smiglak, M.; Holbrey, J. D.; Griffin, S. T.; Reichert, W. M.; Swatloski, R. P.; Katritzky, A. R.; Yang, H.; Zhang, D.; Kirichenko, K.; Rogers, R. D. *Green Chem.* **2007**, *9*, 90.

14 Ohno, H. *Bull. Chem. Soc. Jpn.* **2006**, *79*, 1665.

15 MacFarlane, D. R.; Seddon, K. R. *Aust. J. Chem.* **2007**, *60*, 3.

16 Ngo, H. L.; LeCompte, K.; Hargens, L.; McEwen, A. B. *Thermochim. Acta* **2000**, *357-358,* 97.

17 Fredlake, C. P.; Crosthwaite, J. M.; Hert, D. G.; Aki, S. N. V. K.; Brennecke, J. F. *J. Chem. Eng. Data* **2004**, *49*, 954.

18 Lee, S. *Chem. Commun.* **2006**, 1049.

19 Izgorodina, E. I.; Forsyth, M.; MacFarlane, D. R. *Aust. J. Chem.* **2007**, *60*, 15.

20 Holbrey, J. D.; Visser, A. E.; Spear, S. K.; Reichert, W. M.; Swatloski, R. P.; Broker, G. A.; Rogers, R. D. *Green Chem.* **2003**, *5*, 129.

21 Anderson, J. L.; Ding, R.; Ellern, A.; Armstrong, D. W. *J. Am. Chem. Soc.* **2005**, *127*, 593.

22 Zeng, Z. Phillips, B. S.; Xiao, J. -C.; Shreeve, J. M. *Chem. Mater.* **2008**, *20*, 2719.

23 Gao, Y.; Ye, C.; Twamley, B.; Shreeve, J. M. *Chem. – Eur. J.* **2006**, *12*, 9010..

24 Joo, Y. H.; Shreeve, J. M. *Org. Lett.* **2008**, *10*, 4665.

25 Payagala, T.; Huang, J.; Breitbach, Z. S.; Sharma, P. S.; Armstrong, D. W. *Chem. Mater.* **2007**, *19*, 5848.

26 Artamonova, T. V.; Zatsepina, M. V.; Koldobskii, G. I. Russ. *J. Org. Chem.* **2004**, *40*, 1318.

27 Demko, Z. P.; Sharpless, K. B. *J. Org. Chem.* **2001**, *66*, 7945.

28 Zhao, D.; Fei, Z.; Scopelliti, R.; Dyson, P. J. *Inorg. Chem.* **2004**, *43*, 2197.

29 Borrok, D. M.; Wanty, R. B.; Ridley, W. I.; Wolf, R.; Lamothe, P. J.; Adams, M. *Chem. Geol.* **2007**, *242*, 400.

30 Herrmann, W. A.; Goossen, L. J.; Spiegler, M. *Organometallics* **1998**, *17*, 2162.

31 (*a*) Sheldrick, G. M. *Program for Semiempirical Absorption Correction of Area Detector Data*, University of Göttingen, Germany, 1997; (*b*) Sheldrick, G. M. *SHELXTL*, Version 6.14, Bruker AXS Inc., Madison, WI, 2003.

32 (*a*) Krausa, K.; Moore, G. *J. Am. Chem. Soc.* **1953**, *75*, 1460; (*b*) Kallmann, S.; Steele, C. G.; Chui, N. Y. *Anal. Chem.* **1954**, *28*, 230; (*c*) Bishay, T. Z. *Anal. Chem.* **1972**, *44*, 1087; (*d*) Strelow, F. W. E. *Anal. Chem.* **1978**, *50*, 1359; (*e*) Sweileh, J. A.; El-Nemma, E. M. *Anal. Chim. Acta* **2004**, *523*, 287; (*f*) Archer, C.; Vance, D. J. *Anal. At. Spectrom.* **2004**, *19*, 656; (*g*) Borrok, D. M.; Wanty, R. B.; Ridley, W. I.; Wolf, R.; Lamothe, P. J.; Adams, M. *Chem. Geol.* **2007**, *242*, 400.

33 Svehla, G. Ed. *Vogel's Qualitative Inorganic Analysis*, Longman Scientific & Technical: Essex, U.K., 1987, p. 126.

CHAPTER 4

ZINC-ASSISTED SYNTHESIS OF IMIDAZOLIUM-TETRAZOLATE BI-HETEROCYCLIC ZWITTERIONS WITH VARIABLE ALKYL BRIDGE LENGTH

Taken in part from a prepared manuscript: Drab, D. M.; Smiglak, M.; Shamshina, J. L.; Kelley, S. P.; Rogers, R. D. **2011**, *in preparation*.

Acknowledgements: Kinetic study was performed and evaluated by J. L. Shamshina (The University of Alabama, Tuscaloosa, AL), and refinement of the X-ray diffraction data and presentation of the crystal structure was completed by S. P. Kelley (The University of Alabama, Tuscaloosa, AL).

Abstract

Zinc halide-complexed, alkyl-bridged bi-heterocycles were obtained as zwitterions from the click reaction of a series of *N*-cyanoalkyl-*N*-alkylimidazolium halide ionic liquids with sodium azide.

Introduction

Our group has recently demonstrated a design platform to access multi-heterocyclic ionic liquids (MHILs) systematically by (i) synthesis of heterocycle-forming azoles, (ii) facile cyclization by click methodology to form multi-heterocyclic structures,[1] and (iii) generation of MHILs *via* IL synthetic protocols.[2] Together with the conventional 'dual-functional' approach to IL synthesis,[3,4] the MHIL platform provides new design options to target properties for high-performance applications, including potential alternatives to more traditional oligomeric energetic materials synthesis.[5]

We focused on two methodic changes for the synthesis of 8 ZnX_2-complexed 1-(5-tetrazolidyl)alkyl-3-alkylimidazolium structures (X = halide), including (i) variation of substituent length on the nitrogen atom of the imidazolium core (methyl vs. butyl) and (ii) differences in alkyl-linker chain length. Thus, from a series of *N*-methyl and *N*-butyl-functionalized imidazolium halide salts obtained in a previous study,[6] we selected our clickable starting materials. It is believed that the ionic nature of the *N*-cyanoalkyl-functionalized imidazolium salts would promote the click synthesis of tetrazole rings under Sharpless conditions (e.g., $ZnBr_2$ catalyst in water under mild heating),[1] where reactivity should not be restricted by alkyl substituent length (as is often the case with many neutral nitrile starting materials).[7] Furthermore, the ready formation of the click products as water-insoluble ZnX_2 complexes should allow for easy product separation without the need for a more tedious, pH-sensitive workup protocol, often regarded as problematic for product recovery and purification.[8,9] We have previously shown that Zn can be removed from the click product by a preparatory anion exchange resin technique to isolate either the cationic form of the ligand (as a NH-tetrazole-functionalized chloride salt) or as the tetrazolate-functionalized zwitterion.[2] For this study, however, we report only the preparation of the ZnX_2-complexed click products with variable bridge and *N*-alkyl substituent length that may easily serve as MHIL precursors.

Results and discussion

Synthesis

The precursors **1-8[X]** (Scheme 4.1) were easily obtained *via* alkylation reactions of *N*-methyl- or *N*-butylimidazole with commercially available haloalkylnitriles, where the details of the synthesis and characterization of these compounds has been previously reported.[6] Reactions

of **1-8[X]** with azide anion under Sharpless conditions resulted in the formation of target compounds, **9-16**.[1]

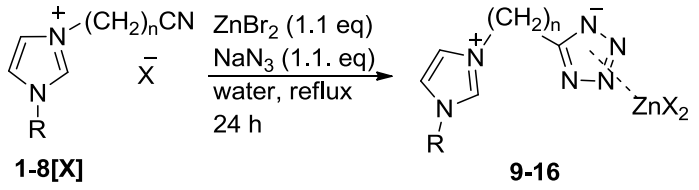

1-8[X] **9-16**

1[Cl]*: R = CH_3, n = 1
2[Br]*: R = CH_3, n = 2
3[Cl]*: R = CH_3, n = 3
4[Cl]*: R = CH_3, n = 4

5[Cl]: R = $(CH_2)_3CH_3$, n = 1
6[Br]: R = $(CH_2)_3CH_3$, n = 2
7[Cl]: R = $(CH_2)_3CH_3$, n = 3
8[Cl]: R = $(CH_2)_3CH_3$, n = 4

9: R=CH_3, n = 1, 96%
10: R=CH_3, n = 2, 38%
11: R=CH_3, n = 3, 46%
12: R=CH_3, n = 4, 74%

13: R = $(CH_2)_3CH_3$, n = 1, 74%
14: R = $(CH_2)_3CH_3$, n = 2, 61%
15: R = $(CH_2)_3CH_3$, n = 3, 70%
16: R = $(CH_2)_3CH_3$, n = 4, 63%

Scheme 4.1. Click reactions of *N*-cyanoalkyl-functionalized imidazolium halide salts (**1-4[X]**, R = methyl; **5-8[X]**, R = butyl) to zwitterionic products (**9-12**, R = methyl; **13-16**, R = butyl). Synthetic yields for all compounds above are reported as percent values. *1-Cyanoalkyl-3-methylimidazolium salt precursors **1[Cl]**,[10] **2[Br]**,[10] **3[Cl]**,[11] and **4[Cl]**[12] have been reported previously, however, all salts **1-8[X]** were prepared as discussed in our recent publication.[6]

N-Cyanoalkyl-*N*-alkylimidazolium halides (**1-8[X]**) were each combined with sodium azide (1.1 eq.) in a 100 mL round-bottom flask and dissolved in 50 mL of deionized water before adding zinc bromide (1.1 eq.) and allowing the mixture to stir at reflux for 24 h on a heated oil bath. During the reaction, the product formed as a white solid which separated from the aqueous solution, and further product precipitation occurred when allowing the reaction mixture to cool to room temperature. To isolate the final product, the solids were washed several times with water prior to filtration and drying in a furnace set to 60 ^{o}C for 24 h.

A subsequent kinetic experiment revealed that reflux is not necessary (*vide infra*), indicating that *N*-cyanoalkyl-substituted imidazolium salts are very well-suited for the click

synthesis of 5-tetrazoles – possibly due to the polar environment created by the ionic starting material and aqueous reaction media.[13] The reaction proceeded smoothly in water with no need of additional co-solvent, where the resultant products (**9**-**16**) precipitated as solids, which were simply filtered from the reaction mixture and dried with no other purification required.

Products **10** and **14** are presumed to be $ZnBr_2$-complexed structures, as only bromide is introduced into the reaction sequence through the use of **2[Br]** and **6[Br]** as starting materials. Compounds obtained from the chloride salts **1**, **3**-**5**, **7**, **8[Cl]** are presumed to form mixed-halide coordination polymers, including products **9**, **11**-**13**, **15**, **16**. The formula unit $ZnBr_{(2-x)}Cl_{(x)}$ may describe the halide content for these structures, supported by the X-ray diffraction analysis of **9**, which showed partial occupancy of the halides when refined as $ZnBr_{0.8}Cl_{1.2}$ (*vide infra*). Although a mixture of halides in the Zn-coordinated product could be avoided by including the same halide in **1**-**8[X]** as in the ZnX_2 salt, the work here explored the click reaction using halide salts from our previously reported work,[6] and $ZnBr_2$ was used for all click reactions to remain consistent with the click conditions reported in the literature.[1]

Single-Crystal X-ray Diffraction

The crystal structure of the Zn-coordinated product *catena*-poly[(bromochlorozinc)-μ-[1-(5-tetrazolato)methyl-3-methylimidazolium]-N_1:N_4], **9** (Figure 4.1), was used in our earlier communication to confirm the product, although the details of this structure were not discussed.[2]

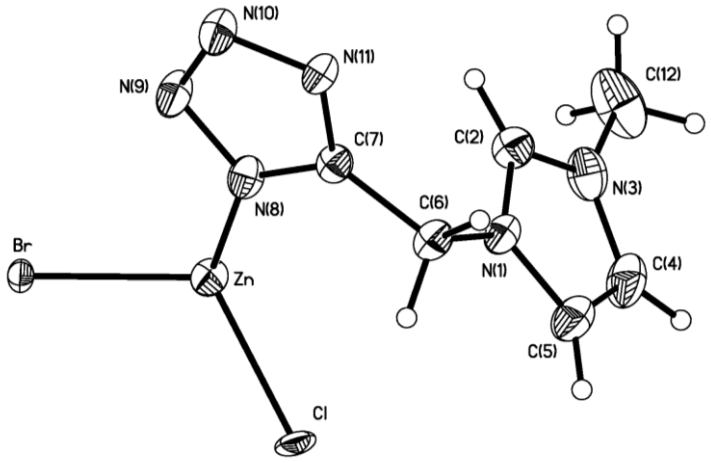

Figure 4.1. ORTEP representation of the asymmetric/formula unit for *catena*-poly[(bromochlorozinc)-μ-[1-(5-tetrazolato)methyl-3-methylimidazolium]-N_1:N_4], **9** (50% probability ellipsoids).

The halide positions showed substitutional disorder of chloride and bromide and were refined to 60% chloride and 40% bromide. The tetrazolate-Zn bonds form an infinite 1D coordination polymer along the crystallographic *b* axis (Figure 4.2).

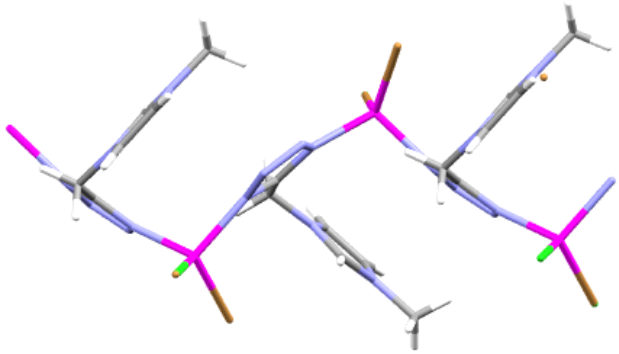

Figure 4.2: A capped-stick packing diagram of **9** showing three units of the coordination polymer along the crystallographic axis *b*.

The overall packing can be described as parallel 1D coordination polymer chains along *b*, forming a lattice of hydrogen bonds along *a* and *c* to give a 3D network (Figure 4.3). We believe

that similar Zn-coordinated polymeric structures are obtained *in situ* from the reaction of **1-8** (representing different *N*-cyanoalkyl and *N*-alkyl substituent lengths) under click conditions. Reaction homology for the Zn-assisted synthesis of tetrazoles has been reported,[1] and more recently the work of Xiong and co-workers concluded that salts of d^{10} metals were effective for the *in situ* formation of 5-tetrazole-based coordination polymers from a variety of neutral nitriles and the azide anion under hydrothermal conditions.[14,15] However, although a large number of Zn-tetrazolate complexes have been reported where the tetrazolate is part of a multi-heterocyclic ligand, their rings are frequently conjugated to force the ligand into planarity.[16]

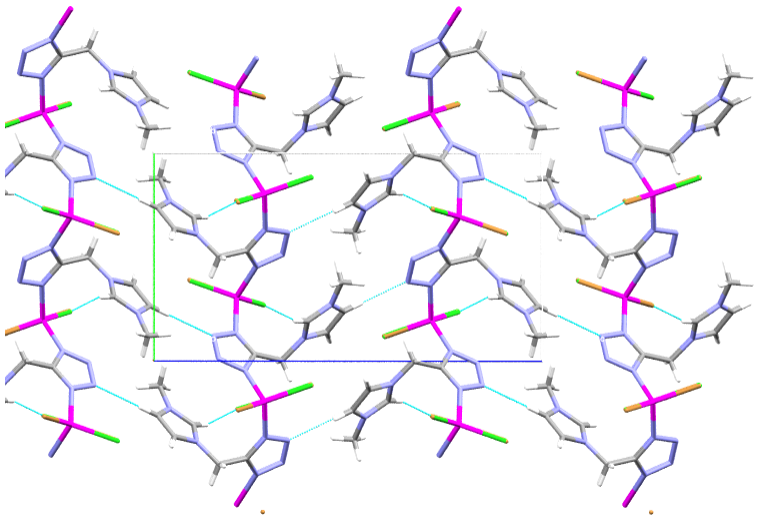

Figure 4.3: Packing of **9** viewed down *c* axis. Polymer chains are oriented vertically and azolate-imidazolium hydrogen bonding is roughly horizontal.

Crystallographic data (excluding structure factors) for the structure of **9** has been deposited with the Cambridge Crystallographic Data Centre as supplementary publication CCDC 765819. Copies of the data can be obtained, free of charge, on application to CCDC, 12 Union Road, Cambridge CB2 1EZ, UK, (fax: +44-(0)1223-336033 or e-mail: deposit@ccdc.cam.ac.uk).

Spectroscopy

^{1}H NMR and ^{13}C NMR spectra verified formation of **9-16**, where the disappearance of a signal for the -C≡N carbon (***δ*** ~ 115-120 ppm) and appearance of a new signal for the C5 carbon of the tetrazole ring (***δ*** ~ 155-160 ppm) was especially diagnostic. In addition, a significant shift of the *α*-carbon next to the carbon atom of the nitrile group (δ ~ 35 ppm) was noted when the cyano group was converted to a tetrazole ring (***δ*** ~ 42-45 ppm) (Scheme 4.2). The above trends are most likely due to the change in hybridization of the nitrile *sp* carbon when converting to the C5 atom of the tetrazole unit (sp^2).

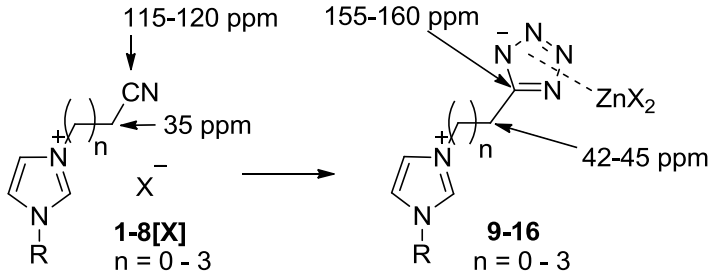

Scheme 4.2. Chemical shift (ppm) of diagnostic signals in the ^{13}C NMR spectra of **1-8[X]** compared with **9-16**.

A considerable change in chemical shifts was also observed in the proton NMR spectra for protons bound to the *α*-carbon next to the nitrile group when converting to tetrazole (Scheme 4.3). The observed degree of change in chemical shift (Δ***δ***, in ppm) increases downfield when comparing compounds with short spacer lengths (Δ***δ*** (ppm) = -0.25, **9**, and -0.02, **13**) and long spacer lengths (Δ***δ*** (ppm) = +0.33, **12**, and +0.34, **16**). One interpretation of this trend is that for the shorter-spaced nitriles, the strong electron-withdrawing effect of the proximal imidazolium cation is countered by the delocalized electron density of the tetrazolate ring system. The downfield chemical shift of the protons on the *α*-carbon of the nitriles decreases with increasing separation from the imidazolium ring (e.g., compare ***δ*** (ppm) = 5.82, **1[Cl]**, 3.26, **2[Br]**, 2.61,

3[Cl], 2.54, **4[Cl]**). However, for click products **9-16**, the degree of downfield shift increased with spacer length when compared with analogous nitriles (e.g., compare δ ($\Delta\delta$) (ppm) = 5.57 (-0.25), **9**, 3.44 (+0.18), **10**, 2.93 (+0.32), **11**, 2.87 (+0.33), **12**).

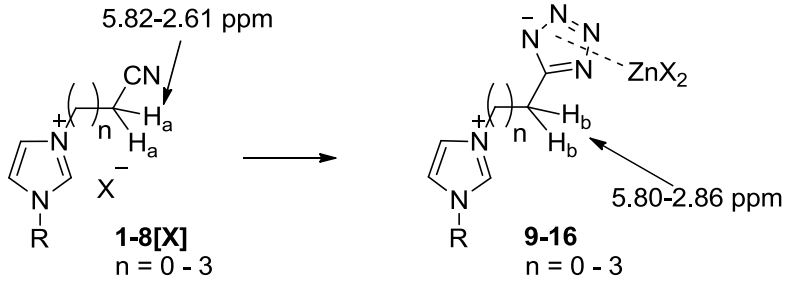

Scheme 4.3. Diagnostic signals in the ^{1}H NMR spectra of **1-8[X]** compared with **9-16**.

The IR spectra also support the formation of the products. The appearance of a new absorption band (ν = 1400-1420 cm^{-1}) indicated formation of a tetrazole ring, and the loss of the -C≡N stretching vibration band present in *N*-cyanoalkyl-functionalized starting materials (ν = 2240 cm^{-1})[17] suggested that the nitrile groups of **1-8[X]** were transformed to the tetrazole moiety in the reaction.

A ^{1}H NMR kinetic study was completed on the click reaction of the **1[Cl]** precursor to determine optimal reaction time, where **1[Cl]** was combined with 1.1 eq. of both $ZnBr_2$ and NaN_3 in D_2O. The experiment was performed using sub-millimole amounts of reagents in an NMR tube (in 1 mL D_2O, 15 mg **1[Cl]**), where the progress of the reaction was checked periodically. A comparison of the disappearing CH_aH_a signal adjacent to the nitrile group *vs.* a newly appearing CH_bH_b signal adjacent to the tetrazole ring served as the basis for quantitative estimation and yield calculation. When nitriles are used as precursors, these two absorptions are separated sufficiently to allow analysis of the mixture by integration.

Conversion to 85% for **9** was observed at room temperature after about 2.5 h (Figure 4.4). Such a fast reaction might be explained by activation of the nitrile functionality for [3+2] dipolar cycloaddition through (i) electrostatic attraction of the azide anion into close proximity to the cation, and (ii) an inductive effect (although decreasing with longer chain lengths) which drives product formation from *N*-cyanoalkyl-functionalized imidazolium precursors. Our results indicate improvement compared with the longer reaction times and harsher conditions required for neutral nitrile substrates in the click synthesis of tetrazoles.[1]

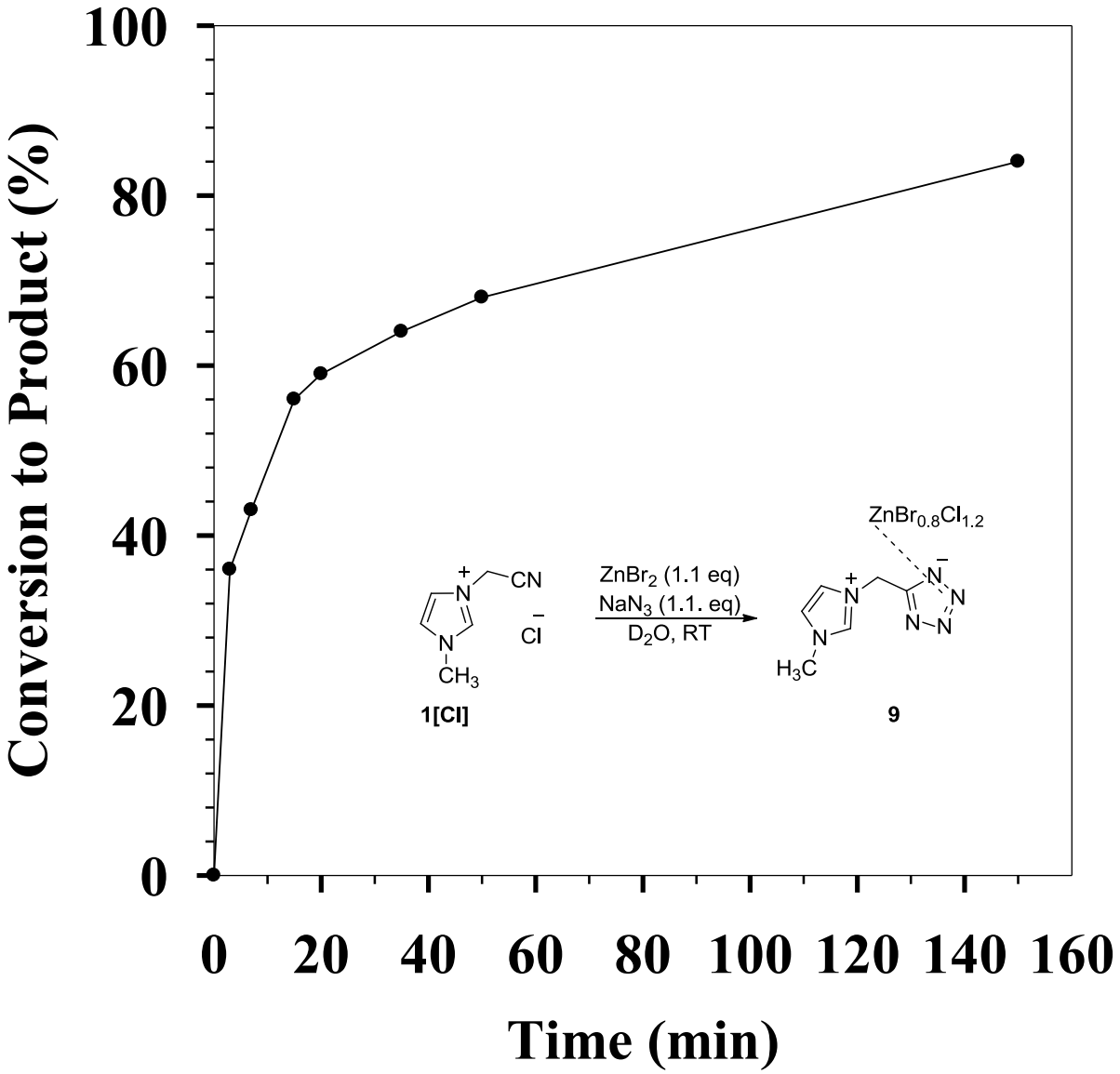

Figure 4.4. Optimization data for the conversion of 1-cyanomethyl-3-methylimidazolium chloride, **1[Cl]**, to zinc-coordination product **9** by zinc-assisted dipolar cycloaddition of sodium azide to **1[Cl]** with $ZnBr_2$ in D_2O for 2.5 h; solid line does not include continuous data, but is shown for visualization only; data is adapted from results reported in a previous study.[2]

Thermal Investigations

The click products **9-16** were analyzed for phase transition temperatures by differential scanning calorimetry (DSC) and for thermal stabilities by thermogravimetric analysis (TGA). Glass transition and melting transition temperatures ($\boldsymbol{T}_g$ and $\boldsymbol{T}_m$, respectively) were determined from the second heating cycle after initially heating the material from ambient temperature to an upper limit based upon the thermal stability of the compound as determined by TGA. Melting transitions, $\boldsymbol{T}_m$, were taken as the onset of a sharp, endothermic peak on heating, and $\boldsymbol{T}_g$ values were identified from the onset of small shifts in heat flow arising from the transition between amorphous glassy to liquid states when heating.

Thermal stabilities (Table 4.1) were assessed by TGA for all prepared compounds and taken as the onset of thermal decomposition for the first 5% weight loss ($\boldsymbol{T}_{5\%onset}$). The $\boldsymbol{T}_{5\%onset}$ values were considered more indicative of thermal stability than the onset of thermal decomposition ($\boldsymbol{T}_{onset}$, included for comparison in parentheses in Table 4.1) which is more commonly reported in the literature.[18] Compounds were heated to 800 ^{o}C at a rate of 5 ^{o}C·min^{-1} with an isothermal hold at 75 ^{o}C for 30 min. Exceptions to this procedure were compounds **9** and **13**, which were heated to 600 ^{o}C and was a sufficient temperature to observe their full decomposition.

Table 4.1. Thermal data summary for click products **9-16**.

Structure	Compound	n	[X]	T_g (°C)[a]	T_m (°C)[a]	$T_{5\%onset}$ (T_{onset}) (°C)[c]
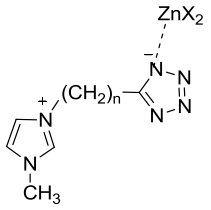	**9**	**1**	**Cl^-/Br^-**	64	---	295 (303)
	10	**2**	**Br^-**	40	---	281 (307)
	11	**3**	**Cl^-/Br^-**	91	196[b]	298 (311)
	12	**4**	**Cl^-/Br^-**	72	---	286 (303)
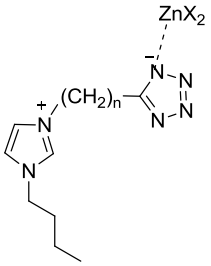	**13**	**1**	**Cl^-/Br^-**	46	40[b]	290 (301)
	14	**2**	**Br^-**	53	44[b]	244 (263)
	15	**3**	**Cl^-/Br^-**	81	---	260 (319)
	16	**4**	**Cl^-/Br^-**	66	---	290 (312)

[a] Melting point (T_m) and/or glass transition temperatures (T_g) were taken from the onset of observed transition and determined by DSC during the second heating cycle at a ramp rate of 5 $^oC \cdot min^{-1}$ after initially melting then cooling all samples to -100 °C. [b] All melting transitions were observed for the initial heating cycle only, where dashed lines (---) indicated that no T_m was observed. [c] Thermal decomposition temperatures were obtained by TGA using a heating ramp of 5 °C min^{-1} under a dried air atmosphere. All values are reported as (i) onset to 5 wt% loss of mass ($T_{5\%onset}$) and (ii) onset to total mass loss (T_{onset}) (parentheses).

The high temperature decomposition of **9-16** were characterized by a two-step weight loss pattern. This trend was also observed for many *N*-cyanoalkyl-functionalized salts in our previous work, where we suggested the formation of thermally-stable carbonaceous materials following initial decomposition.[6] Support for this observation was reported by MacFarlane[19] and others,[20] where the *N*-CH_2CN groups may cyclize or polymerize upon heating to form thermally-stable ring-containing or polymeric systems.

Conclusions

In this report, we have described the synthesis and characterization of 8 new zinc halide complexes of 1-(5-tetrazolidyl)alkyl-3-alkylimidazolium zwitterions, obtained through the click reaction of *N*-cyanoalkyl-functionalized imidazolium halide salts with azide anion and zinc bromide. Work to optimize the reaction conditions suggested *N*-cyanoalkyl-substituted imidazolium salts are ideal for the click synthesis of 5-tetrazoles. These results further extend the preliminary findings of an MHIL synthetic platform to include new tetrazole-based multi-heterocycles, which may find application in a variety of fields (e.g., energetic materials, coordination chemistry, pharmaceuticals, *etc.*).

Experimental Section

Materials and Methods:

All starting materials were purchased from Sigma-Aldrich (Milwaukee, WI) and used as received. The synthesis of the halide precursors **1-8[X]** and their characterization have been recently reported by our group.[6]

Melting point and glass transitions were determined for **9-16** by differential scanning calorimetry (DSC) using a DSC 2920 Modulated DSC, TA Instruments, Inc. (New Castle, DE) cooled with a liquid nitrogen cryostat. The calorimeter was calibrated for temperature and cell constants using indium (melting point 156.61 ^{o}C; $\boldsymbol{C}$ = 28.71 J·g^{-1}). Data were collected at constant atmospheric pressure, with heating at a rate of 5 ^{o}C·min^{-1} using samples between 5-15 mg in aluminum sample pans (sealed and then perforated with a pin-hole to equilibrate pressure from potential expansion of evolved gases). The DSC was adjusted so that zero heat flow was between 0 and -0.5 mW, and the baseline drift was less than 0.1 mW over the temperature range of 0-180 ^{o}C. An empty sample pan served as the reference.

Thermogravimetric analysis (TGA) for compounds **9-16** was performed using a TGA 2950, TA Instrument, Inc. (New Castle, DE). These experiments were conducted under air atmosphere and measured in the dynamic heating regime. Samples between 5-15 mg were heated under atmospheric pressure to 800 ^{o}C (except as noted) under constant heating ramp of 5 ^{o}C min^{-1} with a 30 min isotherm at 75 ^{o}C.

^{1}H and ^{13}C NMR spectra were collected utilizing a Bruker AV-500 (Karlsruhe, Germany) spectrometer operating at 500 MHz for ^{1}H NMR and 125 MHz for ^{13}C NMR spectra, and DMSO-d_6 was used as the solvent. Infrared spectra were obtained by direct measurement of the neat samples utilizing a Perkin-Elmer Spectrum 100 FT-IR instrument (Shelton, CT) featuring an attenuated total reflection (ATR) force gauge. Spectra were obtained in the range of 650 – 4000 cm^{-1}.

Synthetic Protocols:

General procedure for synthesis of zinc halide-complexed 1-(5-tetrazolidyl)alkyl-3-alkylimidazolium zwitterions,* 9-16: N*-cyanoalkyl-*N*-alkylimidazolium halide (**1-8[X]**) (0.77 to 10.6 mmol) was combined with sodium azide (1.1 eq.) in a 100 mL round-bottom flask with 50 mL water and stirred to dissolve with a magnetic stir bar. Zinc bromide was added (1.1 eq.), and the mixture was stirred at reflux overnight. Upon cooling, the resultant white solid was washed several times with water and filtered. The final product was dried at 60 ^{o}C for 24 h in the furnace, and reported yields are based upon the formula weight of the product calculated with $ZnBr_{0.8}Cl_{1.2}$ (**9**), $ZnBr_2$ (**10** and **14**), or ZnBrCl (**11**-**13**, **15**, **16**).

***1-(5-Tetrazolidyl)methyl-3-methylimidazolium·($ZnBr_{0.8}Cl_{1.2}$)* (9):** Compound **9** was prepared from **1[Cl]** (1.662 g, 10 mmol). White powder; ^{1}H NMR (360 MHz, DMSO-d_6) $\boldsymbol{\delta}$ ppm 9.18 (s, 1H), 7.75 (t, J = 1.7 Hz, 1H), 7.68 (t, J = 1.7 Hz, 1H), 5.57 (s, 2H); 3.87 (3H, s); ^{13}C

NMR (125 MHz, DMSO-d_6) $\boldsymbol{\delta}$ ppm 154.1, 138.0, 124.4, 123.5, 42.9, 36.5; FT-IR ($\boldsymbol{\nu}_{max}$): 3498 (w), 3103 (s), 3078 (s), 2076 (s), 1618 (w), 1572 (s), 1446 (s), 1433 (s), 1421 (s), 1340 (m), 1171 (s), 1072 (m), 839 (s), 816 (s), 776 (s), 692 (s) cm^{-1}.

***Optimization data collection for the conversion of 1-cyanomethyl-3-methylimidazolium chloride, 1[Cl], to zinc-coordination product, 9*: 1[Cl]** (0.015 g, 0.010 mmol) was dissolved with 1.1 eq. of both $ZnBr_2$ and NaN_3 in D_2O (1 mL). The progress of the reaction was monitored by ^1H NMR spectroscopy, where 85% conversion to **9** was observed at room temperature after about 2.5 h. The experiment was performed in a borosilicate glass NMR tube (5 mm diameter, thin wall, 7 inches length, Wilmad LabGlass, Vineland, NJ) where the progress of the reaction was checked periodically with ^1H NMR. A comparison of the signals for the C$\mathbf{H}_2$ peaks of the α-carbon nearest the nitrile precursor (**1-8[X]**) and tetrazole product (**9-16**) served as the measurable to quantify the estimated conversion for the click reaction.

***1-(2-(5-Tetrazolidyl)ethyl)-3-methylimidazolium·($ZnBr_2$)* (10):** Compound **10** was prepared from **2[Br]** (0.491 g, 2.5 mmol). White powder; ^1H NMR (360 MHz, DMSO-d_6) $\boldsymbol{\delta}$ ppm 9.08 (s, 1H), 7.65 (td, J = 4.4, 1.8 Hz, 2H), 4.58 (t, J = 6.9 Hz, 2H), 3.84 (s, 3H), 3.45 (t, J = 6.9 Hz, 2H); ^{13}C NMR (125 MHz, DMSO-d_6) $\boldsymbol{\delta}$ ppm 157.9, 137.4, 124.1, 122.9, 48.1, 36.4, 26.2; FT-IR ($\boldsymbol{\nu}_{max}$): 3569 (m), 3103 (m), 3098 (m), 2146 (m), 2066 (s), 1575 (m), 1560 (m), 1487 (m), 1421 (s), 1335 (m), 1161 (s), 1082 (m), 854 (s), 761 (s), 705 (m) cm^{-1}.

***1-(3-(5-Tetrazolidyl)propyl)-3-methylimidazolium·($ZnBr_{2-x}Cl_x$)* (11):** Compound **11** was prepared from **3[Cl]** (1.963 g, 10.6 mmol). White powder; ^1H NMR (500 MHz, DMSO-d_6) $\boldsymbol{\delta}$ ppm 9.10 (s, 1H), 7.70 (d, J = 25.6 Hz, 2H), 4.21 (t, J = 6.4 Hz, 2H), 3.85 (s, 3H), 3.00-2.86 (m, 2H), 2.18 (t, 2H); ^{13}C NMR (125 MHz, DMSO-d_6) $\boldsymbol{\delta}$ ppm 160.3, 137.0, 124.0, 122.7, 48.8, 36.3,

29.0, 21.3; FT-IR (ν_{max}): 3518 (w), 3104 (m), 3083 (m), 2066 (s), 1570 (s), 1560 (s), 1489 (s), 1439 (s), 1428 (s), 1156 (s), 1064 (m), 837 (s), 748 (s), 698 (m) cm^{-1}.

1-(4-(5-Tetrazolidyl)butyl)-3-methylimidazolium·($ZnBr_{2-x}Cl_x$) **(12):** Compound **12** was prepared from **4[Cl]** (0.815 g, 4.1 mmol). Yellowish solid; ^{1}H NMR (500 MHz, DMSO-d_6) δ ppm 9.07 (s, 1H), 7.68 (d, J = 24.3 Hz, 2H), 4.14 (t, J = 6.9 Hz, 2H), 3.83 (s, 1H), 2.87 (t, J = 6.8 Hz, 3H), 1.79-1.75 (m, 2H), 1.58 (q, 2H); ^{13}C NMR (125 MHz, DMSO-d_6) δ ppm 161.3, 137.0, 124.1, 122.7, 49.1, 36.4, 29.6, 25.6, 23.7; FT-IR (ν_{max}): 3514 (w), 3104 (w), 2946 (w), 2061 (s), 1570 (s), 1486 (m), 1426 (s), 1337 (m), 1161 (s), 1074 (m), 1019 (w), 829 (m), 743 (s) cm^{-1}.

1-(5-Tetrazolidyl)methyl-3-butylimidazolium·($ZnBr_{2-x}Cl_x$) **(13)**: Compound **13** was prepared from **5[Cl]** (1.000 g, 3.8 mmol). White powder; ^{1}H NMR (500 MHz, DMSO-d_6) δ ppm 9.26 (s, 1H), 7.78 (d, J = 29.4 Hz, 2H), 5.80 (s, 2H), 4.20 (t, J = 7.0 Hz, 2H), 1.83-1.72 (m, 2H), 1.26 (m, J = 14.3, 7.0 Hz, 2H), 0.90 (t, J = 7.2 Hz, 3H); ^{13}C NMR (125 MHz, DMSO-d_6) δ ppm 156.2, 136.9, 123.3, 122.9, 49.1, 44.0, 31.7, 19.2, 13.7; FT-IR (ν_{max}): 3098 (s), 2946 (m), 2865 (w), 2075 (m), 1565 (s), 1441 (s), 1335 (m), 1161 (s), 1138 (m), 1075 (m), 822 (s), 746 (s), 710 (s), 672 (s) cm^{-1}.

1-(2-(5-Tetrazolidyl)ethyl)-3-butylimidazolium·($ZnBr_2$) **(14):** Compound **14** was prepared from **6[Br]** (0.198 g, 0.77 mmol). White powder; ^{1}H NMR (500 MHz, DMSO-d_6) δ ppm 9.18 (s, 1H), 7.77 (s, 1H), 7.75 (s, 1H), 4.60 (t, J = 6.7 Hz, 2H), 4.13 (t, J = 7.0 Hz, 2H), 3.51 (t, J = 6.5 Hz, 2H), 1.70 (m, J = 7.1 Hz, 2H), 1.18 (m, J = 7.5 Hz, 2H), 0.85 (t, J = 7.3 Hz, 3H); ^{13}C NMR (125 MHz, DMSO-d_6) δ ppm 153.5, 136.7, 122.7, 48.8, 46.4, 31.4, 24.0, 18.8, 13.4; FT-IR (ν_{max}): 3572 (w), 3402 (w), 3140 (w), 3106 (w), 2962 (w), 2962 (w), 2934 (w), 2873

(w), 2161 (m), 2061 (s), 1561 (m), 1491 (w), 1439 (s), 1338 (m), 1288 (w), 1240 (w), 1158 (s), 1108 (w), 1070 (w), 1027 (w), 953 (w), 922 (w), 826 (m), 747 (m) cm^{-1}.

1-(3-(5-Tetrazolidyl)propyl)-3-butylimidazolium·(ZnBr$_{2-x}$Cl$_x$) **(15):** Compound **15** was prepared from **7[Cl]** (1.020 g, 4.5 mmol). White powder; ^{1}H NMR (500 MHz, DMSO-d_6) $\boldsymbol{\delta}$ ppm 9.14 (s, 1H), 9.14 (s, 1H), 7.73 (s, 1H), 4.16 (t, J = 6.8 Hz, 2H), 4.11 (t, J = 7.2 Hz, 2H), 2.86 (t, J = 7.3 Hz, 2H), 2.20-2.11 (m, 2H), 1.78-1.69 (m, 2H), 1.22 (dd, J = 14.9, 7.4 Hz, 2H), 0.85 (t, J = 7.3 Hz, 3H); ^{13}C NMR (125 MHz, DMSO-d_6) $\boldsymbol{\delta}$ ppm 160.3, 136.5, 122.9, 122.9, 49.1, 48.9, 31.6, 28.9, 21.4, 19.3, 13.8; FT-IR ($\boldsymbol{\nu}_{max}$): 3493 (w), 3108 (w), 2942 (w), 2061 (s), 1565 (s), 1426 (s), 1337 (m), 1161 (s), 1074 (m), 1021 (s), 834 (m), 743 (s) cm^{-1}.

1-(4-(5-Tetrazolidyl)butyl)-3-butylimidazolium·(ZnBr$_{2-x}$Cl$_x$) **(16):** Compound **16** was prepared from **8[Cl]** (1.039 g, 4.3 mmol). Dark yellow waxy solid; ^{1}H NMR (500 MHz, DMSO-d_6) $\boldsymbol{\delta}$ ppm (9.19 (s, 1H), 7.77 (d, J = 10.0 Hz, 2H), 4.32-3.89 (m, 4H), 2.92 (t, J = 7.3 Hz, 2H), 1.79 (dd, J = 14.8, 7.2 Hz, 4H), 1.64-1.55 (m, 2H), 1.26 (dd, J = 14.9, 7.4 Hz, 2H), 0.90 (t, J = 7.3 Hz, 3H); ^{13}C NMR (125 MHz, DMSO-d_6) $\boldsymbol{\delta}$ ppm 161.0, 136.3, 122.9, 122.8, 49.1, 49.1, 31.6, 29.4, 25.5, 23.8, 19.3, 13.7; FT-IR ($\boldsymbol{\nu}_{max}$): 3503 (w), 3099 (w), 2956 (w), 2066 (s), 1560 (s), 1489 (m), 1429 (s), 1158 (s), 1075 (m), 1019 (w), 829 (m), 743 (s) cm^{-1}.

X-ray diffraction analysis

Crystals of **9** were grown by the addition of a few drops of concentrated HNO_3 (70% w/w) to dissolve the powder and then, after evaporating to near dryness, acetone was added to wash the residual material which then formed crystals upon slow evaporation of the solvent at room temperature. Single-crystal X-ray diffraction data were collected on a Bruker CCD area detector-equipped diffractometer (Madison, WI) with graphite-monochromated Mo-$K\alpha$ radiation (λ = 0.71073 Å). The crystal of **9** was cooled to -100 ^{o}C with a stream of nitrogen gas.

SHELXTL-5 software was used for structure solution and refinement,[21,22] with refinement by using full-matrix least-squares methods on F^2. All atoms were readily located and the positions of all non-hydrogen atoms were refined anisotropically, where all hydrogen atoms were located in calculated positions riding on the bonded atom.

The halide positions exhibited substitutional disorder of chloride and bromide and were refined as 60% chloride and 40% bromide. Both sites were refined with the same occupancy and, from the crystallographic data, it is not clear whether the structure consisted of disordered $ZnCl_2/ZnBr_2$ units or if ZnClBr was also present.

Acknowledgements

This research was supported by the Air Force Office of Scientific Research (Grant FA9550-10-1-0521).

References

1 Demko, Z. P.; Sharpless, K. B. *J. Org. Chem.* **2001**, *66*, 7945.

2 Drab, D. M.; Shamshina, J. L.; Smiglak, M.; Hines, C. C.; Cordes, D. B.; Rogers, R. D. *Chem. Commun.* **2010**, *46*, 3544.

3 Katritzky, A. R.; Singh, S.; Kirichenko, K.; Smiglak, M.; Holbrey, J. D.; Reichert, W. M.; Spear, S. K.; Rogers, R. D. *Chem. – Eur. J.* **2006**, *12*, 4630.

4 Smiglak, M.; Hines, C. C.; Wilson, T. B.; Singh, S.; Vincek, A. S.; Kirichenko, K.; Katritzky, A. R.; Rogers, R. D. *Chem. – Eur. J.* **2010**, *16*, 1572.

5 Koldobskii, G. I. *Russ. J. Org. Chem.* **2006**, *42*, 469.

6 Drab, D. M.; Smiglak, M.; Shamshina, J. L.; Kelley, S. P.; Schneider, S.; Hawkins, T. W.; Rogers, R. D. *New J. Chem.* **2010**, *submitted*.

7 Himo, F.; Demko, Z. P.; Noodleman, L.; Sharpless, K. B. *J. Am. Chem. Soc.* **2002**, *124*, 12210.

8 Amantini, D.; Beleggia, R.; Fringuelli, F.; Pizzo, F.; Vaccaro, L. *J. Org. Chem.* **2004**, *69*, 2896.

9 Schmidt, B.; Meid, D.; Kieser, D. *Tetrahedron* **2007**, *63*, 492.

10 Zhao, D.; Fei, Z.; Scopelliti, R.; Dyson, P. J. *Inorg. Chem.* **2004**, *43*, 2197.

11 Tao, G. –H.; Zou, M.; Wang, X. –H.; Chen, Z. –Y.; Evans, D. G.; Kou, Y. *Aust. J. Chem*. **2005**, *58*, 327.

12 Zhao, D.; Fei, Z.; Ohlin, C. A.; Laurenczy, G.; Dyson, P. J. *Chem. Commun.* **2004**, 2500.

13 Himo, F.; Demko, Z. P.; Noodleman, L.; Sharpless, K. B. *J. Am. Chem. Soc.* **2003**, *125*, 9983.

14 Xue, X.; Wang, X. –S.; Wang, L. –Z.; Xiong, R. –G.; Abrahams, B. F.; You, X. –Z.; Xue, Z. –L.; Che, C. –M. *Inorg. Chem.* **2002**, *41*, 6544.

15 Zhao, H.; Qu, Z. –R.; Ye, H. –Y.; Xiong, R. –G. *Chem. Soc. Rev.* **2008**, *37*, 84.

16 Tong, X. L.; Wang, D. Z.; Hu, T. L.; Song, W. C.; Bu, X. H. *Crys. Growth. Des.* **2009**, *9*, 2280.

17 Zhang, Q.; Li, Z.; Zhang, J.; Zhang, S.; Zhu, L.; Yang, J.; Zhang, X.; Deng, Y. *J. Phys. Chem. B* **2007**, *111*, 2864.

18 Wooster, T. J.; Johanson, K. M.; Fraser, K. J.; MacFarlane, D. R.; Scott, J. L. *Green Chem.* **2006**, *8*, 691.

19 MacFarlane, D. R.; Forsyth, S. A.; Golding, J.; Deacon, G. B. *Green Chem.* **2002**, *4*, 444.

20 Golub, A. M.; Kohler, H.; Skopenko, V. V. In *Chemistry of Pseudohalides*; Elsevier: Berlin, 1986.

21 Sheldrick, G. M.; In *Program for Semiempirical Absorption Correction of Area Detector Data*; University of Göttingen: Germany, 1997.

22 Sheldrick, G. M.; In *SHELXTL (Version 6.14)*; Bruker AXS Inc.: Madison, WI, 2003.

CHAPTER 5

REACTIVITY OF *N*-CYANOALKYL-SUBSTITUTED IMIDAZOLIUM HALIDE SALTS BY SIMPLE ELUTION THROUGH AN AZIDE ANION EXCHANGE RESIN

Acknowledgement: S. P. Kelley (The University of Alabama, Tuscaloosa, AL) collected and refined X-ray diffraction data for the amide structure presented within.

Abstract

Certain *N*-cyanoalkyl-functionalized imidazolium halide salts unexpectedly underwent nitrile hydrolysis to amides, as well as dipolar cycloaddition to tetrazoles when eluted on azide anion exchanged resin suggesting convenient and recyclable resin-based approaches to amide- and tetrazole-based products.

In a recent communication of a design platform for the synthesis of multi-heterocyclic ionic liquids (MHILs) we described a general approach to tetrazole-based multi-heterocycles and corresponding MHILs, from *N*-cyanoalkyl-functionalized azoles.[1] The approach utilized click chemistry[2] followed by strategic conversion of formed azoles into MHILs. Seeking even more efficient synthetic methods, we turned to the work of Hawkins and co-workers, where they had reported the preparation of azolium azides by an azide anion exchange technique.[3] We believed such azide-based ILs would be interesting precursors for zwitterionic products, because the 1,3-dipolar cycloaddition reaction would occur between two ions of a single salt (as in the approach highlighted in Scheme 5.1), which might have benefits such as improved atom economy (all

atoms in the starting materials would be included in the zwitterionic product). Furthermore, the preparation of azolium azides with azide anion exchange resin has several advantages over other azide anion sources, including simple regeneration of the supported reagent,[4] and good exchange conversion (typically < 20 ppm of residual precursor anion).[5]

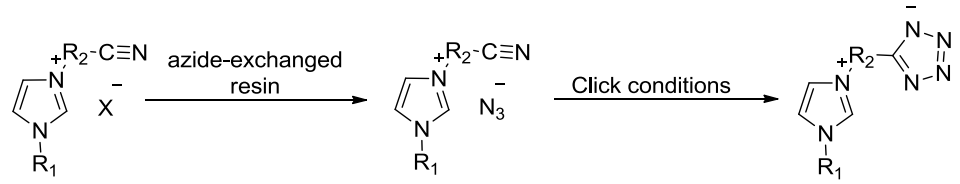

Scheme 5.1. Planned synthesis of azide-based ILs as precursors for zwitterionic products (X^- any halide).

Structurally similar *N*-cyanoalkyl-functionalized imidazolium RTILs were utilized for this investigation. Nitrile-terminated alkylene linkages included short linear chains (**2[Cl]** and **3[Cl]**), long linear chains (**1[Br]**) and branched (**4[Br]**), as shown in Scheme 5.2. Under anion exchange reaction conditions, it was found that the structure of starting N-cyanoalkyl-functionalized imidazolium cations greatly affects the reaction outcome; results are summarized in Scheme 5.2. Thus, when starting azoles were eluted on azide anion exchanged resin, the desired anion exchange occurred with **1[Br]**, the substrate containing *n*-hexylene $(CH_2)_6$ linker between terminal nitrile and imidazolium ring. However, the unexpected formation of a mixture of tetrazole and hydrolysis products was observed for substrates with a single carbon atom between nitrile and imidazolium ring, **2[Cl]**, **3[Cl]** and **4[Br]**, under otherwise identical conditions. Although the preparatory use of azide anion exchange resin has been reported for various synthetic applications,[6-9] there continues to be high interest in discovering new and improved routes for the hydrolysis of nitriles, where typically the use of high temperatures or metal catalysts[10] or the persistence of sequential hydration to carboxylic acid products when reacting in aqueous media[11] have been technical challenges. Similarly, conventional methods to

prepare tetrazoles from nitriles frequently use hazardous hydrazoic acid or require tedious separation of product from solvent, presenting obstacles for scale-up considerations. The results reported here suggest that by selection of the appropriate reactive *N*-cyanoalkyl-functionalized imidazolium cations, where the desired reactions can be accomplished by simple elution through an azide anion exchange resin under ambient conditions.

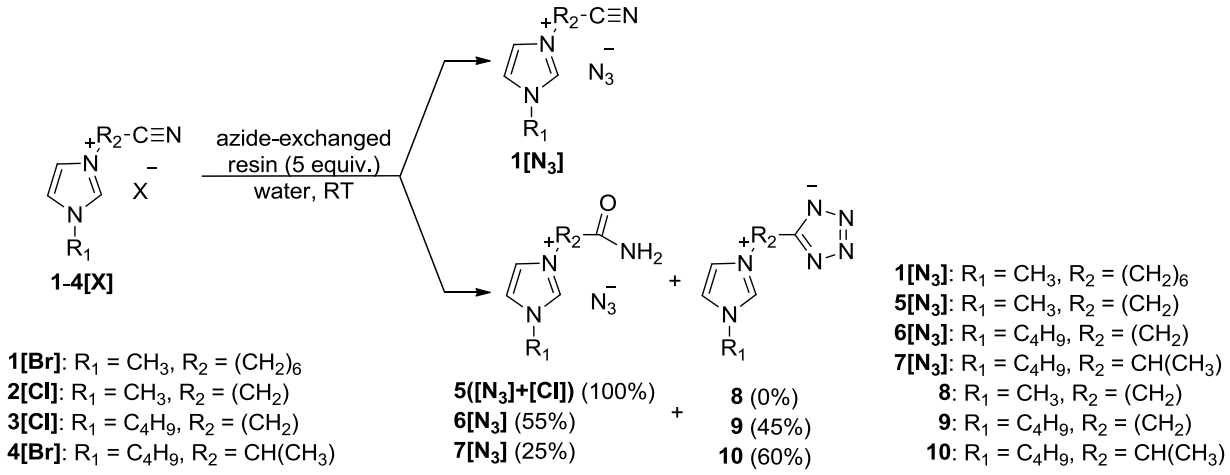

Scheme 5.2. Elution of *N*-cyanoalkyl-functionalized imidazolium halide salts (**1-4[X]**) on azide-exchanged resin columns resulted in anion exchange (**1[N_3]**), anion exchange with reaction of the cation to pure amide-functionalized azide (**5[N_3]**), or a mixture of amide with tetrazolate-functionalized zwitterion (**6[N_3]** + **9** or **7[N_3]** + **10**).

Halide precursors **1-4[X]** were prepared as described in a previous study.[12] Amberlite IRA-400 strongly basic anion exchange resin (16-50 mesh, 8% styrene-divinylbenzene copolymer cross-linkage) was converted from the commercially available Cl^- form to the N_3^- form based on previously reported methods,[13] where the resin was first washed with 2 bed volumes of deionized water to prepare a slurry which was then introduced into a glass chromatographic column (diameter = 1 cm, height = 10 or 50 cm). After allowing settling by eluting the water, the resin was converted to OH^- form by eluting with 20 bed volumes of 1 M NaOH at a rate of 2 cm/min. The complete removal of chloride anion was assessed by a spot-test, where 1% (w/w) $AgNO_3$ solution was added to an equal volume of the sample (*ca.* 0.5 mL

each) after neutralization with a few drops of concentrated HNO_3 (70% w/w). The OH^- form of the resin was then washed with 2 bed volumes of water to remove excess NaOH. To convert the resin to the N_3^- form, the column was eluted with 2 bed volumes of 0.5 M NaN_3, and the final pH was found to be ~ 7 using indicator paper. Final conditioning of the azide resin column was completed by washing with 5 bed volumes of water prior to introduction of the sample.

Salts **1-4[X]** were introduced onto the N_3^--resin column (1 cm diameter; 8 cm length; prepared from 5 eq. of the resin) as *ca.* 5 mmol halide/15 mL water at a rate of 2 cm/min. After rinsing the column with an additional 2 bed volumes of water, the eluted fractions were combined and set to dry under air stream overnight followed by additional drying under high vacuum for 24 h. The eluted products' structures were confirmed by ^1H and ^{13}C NMR, as well as FT-IR spectroscopy.

The precursor with the longest *N*-cyanoalkyl chain (-$(CH_2)_6$, **1[Br]**) formed the anticipated azide-exchanged salt **1[N_3]**. The nitrile carbon signal in the ^{13}C NMR spectrum ($\boldsymbol{\delta}$ = 115-119 ppm) and the appearance of a strong signal for the free-azide anion in the IR ($\boldsymbol{\nu}_{max}$ = 2000-2005 cm^{-1}) both supported formation of this salt. In contrast, halides with a single-carbon linker (**2[Cl], 3[Cl]**, and **4[Br]**) reacted to form either pure amide (as in cation of **5**) or a mixture of amide with tetrazole (as in (**6[N_3]** + **9**) and (**7[N_3]** + **10**)). The ^1H NMR spectra showed evidence for the formation of the amide group with a doublet (e.g., $\boldsymbol{\delta}$ = 8.01 ppm, 7.52 ppm for 2H in **5**) characteristic of the apparent separate signals for C(O)N**H_2** due to restricted rotation of the amide group on the time-scale of the NMR experiment. Temperature gradient and deuterium exchange ^1H NMR experiments were conducted on **5** to confirm the amide structure (see Experimental Section).

^{13}C NMR spectra for the eluted products of **2[Cl]**, **3[Cl]** and **4[Br]** also supported the formation of amide (e.g., **5**) or amide and tetrazole in mixture (e.g., (**6[N$_3$]** + **9**), (**7[N$_3$]** + **10**)), where there was a loss of the nitrile carbon signal (δ = 115-119 ppm) and the appearance of a new signal for the carbonyl C=O carbon (δ = 167 ppm). In the FT-IR spectrum, the presence of peaks characteristic for both the carbonyl (ν_{max} = 1691 cm^{-1}), as well as the free azide anion (ν_{max} = 2019 cm^{-1}) are in agreement with NMR data.

Structural data for the hydrate of **5[Cl]** (also present alongside with **5[N$_3$]**) was obtained by single-crystal X-ray diffraction using a crystal obtained from dissolving **5** in ethanol/acetonitrile (1:4) followed by slow vapor diffusion of diethyl ether for several days at room temperature. The imidazolium and amide portions of the molecule are planar with typical bond lengths and angles. Further discussion of the crystal packing is included in the Experimental Section.

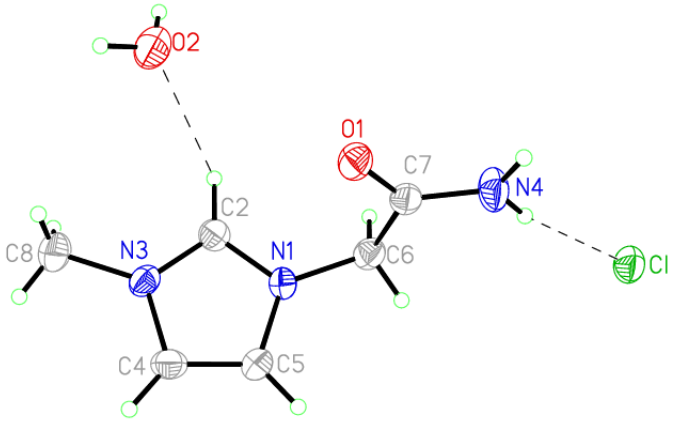

Figure 5.1. ORTEP (50% probability ellipsoids) illustration of the asymmetric/formula unit of **5[Cl]·H$_2$O.**

Unlike **2[Cl]** which forms only the amide **5**, **3[Cl]** and **4[Br]** formed mixtures of the amide and tetrazole. Identification of the mixed products (**6[N_3]** + **9** and **7[N_3]** + **10**) was supported by the presence of both tetrazole carbon (δ = 156 ppm) and carbonyl carbon (δ = 167 ppm) peaks in the ^{13}C NMR spectrum. Furthermore, ^{1}H and ^{13}C NMR data indicate the presence of two distinct imidazolium-based products. The integration of ^{1}H NMR signals was used to estimate the ratio of amide to tetrazole product in each case (compare **5[N_3]** (100% amide), **6[N_3]** + **9** (55% amide, 45% zwitterion), and **7[N_3]** + **10** (25% amide, 60% zwitterion, and 15% unreacted starting material).

Discussion

The difference between the reactivity of the cations on the resin might be explained mostly by the electronic effect. For the nitrile **1[Br]** with greater separation from the imidazolium core, simple exchange of the bromide anion for azide **1[N_3]** was observed. This might be due to 6-carbon distance between the nitrile group and the imidazolium core of this cation. The linker increase weakens the electron-withdrawing effect of positively charged imidazolium ring (as dipole induction rapidly diminishes with increasing distance), where support from studies of group contributions on the inductive effect from different charged and uncharged functionalities across variable chain lengths have been reported.[14] Computational results also indicated that electron-withdrawing substituents (e.g., imidazolium cation) activate the nitrile for both tetrazole formation as well as hydration,[15] where increasing distance from the imidazolium cation renders the nitrile group unreactive. This is directly correlated with the decrease of reactivity of nitrile group, and no effect of attached imidazolium is observed on **1[Br].** Therefore, only anion exchange product was isolated.

By contrast, in substrates **2[Cl]**, **3[Cl]** and **4[Br]** the nitrile group is separated from the imidazolium ring by a single carbon atom. Therefore, the α-hydrogen becomes quite acidic, and CH_2 therefore might be deprotonated by azide resulting in an intermediate which readily undergoes hydrolysis to amides followed by anion exchange, forming **5[N_3]**, **6[N_3]** and **7[N_3]**, as shown in Scheme 5.3 for substrate **2[Cl]**. The hydrolysis rate decreases for **4[Br]**, which is consistent with the donating effect of CH_3-group in branched ((CH)CH_3) linker. This donating effect contributes to decrease of electrophilicity of nitrile carbon and therefore results in slower reaction.

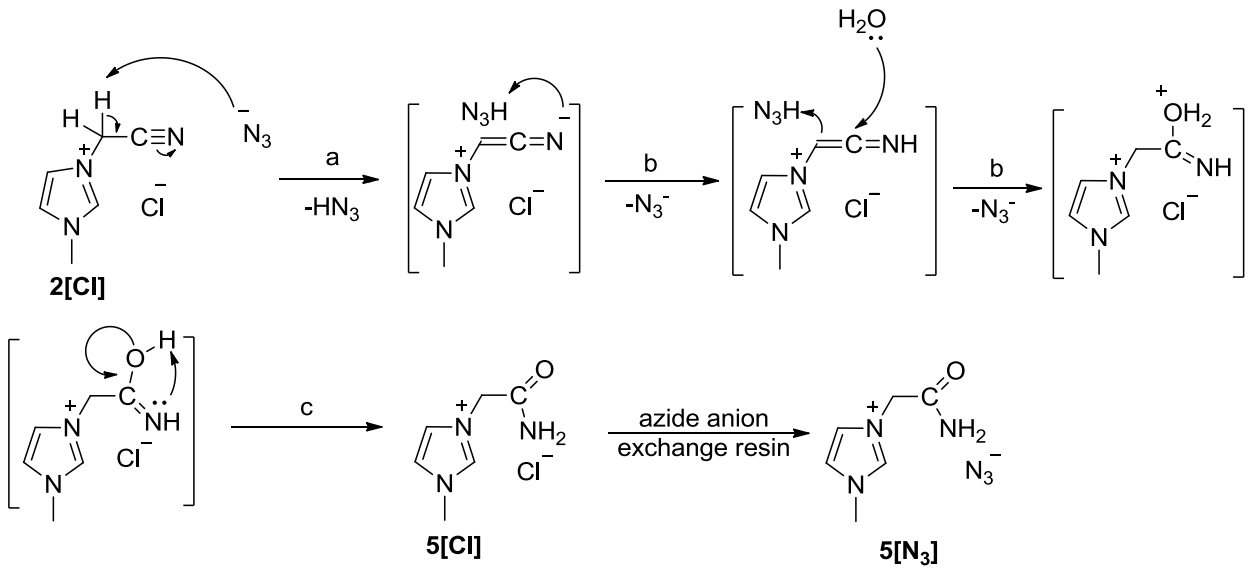

Scheme 5.3. Proposed mechanism for the hydration of 1-cyanomethyl-3-methylimidazolium chloride, **5[Cl]**, followed by azide exchange to form the 1-(acetamido)methyl-3-methylimidazolium azide product, **5[N_3]**.

The structures of **2[Cl]** and **3[Cl]** are similar, yet each cation shows different reactivity for hydrolysis under the same elution conditions (Scheme 5.3). The difference in reactivity would then appear to be related to the differing lengths of the alkyl chains on imidazolium nitrogen N3. Aromatic alkyl substituents are more electron-donating with increasing chain

length (e.g., alkyl inductive effect).[16] The longer alkyl side chain of **3[Cl]** may be able to donate enough electron density to reduce the reactivity of the nitrile carbon towards nucleophiles. This position is supported both by chemical theory[17] and experimental results, where longer reaction times and higher temperatures were required for the hydration of aromatic nitriles featuring longer alkyl substituents (e.g., butyl *vs.* methyl).[11,18]

The same electronic effect is responsible for formation of tetrazoles **9** and **10** from **3[Cl]** and **4[Br]**, and the click and hydrolysis reactions compete with each other. The key step in formation of tetrazoles **9** and **10** is the azide-nitrile cycloaddition, a click process where the nitrile is activated by a strong electron-withdrawing imidazolium ring. Thus, the electronegative imidazolium assists in the formation of a partial positive charge on the nitrile carbon and facilitates the approach of the azide anion. This is supported by the fact that trifluoroacetonitrile has been shown to react rapidly with sodium azide at room temperature in the absence of any catalyst.[19]

With possible coordination of the nitrile to the Lewis acidic cationic surface of the exchange resin polymer,[20] a concerted cycloaddition of azide *via* the nitrile carbon and ring closure by N-N bond formation results in the formed tetrazolate moiety.[21] The reactivity of **4[Br]** to form tetrazole product, **10**, over the hydration product **7[N_3]**, may occur due to the bromide anion as opposed to the chloride anions in **2[Cl]** and 3**[Cl]** (Scheme 5.4). Bromide exchange for azide was expected to be very complete (Scheme 5.4a), as the size and selectivity of azide is similar to that of chloride, and both azide and chloride have lower affinity towards the resin than bromide, as mentioned previously. Anion exchange must occur before the cycloaddition can happen because the tetrazole is a net neutral molecule, although hydrolysis can

occur before as evidenced by the observation of amide chloride salt **5[Cl]**. Once exchanged with [Cl^-], the azide anion is free for nucleophilic attack on the nitrile carbon (Scheme 5.4b), which results in an imidoyl azide in equilibrium with the observed 5-tetrazolate-functionalized zwitterion, **10** (Scheme 5.4c). Therefore, the prevalence of the tetrazolate form for **4[Br]** is due to the presence of an electron-donating methyl substituent on the α-carbon and bromide as anion.

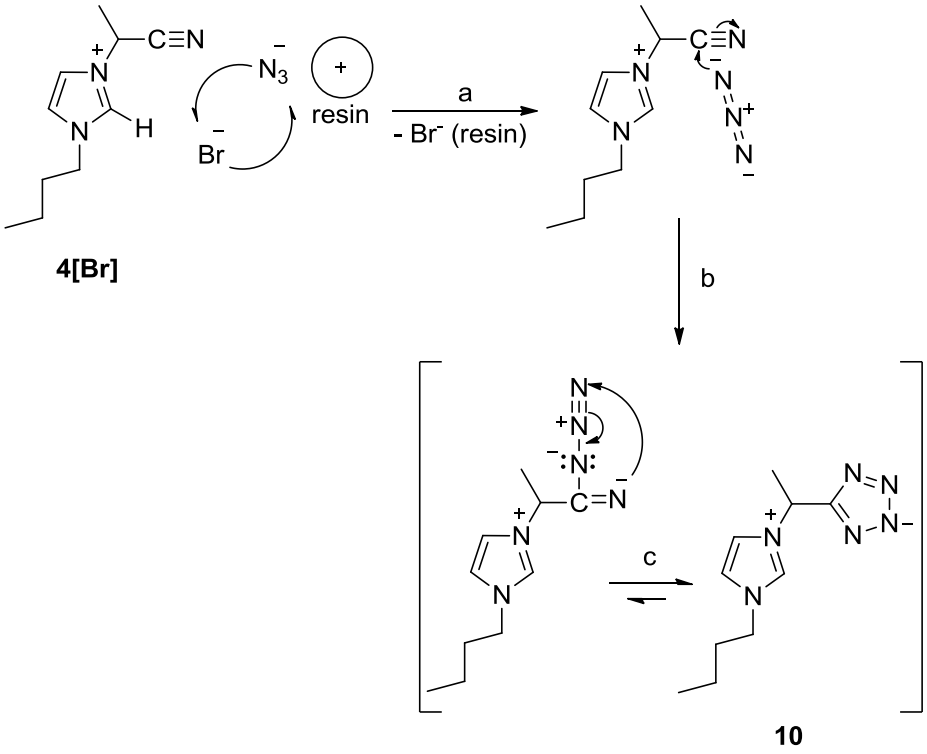

Scheme 5.4. Higher reactivity of 1-butyl-3-(1-cyanoethyl)imidazolium bromide, **4[Br]**, for tetrazole formation.

As the products were obtained by simple aqueous elution of the halide precursors through an azide exchange resin column, our results point towards a potentially useful and efficient technique for the synthesis of amide- and tetrazole-functionalized heterocycles with a variety of applications (such as pharmaceuticals and energetic materials synthesis). In future applications,

this technique could prove to be an easy preparatory route to improve the conventional processing and manufacture of commodity chemicals, where an understanding of the requisite substitution patterns and their electronic effects upon substrate reactivity would be key for meeting this challenge.

Experimental Section

Materials and Methods:

All reagents were used as received from commercial sources (Sigma-Aldrich, Milwaukee, WI) unless otherwise specified. All solvents were of 'solvent-grade' and were used without additional purification.

All ^{1}H and ^{13}C NMR spectra were obtained using a Bruker AV-500 (Karlsruhe, Germany) spectrometer operating at 500 or 125 MHz, respectively. Infrared (IR) analyses were obtained by measuring the absorption of neat samples using a Perkin-Elmer 100 FT-IR instrument, Perkin-Elmer (Shelton, CT) featuring and attenuated total reflectance (ATR) force gauge, and all spectra were obtained in the range of ν_{max} = 650-4000 cm^{-1}.

Single crystals of **5[Cl]·H_2O** were grown from **5[N_3]** by slow diffusion of diethyl ether into a 1:4 methanol:acetonitrile solution. Single crystal X-ray diffraction data were collected on a Bruker Apex II diffractometer with a CCD area detector using graphite monochromated Mo-*K*α radiation. Data were integrated with Bruker SAINT and an absorption correction was performed using Bruker AXScale.[22] Structure solution was carried out using the SHELXTL-97 suite from Bruker.[23]

The structure was solved by direct methods and refined by full matrix least squares refinement on F^2. All non-hydrogen atoms and hydrogen atoms bonded to N and O atoms were located from the difference map. Hydrogen atoms bonded to carbon atoms were placed in calculated positions, and hydrogen atoms on C8 were found to be disordered in two conformations offset from each other by 60°. These hydrogen atoms were not refined and held at 50% occupancy. For all other hydrogen atoms, coordinates were free to refine and thermal parameters were allowed to ride on the bonded atom.

Thermogravimetric analysis (TGA) was used to obtain thermal stability data (onset of 5% thermal decomposition, $\boldsymbol{T}_{5\%onset}$) for compounds (**1[N$_3$]** and **5[N$_3$]**) using a TGA 2950, TA Instruments, Inc. (New Castle, DE). All experiments were conducted under an air atmosphere and measured in the dynamic heating regime. Samples weighing between 5-15 mg were heated from 30-600 ^{o}C at a ramp rate of 5 ^{o}C/min, where a 30 min isotherm occurred at 75 ^{o}C.

Differential scanning calorimetry (DSC) was used to determine phase transitions (glass ($\boldsymbol{T}_g$), melting ($\boldsymbol{T}_m$), or liquid-liquid ($\boldsymbol{T}_{l\text{-}l}$) transitions, and crystallization ($\boldsymbol{T}_{cryst}$), when observed) for all precursors and pure products using a DSC 2920 Modulated DSC, TA Instruments, Inc. (New Castle, DE) cooled with a liquid nitrogen cryostat. The calorimeter was calibrated for temperature and cell constants using indium ($\boldsymbol{T}_m$ = 156.61 ^{o}C; $\boldsymbol{C}$ = 28.71 J g^{-1}). Data were collected at atmospheric pressure, where samples were initially heated at a rate of 5 ^{o}C·min^{-1} to a temperature not to exceed 50 ^{o}C below the measured $\boldsymbol{T}_{5\%onset}$ (obtained from TGA). The sample was then held for a 5 min isotherm prior to two cycles of cooling and heating (back to upper temperature limit from first heating) at a rate of 5 ^{o}C min^{-1} spaced by 5 minute isothermal holding at lower (T = -100 ^{o}C, unless otherwise stated) and upper (as indicated above) endpoint

temperatures. Samples between 5-15 mg were used in aluminum sample pans (sealed, then perforated with a pin-hole to equilibrate pressure resulting from potential expansion of evolved gases). The DSC was adjusted so that zero heat flow was between 0 and -0.5 mW, and the baseline drift was less than 0.1 mW over the temperature range of 0-180 ^{o}C. An empty sample pan served as the reference. Temperatures reported for the glass transition ($\boldsymbol{T}_g$) and melting ($\boldsymbol{T}_m$) were established as the onset temperature for the endothermic change in heat flow measured through the material and as the onset temperature for the exothermic change in heat flow measured in the case of observed crystallization ($\boldsymbol{T}_{cryst}$).

Temperature gradient ^{1}H NMR analysis for the amide structure was completed by dissolving 10 mg of **5[N$_3$]•H$_2$O** in DMSO-d_6 in a glass NMR tube and collecting 16 scan data sets on a 500 MHz frequency at different temperatures equilibrated by the NMR probe (T (K) = 298, 313, 323). Deuterium exchange was observed by cooling the same sample to 298 K and adding 2 drops of deuterium oxide (D_2O). After agitating and waiting 20 min, a 16 scan data set was collected on the 500 MHz instrument.

Synthetic Protocols for the Formation of Major Products:

***General procedure for the preparation of azide-exchanged anion exchange resin*:** Amberlite IRA-400 (Cl^- form) resin was first washed with 2 bed volumes of deionized water to prepare a slurry, which was then introduced into a glass chromatographic column (diameter = 1 cm, height = 10 or 50 cm). After settling, the resin is converted to OH^- form by eluting with 20 bed volumes of 1 M NaOH at a rate of 2 cm/min. The complete removal of chloride anion is assessed by a spot-test, where 1 % (w/w) $AgNO_3$ solution is added to an equal volume of the sample (*ca.* 0.5 mL each) after neutralization with a few drops of concentrated HNO_3 (70%

w/w). The OH- form of the resin is then washed with 2 bed volumes of water to remove excess NaOH. To convert the resin to the N_3^- form, the column is eluted with 2 bed volumes of 0.5 M NaN_3, where the final pH is checked for neutrality (pH ~ 7 using indicator paper). Final conditioning of the azide resin column was completed by washing with 5 bed volumes of water prior to introduction of the sample.

***General procedure for the elution of N-cyanoalkyl-functionalized imidazolium halides on azide exchanged resin*:** The synthesis and characterization of all halides (**1[Br]**, **2[Cl]**, **3[Cl]**, and **4[Br]**) have been reported.[10] *N*-cyanoalkyl halide samples (**1-4[X]**) were introduced onto the N_3^--resin column as *ca.* 5 mmol halide/15 mL water at a rate of 2 cm/min. After eluting the halide solution into the column, a final rinsing with 20 mL water, combining all eluted fractions, and removal of water by air stream prior to high vacuum drying overnight concluded the isolation of pure products (**1[N_3]** and **5[N_3]**) and mixtures **6[N_3]** + **9** and **7[N_3]** + **10**.

Preparation of 1-(6-cyanohexyl)-3-methylimidazolium azide (**1[N_3]**): Compound **1[N_3]** was prepared from **1[Br]** (1.373 g, 5.1 mmol). Amber liquid (61%); ^{1}H NMR (500 MHz, DMSO-d_6) $\boldsymbol{\delta}$ ppm 9.14 (s, 1H), 7.78 (t, 1H), 7.71 (t, 1H), 4.16 (t, 2H), 3.85 (s, 3H), 2.49 (m, 3H), 1.52 (m, 2H), 1.38 (m, 2H), 1.28 (m, 2H), 1.23 (t, 2H); ^{13}C NMR (125 MHz, DMSO-d_6) $\boldsymbol{\delta}$ ppm 136.5, 123.6, 122.2, 120.6, 48.6, 35.7, 29.0, 27.3, 24.6, 24.4, 16.0. FT-IR ($\boldsymbol{\nu}_{max}$ in cm^{-1}): 3707 (w), 3665 (w), 3376 (w), 3309 (w), 3145 (w), 2938 (s), 2864 (m), 2242 (w), 2000 (vs), 1644 (w), 1571 (m), 1456 (w), 1426 (w), 1332 (m), 1168 (s), 1055 (s), 1033 (s), 1015 (s), 840 (w), 756 (w), 736 (w).

Preparation of 1-(acetamido)methyl-3-methylimidazolium azide (**5[N_3]**): Compound **5[N_3]** was prepared from **2[Cl]** (0.788 g, 5.0 mmol). Brown solid (98%); ^{1}H NMR (500 MHz,

DMSO-d_6) $\boldsymbol{\delta}$ ppm 9.13 (s, 1H), 8.01 (s, 1H), 7.70 (s, 2H), 7.52 (s, 1H), 4.98 (s, 2H), 3.89 (s, 3H); ^{13}C NMR (125 MHz, DMSO-d_6) $\boldsymbol{\delta}$ ppm 166.7, 137.7, 123.8, 122.9, 50.4, 35.7. FT-IR ($\boldsymbol{\nu}_{max}$ in cm^{-1}): 3442 (w), 3391 (w), 3314 (w), 3148 (s), 3109 (s), 3090 (s), 2985 (w), 2945 (w), 2019 (vs), 1692 (vs), 1626 (s), 1571 (s), 1470 (w), 1440 (w), 1396 (s), 1381 (w), 1352 (m), 1303 (s), 1208 (m), 1166 (s), 1092 (w), 1033 (w), 974 (w), 850 (s), 775 (w), 757 (w), 672 (w).

Preparation of 1-(acetamido)methyl-3-butylimidazolium azide + 1-(5-tetrazolidyl)-methyl-3-methylimidazolium (**6[N$_3$]** + **9**, 55:45 mixture): The mixture of compound **6[N$_3$]** + **9** was prepared from **3[Cl]** (1.231 g, 6.0 mmol). Amber liquid (70%); ^{1}H NMR (500 MHz, DMSO-d_6) $\boldsymbol{\delta}$ ppm 9.27 (s, 1H), 9.17 (s, 1H), 7.98 (s, 1H), 7.85 (d, 2H), 7.71 (d, 2H), 7.54 (s, 1H), 5.53 (s, 2H), 4.96 (s, 2H), 4.21 (t, 2H), 4.18 (t, 2H), 1.76 (m, 2H), 1.73 (m, 2H), 1.26 (m, 2H), 1.21 (m, 2H), 0.91 (t, 3H), 0.88 (t, 3H); ^{13}C NMR (125 MHz, DMSO-d_6) $\boldsymbol{\delta}$ ppm 166.7, 155.7, 137.3, 136.1, 124.0, 122.9, 122.2, 121.7, 50.5, 48.6, 48.5, 44.8, 31.4, 31.3, 18.8, 18.7, 13.2. FT-IR ($\boldsymbol{\nu}_{max}$ in cm^{-1}): 3330 (w), 3148 (w), 3099 (w), 2965 (w), 2925 (w) 2204 (w), 2009 (vs), 1694 (s), 1671 (w), 1565 (m), 1466 (w), 1403 (w), 1310 (w), 1165 (m), 1143 (w), 1036 (w), 861 (w), 753 (m).

1-(acetamido)methyl-3-butylimidazolium azide + 1-(5-tetrazolidyl)methyl-3-methyl-imidazolium (**7[N$_3$]** + **10**, 25:60 mixture with 15% **4[N$_3$]**): The mixture of compound **7[N$_3$]** + **10** was prepared from **4[Br]** (1.678 g, 6.5 mmol). Amber liquid (83%); ^{1}H NMR (500 MHz, DMSO-d_6) $\boldsymbol{\delta}$ ppm 9.36 (s, 1H), 9.34 (s, 1H), 8.13 (s, 1H), 7.97 (s, 2H), 7.78 (s, 2H), 7.59 (s, 1H), 5.94 (m, 1H), 5.17 (m, 1H) 7.54 (s, 1H), 4.22 (t, 2H), 4.18 (t, 2H), 1.80 (d, 3H), 1.76 (d, 3H), 1.73 (m, 2H), 1.71 (m, 2H), 1.28 (m, 2H), 1.20 (m, 2H), 0.92 (t, 3H), 0.89 (t, 3H); FT-IR ($\boldsymbol{\nu}_{max}$ in

cm^{-1}): 3330 (w), 3148 (w), 3099 (w), 2965 (w), 2925 (w) 2204 (w), 2009 (vs), 1694 (s), 1671 (w), 1565 (m), 1466 (w), 1403 (w), 1310 (w), 1165 (m), 1143 (w), 1036 (w), 861 (w), 753 (m).

This research was supported by the Air Force Office of Scientific Research (Grant FA9550-10-1-0521).

References:

1 Drab, D. M.; Shamshina, J. L.; Smiglak, M.; Hines, C. C.; Cordes, D. B.; Rogers, R. D. *Chem. Commun.* **2010**, *46*, 3544.

2 Demko, Z. P.; Sharpless, K. B. *J. Org. Chem.* **2001**, *66*, 7945.

3 Schneider, S.; Hawkins, T.; Rosander, M.; Mills, J.; Brand, A.; Hudgens, L.; Warmoth, G.; Vij, V. *Inorg. Chem.* **2008**, *47*, 3617.

4 *AG 1, AG MP-1, and AG 2 Strong Anion Exchange Resin: Instruction Manual*, BioRad Laboratories: Hercules, CA (LIT212 Rev C; accessed online August 17, 2010; http://www.biorad.com/webroot/web/pdf/lsr/literature/ 9114_AG_1.pdf)

5 Dinarès, I.; de Miguel, C. G.; Ibáñez, A.; Mesquida, N.; Alcalde, E. *Green Chem.* **2009**, *11*, 1507.

6 Lakshman, M.; Nadkarni, D. V.; Lehr, R. E. *J. Org. Chem.* **1990**, *55*, 4892.

7 Lu, Y.; Taylor, R. T. *Tetrahedron Lett.* **2003**, *44*, 9267.

8 Blass, B. E.; Coburn, K. R.; Faulkner, A. L.; Seibel, W. L.; Srivastava, A. *Tetrahedron Lett.* **2003**, *44*, 2153.

9 Sreekumar, R.; Padmakumar, R.; Rugmini, P. *Chem. Commun.* **1997**, 1113.

10 Drab, D. M.; Smiglak, M.; Shamshina, J. L.; Kelley, S. P.; Schneider, S.; Hawkins, T. W.; Rogers, R. D. *New J. Chem.* **2010**, *submitted*.

11 Hassner, H.; Stern, M. *Angew. Chem., Int. Ed.* **1986**, *25*, 478.

12 Cherkasov, A. R.; Galkin, V. I.; Cherkasov, R. A. *J. Phys. Org. Chem.* **1998**, *11*, 437.

13 Exner, O. *J. Phys. Org. Chem.* **1999**, *12*, 265.

14 Himo, F.; Demko, Z. P.; Noodleman, L.; Sharpless, K. B. *J. Am. Chem. Soc.* **2002**, *124*, 12210.

15 Adcock, W.; Khor, T. –C. *J. Org. Chem.* **1978**, *43*, 1272.

16 Loew, G. H.; Chang, S.; Berkowitz, D. *J. Mol. Evol.* **1975**, *5*, 131.

17 Lee, J.; Kim, M.; Chang, S.; Lee, H. –Y. *Org. Lett.* **2009**, *11*, 5598.

18 Norris, W. P. *J. Org. Chem.* **1962**, *27*, 3248.

19 Jacobsen, H.; Burke, H.; Doering, S.; Kehr, G.; Erker, G.; Froehlich, R.; Meyer, O. *Organometallics* **1999**, *18*, 1724.

20 Paul, P. Nag, R. *Inorg. Chem.* **1987**, *26*, 2969.

21 Hay, R. W. MacLaren, F. M. *Transition Met. Chem.* **1999**, *24*, 398.

CHAPTER 6

AZOLIUM AZIDES TO AZOLATES: TETRAZOLE-BASED MULTI-HETEROCYCLIC IONIC LIQUIDS BY A MODULAR METAL-FREE CLICK STRATEGY

Abstract

We report multi-heterocyclic ionic liquids obtained *via* click reaction of azolium azide salts with alkylcyano-substituted azoles without using metals or solvents.

Multi-heterocyclic ionic liquids (MHILs) have received recent attention and are often obtained following synthetic methods (e.g., *N*-alkylation,[1] anion exchange) that are comparable to those used for acyclic and monocyclic ionic liquid (IL) systems. They are attractive candidate ions for making ILs as a result of additional design options that include variation of symmetry (same or different heterocycles,[2] bridge units,[3] heterocyclic substituents[4]), localization of formal charges in separate parts of the MHIL structure,[5] and flexible bridge units.[6] A heightened interest to understand how properties change with modifications of MHIL structure has led to an increase in research contributions from various diverse fields including energetic materials,[7] high-temperature chromatographic media,[8] IL-supported catalysts,[9] organometallic catalysts,[10] and chemical separations,[6a] to name but a few.

Our group recently reported a design platform for the synthesis of MHILs that demonstrated a facile approach to access MHILs and their precursors using a combination of

click chemistry[11] and IL-based synthetic strategies.[12] For example, both anionic and cationic MHIL components could be obtained by either a deprotonation-decarboxylation reaction previously explored by our group (Scheme 6.1a)[13] or through a Bronstëd acid-base reaction (Scheme 6.1b).[14] These transformations in structure and charge show the versatility of MHIL design and, as a result, have inspired us to further develop MHIL synthetic methodology.

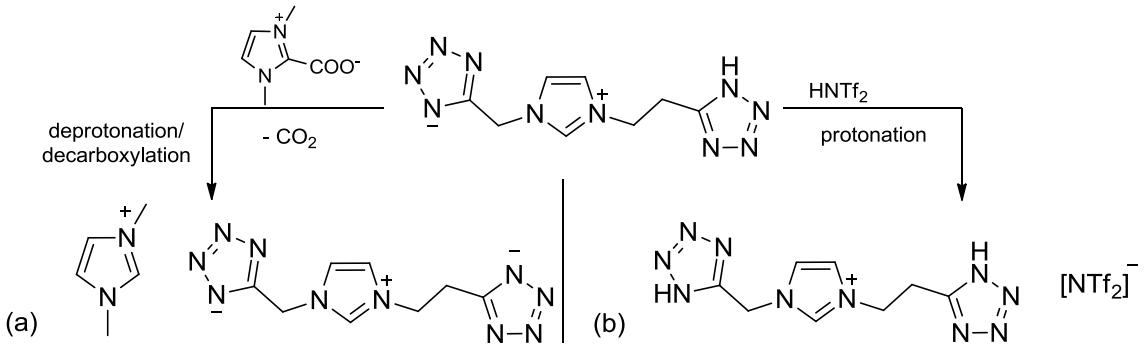

Scheme 6.1. A comparison of IL-based synthetic strategies (a) deprotonation/decarboxylation[13] and (b) protonation[14] that have been applied to MHIL synthesis.

Recently, azolium azide-based ILs have been reported as reaction media,[15] reagents,[16] or both,[17] including evaluation as candidates for safer energetic materials alternatives.[18] We thus targeted azolium azides as starting materials for the click synthesis of azolium azolate MHILs (Scheme 6.2). Azolium azides feature the required azide anion to form tetrazoles upon reaction with nitriles, and the azolium cation remains to complete the azolium azolate product structure. Thus a well-known 'dual-functional' design capacity[19] of ILs is evoked, whereby structural modification can be imposed independently at the site of the cation (from the azolium azide), as well as the anion (through the nitrile precursor). If successful, this new click reaction route to MHILs would further develop our original design platform to include multi-heterocyclic

structures of the azolium azolate class, which have recently been investigated by our group[20] and others[21] as potential energetic ionic liquids.

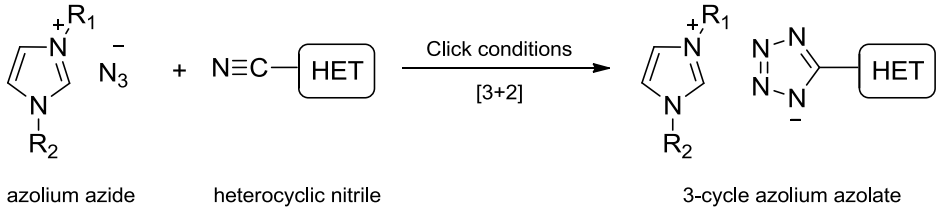

Scheme 6.2. New synthetic method proposed for MHILs by click synthesis of multi-heterocyclic azolium azolates from azolium azides and nitrile-functionalized heterocycles.

To the best of our knowledge, the determination of the reactivity between azolium azides and nitrile-functionalized heterocycles under click conditions has not yet been reported. We believe that the synthetic flexibility and exclusion of metals and solvent in this approach would have valuable impact by introducing new synthetic approaches to both azolium azolates as well as tetrazole-based targets by click chemistry. Herein, the successful click synthesis is described for MHIL azolium azolates from the click reaction of 1-butyl-3-methylimidazolium azide, **1[N_3]**, and 4-amino-1-butyl-1,2,4-triazolium azide, **2[N_3]** with *N*-(2-cyanoethyl)-functionalized azoles (**3** and **4**) (Scheme 6.3), where each azolium azolate features different heterocyclic combinations *via* the cation and anion.

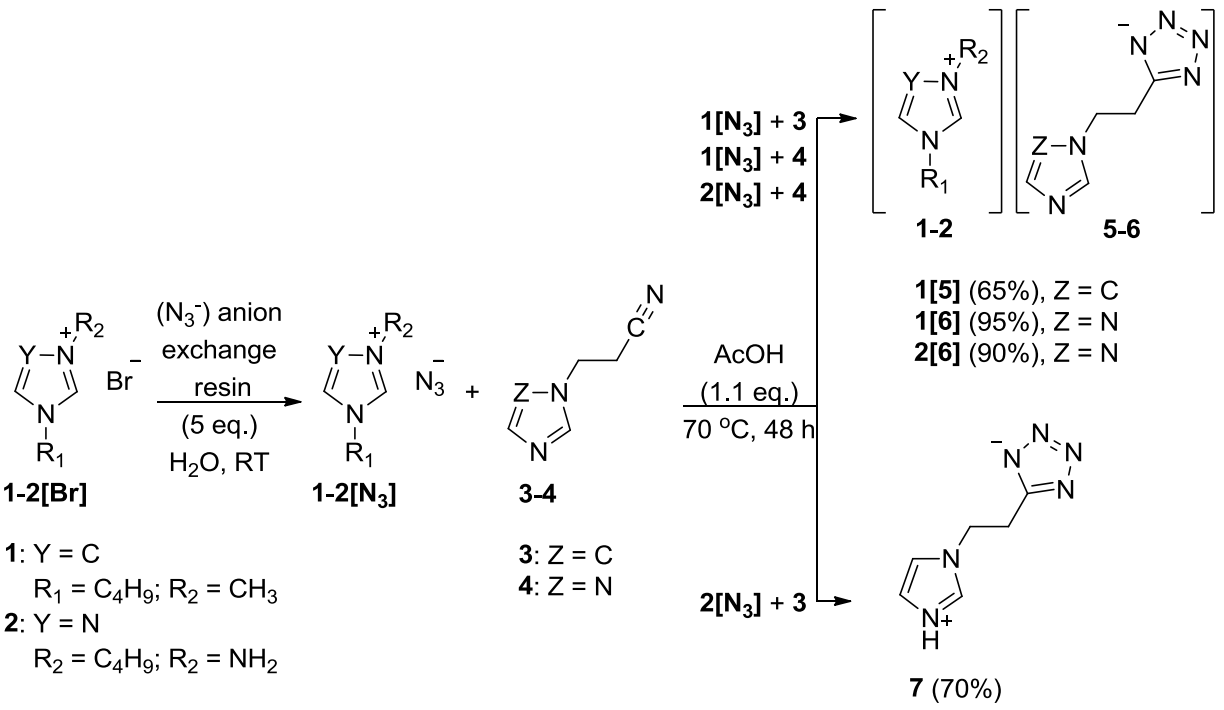

Scheme 6.3. Click synthesis of azolium azolate MHILs [1-butyl-3-methylimidazolium][5-(2-(imidazol-1-yl)ethyl)tetrazolate], **1[5]**, [1-butyl-3-methylimidazolium][5-(2-(1,2,4-triazol-1-yl)ethyl)tetrazolate], **1[6]**, and [4-amino-1-butyl-1,2,4-triazolium][5-(2-(1,2,4-triazol-1-yl)ethyl)tetrazolate], **2[6]**, from the reaction of *N*-2-cyanoethyl-functionalized azoles (**3-4**) with azolium azides (**1-2[N_3]**) formed by azide anion exchange from azolium bromides (**1-2[Br]**). A protonated anion bi-heterocyclic product, **7**, was formed from the reaction of azide **2[N_3]** with azole **3**.

Azolium azides **1-2[N_3]** were prepared by anion exchange of **1[Br]**[22] and **2[Br]**[23] *via* aqueous elution on an azide form of Amberlite IRA-400 resin (preparation described in Experimental Section). Based on the exchange capacity of the dry resin (3.8 meq/g resin), 5 eq. of azide anion exchange resin was used for each sample, and the isolated azides were obtained in excellent yield upon drying (90%, **1[N_3]**; 97%, **2[N_3]**).

The synthesis of the azolium azolates by click reaction proceeded by combining 1.2 - 4.4 mmol of azides **1-2[N_3]** with about 1.5 eq. of *N*-(2-cyanoethyl)-functionalized azole **3-4** in a

small vial to which 1.1 eq. of glacial acetic acid was added. Protonation of the nitrile N atom by acetic acid activated the nitrile for nucleophilic attack by the azide anion, forming a δ^+ charge at the nitrile carbon by the azide anion.[24] The use of acetic acid to activate nitriles for tetrazole formation from inorganic azide salts has been previously reported.[25]

Each vial was stirred for 48 h in an oil bath heated to 70 ^{o}C prior to cooling to room temperature, washing each sample several times with ethyl acetate, and then setting the sample to dry under high vacuum for 48 h at 70 ^{o}C. Without optimization of the reaction conditions, azolium azolate products [1-butyl-3-methylimidazolium][5-(2-(imidazol-1-yl)ethyl)tetrazolate], **1[5]**, [1-butyl-3-methylimidazolium][5-(2-(1,2,4-triazol-1-yl)ethyl)tetrazolate], **1[6]**, and [4-amino-1-butyl-1,2,4-triazolium][5-(2-(1,2,4-triazol-1-yl)ethyl)tetrazolate], **2[6]**, were each obtained as viscous liquids at room temperature, where yields were fair to excellent (65%, **1[5]**; 95%, **1[6]**; 90%, **2[6]**). The reaction of azolium azide **2[N$_3$]** with azole **3** led to the formation of the protonated zwitterion product, **7**, which readily formed as a white solid (yield = 70%) with a melting point of 81 ^{o}C.

The isolation of the zwitterion **7** might be explained by the difference in the pK_a values of the imidazole *vs.* triazole rings in **[5]**$^-$ *vs.* **[6]**$^-$. The pK_a values increases in the order 1-alkylimidazole (N**H**, pK_a = 7.12 - 7.16) > acetic acid (CH$_3$COO**H**, pK_a = 5) > 1-alkyl-1,2,4-triazole (N**H**, pK_a = 3.20 - 3.40).[26] It follows that the formation of the 1,2,4-triazole-based anion **[6]**$^-$ would be favored over the protonated anion due to its high acidity and loss of proton to available acetate. Thus, the formation of **1[6]** and **2[6]** are strongly favored by a high pH gradient, with acetic acid removed during purification.

In the case of compound **7**, 1-(2-(5-tetrazolidyl)ethyl)-3H-imidazolium, the acidity of the bi-heterocyclic imidazole ring is much lower than that of acetic acid, allowing the available proton to reside on the more basic imidazole. Slight differences in the concentration of acid or starting materials may be responsible for the precipitation of **7**, where in the same oil bath **2[6]** was obtained as a room-temperature IL. Precipitation of **7** may also be effected by the cation, where the amino NH protons of 4-amino-1-alkyl-1,2,4-triazolium salts were previously reported as good hydrogen bond donors that directed solid-state aggregation with suitable anionic acceptor groups.[27] Oxygen-containing anions such as nitrate and perchlorate are particularly good hydrogen bond acceptors,[28] where in this case the acetate anion could serve as a suitable acceptor with two available electron-rich oxygen atoms available for bonding.

^{1}H and ^{13}C NMR as well as FT-IR spectroscopies were used to confirm the formation of products and verify purity of both precursors and products (see Experimental Section for details). For ^{1}H NMR, the stoichiometric ratio of the *N*-alkyl protons of the cation and the $(CH_2)_2$ protons of the anion indicated that the product was isolated without excess of either starting azolium azide (**1-2[N_3]**) or azole (**3-4**). The zwitterionic structure, **7**, was determined in a similar way, where the 4-amino-1-butyl-1,2,4-triazolium cation (**2**) was not observed in the proton spectrum.

^{13}C NMR spectroscopy was used diagnostically to confirm the absence of the nitrile functionality (δ = 115-120 ppm) and the formation of the tetrazole moiety (δ = 155-160 ppm) in all click products. FT-IR spectroscopy also confirmed the purity from residual starting materials, where the absorptions characteristic for the C≡N stretch (ν_{max} = 2250 cm^{-1}), as well as asymmetric stretch for the free azide anion (ν_{max} = 2000-2010 cm^{-1}) were minimal for the spectra of the azolium azolate products (see Experimental Section for details).

All starting materials and products underwent thermogravimetric analysis (TGA), as well as differential scanning calorimetry (DSC) analysis to assess their relative thermal stabilities and observable phase transitions, respectively. The parameters used for all thermal data collection are described in the Experimental Section, where the data obtained are summarized in Table 6.1 and compared with available data values from the literature.

Table 6.1. Summary of thermal data for azolium bromides (**1-2[Br]**) and azide (**1-2[N_3]**) precursors and azolium azolate (**1[5]**, **1[6]**, and **2[6]**) and zwitterion (**7**) products.

Cation/Zwitterion Structure	Compound	T_g (^oC)[a]	T_m (T_{cryst}) (^oC)[a]	$T_{5\%onset}$ (T_{onset}) (^oC)[b]
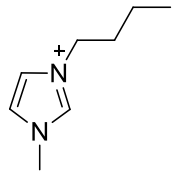 **1**	**1[Br]**	-72 Lit. = -50[29]	64[c] (25)[d]	225 (265) (Lit. = 273)[22]
	1[N_3]	-70	none observed Lit. = 36[18]	191 (214) (Lit. = 222)[18]
	1[5]	-53	none observed	179 (242)
	1[6]	-54	none observed	196 (232)
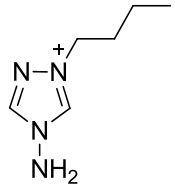 **2**	**2[Br]**	-42	36[c] Lit. = 47.5-49[23] (3.2)[d]	155 (173)
	2[N_3]	-43	none observed	124 (138)
	2[6]	-33	none observed	168 (235)
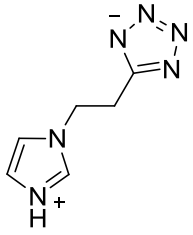 **7**	**7**	-52	81[e] 45 and 67 (37)[f]	194 (220)

[a] Melting point (T_m) and/or glass transition temperatures (T_g) were taken as the onset of observed transition and determined by DSC during the second heating cycle at a ramp rate of 5 $^oC \cdot min^{-1}$ after initially melting then cooling all samples to -100 °C. [b] Thermal decomposition temperatures were obtained by TGA using a heating ramp of 5 °C min^{-1} under a dried air atmosphere. All values are reported as (i) onset to 5 weight % loss of mass ($T_{5\%onset}$) and (ii) onset to total mass loss (T_{onset}) (parentheses). [c] Melting transition observed for 2nd and 3rd heating cycles. [d] Crystallization on heating from super-cooled liquid phase. [e] Initial melting on initial heating and dual melting transitions observed for subsequent heating cycles. [f] Crystallization on cooling cycles.

The glass transition temperatures (T_g) for precursors (e.g., compare T_g = -72 ^{o}C, **1[Br]**, to -70 ^{o}C, **1[N_3]**, and -42 ^{o}C, **2[Br]**, to -43 ^{o}C, **2[N_3]**, Table 6.1) and products (compare T_g = -53 ^{o}C, **1[5]**, to -54 ^{o}C, **1[6]**) have similar values for identical cations, which may be a result of the similar interactions between neighboring ions.[30] The observed lower T_g values for azides versus

bromides have been previously reported.[18] Although azolate anions with different numbers of nitrogen atoms have been found to vary in glass transition temperatures,[20c] azolium azolates **1[5]** and **1[6]** have very similar T_g values, where a strong effect of the common cation structure is implied. The DSC data for **7** indicate a mixture of polymorphic structures in the crystalline solid. Initial heating shows T_m = 81 ^oC, a crystallization upon cooling (T_{cryst} = 37 ^oC) and two distinct melting endotherms on the second and third heating cycles (T_m = 67 ^oC and T_m = 45 ^oC).

The azolium azides were the least stable of all compounds (Table 6.1), as observed when comparing azolate to bromide salts of 1-butyl-3-methylimidazolium ILs ($T_{5\%onset}$ = 179 ^oC, **1[5]**, 196 ^oC, **1[6]**, 225 ^oC, **1[Br]**). This agrees with previous reports comparing azolium azides with halides.[18] Overall, the 4-amino-1-butyl-1,2,4-triazolium series are the least thermally stable.

We have demonstrated that MHILs can be prepared by the click reaction of an azolium azide salt with a neutral cyanoazole precursor. This complements our previously published routes to such compounds by reacting *N*-cyanoalkyl-functionalized azolium cations with azide anion,[12] and pointing towards the design of new MHIL products from either the azolium cation or the neutral nitrile precursors (e.g., type of cycle and substituents). The resulting compartmentalized functionality can be exploited to target performance properties for a diverse set of applications (e.g., drug design, energetic materials, *etc.*). The benefits of asymmetric multi-heterocyclic structures and properties inherent to the IL form (e.g., low melting point, high thermal stability) may, thus, be systematically accessed.

Experimental Section

Materials and methods:

All reagents were from commercial sources (Sigma-Aldrich, Milwaukee, WI) and used as received, unless otherwise specified. All solvents were of 'solvent-grade' and were used without further purification.

All ^{1}H and ^{13}C NMR spectra were obtained with a Bruker AV-500 (Karlsruhe, Germany) spectrometer operating at 500 or 125 MHz, respectively. Infrared (IR) analyses were acquired from neat samples using a Perkin-Elmer 100 FT-IR instrument (Shelton, CT) which featured an attenuated total reflectance (ATR) force gauge, where all spectra were obtained in the range of $\boldsymbol{\nu}_{max}$ = 650 – 4000 cm^{-1}.

Thermogravimetric analyses (TGAs) were obtained for samples using a TGA 2950, TA Instruments, Inc. (New Castle, DE). All experiments were conducted under an air atmosphere and measured in the dynamic heating regime. Samples weighing between 5-15 mg were heated from 30-600 ^{o}C at a ramp rate of 5 ^{o}C/min, where a 30 min isotherm occurred at 75 ^{o}C. Click products (**[1][5]**, **[1][6]**, **[2][6]** and **7**) were recollected with an upper temperature limit of 800 ^{o}C in order to capture the complete thermal decomposition of these materials. Thermal stability for all materials was taken as the onset temperature for decomposition of the first 5% of the sample ($\boldsymbol{T}_{5\%onset}$).

Melting point/glass transition analyses were completed by differential scanning calorimetry (DSC) using a DSC 2920 Modulated DSC, TA Instruments, Inc. (New Castle, DE) equipped with a liquid nitrogen cryostat for cooling. The calorimeter was calibrated for temperature and cell constants using an indium standard ($\boldsymbol{T}_m$ = 156.61 ^{o}C; $\boldsymbol{C}$ = 28.71 J g^{-1}). All

data were collected at atmospheric pressure, where samples were initially heated at a rate of 5 $^{o}C \cdot min^{-1}$ to a temperature 50 ^{o}C below the measured $\boldsymbol{T}_{5\%onset}$ (obtained from TGA), then a 5 min isotherm prior to two cycles of cooling (to $\boldsymbol{T}$ = -100 ^{o}C) and heating. Samples between 5-15 mg were used in aluminum sample pans (sealed, then perforated with a pin-hole). The DSC was adjusted for zero heat flow between 0 and -0.5 mW, and the baseline drift was less than 0.1 mW over the temperature range of 0-180 ^{o}C. An empty sample pan served as the reference. Temperatures reported for the glass transition ($\boldsymbol{T}_g$) and melting ($\boldsymbol{T}_m$) were taken as the onset temperature for the endothermic change in heat flow and onset temperature for the exothermic change in heat flow in the case of observed crystallization ($\boldsymbol{T}_{cryst}$).

Elemental analyses were obtained by submitting samples **2[N$_3$]**, **1[5]**, **2[5]**, **1[6]**, and **7** for combustion analysis using a CHN analyzer (Galbriath Laboratories, Inc., Knoxville, TN) with a detection limit > 0.5%.

Synthetic protocols for the formation of major products:

General protocols for the synthesis of azolium azides **(1-2[N$_3$]):** Azolium bromides (**1[Br]**[22] and **2[Br]**[23]) were formed by methods previously reported by others, and the protocol for their exchange to azolium azides (**1-2[N$_3$]**) is described below and is based on a protocol described by Hawkins and co-workers.[18a]

General procedure for the preparation of azide-exchanged anion exchange resin**:** Amberlite IRA-400 (Cl^- form) resin was first washed with 2 bed volumes of deionized water to prepare a slurry, which was then introduced into a glass chromatographic column (diameter = 1 cm, height = 10 or 50 cm). After settling, the resin is converted to OH^- form by eluting with 20 bed volumes of 1 M NaOH at a rate of 2 cm/min. The complete removal of chloride anion is

assessed by a spot-test, where 1% (w/w) $AgNO_3$ solution is added to an equal volume of the sample (*ca.* 0.5 mL each) after neutralization with a few drops of concentrated HNO_3 (70% w/w). The OH^- form of the resin is then washed with 2 bed volumes of water to remove excess NaOH. To convert the resin to the N_3^- form, the column is eluted with 2 bed volumes of 0.5 M NaN_3, where the final pH is checked for neutrality (pH ~ 7 using indicator paper). Final conditioning of the azide resin column was completed by washing with 5 bed volumes of water prior to introduction of the sample.

***General procedure for the elution of halide salts* (1-2[Br]) *on azide-exchanged resin for isolation of azides* (1-2[N_3]):** For the formation of azides **1-2[N_3]**, yields were not optimized, and a general procedure may be followed. Halide salts (**1-2[Br]**, *ca.* 5 mmol each) were dissolved in 15 mL deionized water and introduced to the azide resin column prepared for 5 eq. of anion exchange capacity (exchange capacity of resin = 3.8 meq/g dry resin, about 7-8 g dry resin weight). At a rate of about 2 cm/min, the samples were eluted and collected in small Erlenmeyer flasks. The column is then washed with an additional 20 mL of water to ensure complete removal of **1-2[N_3]** from the resin, and all aqueous fractions are combined, dried over an air stream to concentrate, where final drying is finished in a high vacuum oven for 48 h at 70 ^oC.

***Preparation of 1-butyl-3-methylimidazolium azide* (1[N_3]):** Compound **1[N_3]** was prepared from **1[Br]** (1.373 g, 5.1 mmol). Amber liquid, water soluble (90%); ^1H NMR (500 MHz, DMSO-*d6*) $\boldsymbol{\delta}$ ppm 9.14 (s, 1H), 7.78 (t, 1H), 7.71 (t, 1H), 4.16 (7, 2H), 3.85 (s, 3H), 2.49 (m, 3H), 1.52 (m, 2H), 1.38 (m, 2H), 1.28 (m, 2H), 1.23 (t, 2H); ^{13}C NMR (125 MHz, DMSO-*d6*) $\boldsymbol{\delta}$ ppm 136.5, 123.6, 122.2, 120.6, 48.6, 35.7, 29.0, 27.3, 24.6, 24.4, 16.0; FT-IR ($\boldsymbol{\nu}_{max}$ cm^{-1}):

3391 (w), 3145 (w), 3084 (w), 2960 (w), 2935 (w), 2873 (w), 2005 (vs), 1640 (bw), 1570 (m), 1464 (w), 1428 (w), 1382 (w), 1336 (w), 1167 (s), 1115 (w), 848 (w), 754 (m).

***Preparation of 4-amino-1-butyl-1,2,4-triazolium azide* (2[N_3]):** Compound **2[N_3]** was prepared from **2[Br]** (1.173 g, 5.3 mmol). Amber liquid, water soluble (97%); ^{1}H NMR (500 MHz, DMSO-*d6*) δ ppm 10.74 (s, 1H), 9.34 (s, 1H), 8.03 (s, 2H), 4.34 (t, 2H), 1.79 (m, 2H), 1.28 (m, 2H), 0.89 (t, 3H); 13C NMR (125 MHz, DMSO-*d6*) δ ppm 145.3, 144.4, 142.9, 51.8, 30.5, 25.4, 13.6. FT-IR (ν_{max} in cm^{-1}): 3230 (w), 3112 (w), 2961 (w), 2937 (w), 2875 (w), 2005 (vs), 1631 (m), 1561 (w), 1523 (w), 1464 (w), 1406 (w), 1381 (w), 1326 (w), 1164 (m), 1114 (w), 1073 (w), 987 (m), 880 (w), 754 (w); elemental analysis calcd (%) for $C_6H_{13}N_7$: C 39.33, H 7.15, N 53.49; found: C 42.61, H 7.30, 31.92.

***General procedure for the synthesis of azolium azolate MHILs* (1[5], 1[6], and 2[6]) *and zwitterionic* (7) *products*:** The preparation of *N*-2-cyanoethyl-functionalized imidazole, **3**, and 1,2,4-triazole, **4**, have been previously reported by our group in other work.[12] Azolium azides **1-2[N_3]** (*ca.* 4 mmol) were combined with azole **3-4** (1.23-1.26 eq.) in small scintillation vials equipped with magnetic stir bars, to which glacial acetic acid (1.1 eq.) was added. The vials are sealed with screw caps and set to stir on a heated oil bath for 48 h at 70 ^{o}C. After cooling the vials to room temperature, each was washed several times with ethyl acetate while agitating the reaction mixture with a vortex stirrer. The remaining viscous liquids were set to dry in a high vacuum oven for 48 h at 70 ^{o}C to remove residual solvent and acetic acid to obtain MHILs **1[5]**, **1[6]**, and **2[6]** which were liquid at room temperature. The combination of **2[N_3]** and **3** resulted in a white, solid product, which readily precipitated from solution and was filtered and washed with ethyl acetate prior to drying under high vacuum for 48 h at 70 ^{o}C.

***Preparation of [1-butyl-3-methylimidazolium] [5-(2-(imidazol-1-yl)ethyl)tetrazolate]* (1[5]):** Compound **1[5]** was prepared from **1[N_3]** (0.641 g, 3.5 mmol) and **3** (0.536 g, 4.4 mmol). Amber liquid, water soluble (65%); ^{1}H NMR (500 MHz, DMSO-*d6*) δ ppm 9.21 (s, 1H), 7.79 (d, 1H), 7.72 (d, 1H), 7.70 (s, 1H), 7.14 (d, 1H), 6.81 (d, 1H), 4.28 (t, 2H), 4.16 (t, 2H), 3.85 (s, 3H), 3.10 (t, 2H), 1.74 (m, 2H), 1.24 (m, 2H), 0.89 (t, 3H); ^{13}C NMR (125 MHz, DMSO-*d6*) δ ppm 157.2, 137.1, 136.5, 127.9, 122.2, 119.3, 48.5, 45.4, 35.7, 31.3, 27.6, 21.2, 13.2. FT-IR (ν_{max} in cm^{-1}): 3414 (w), 3108 (w), 2961 (w), 2936 (w), 2875 (w), 2483 (bw), 1956 (bw), 1571 (m), 1511 (m), 1455 (w), 1364 (s), 1262 (vs), 1168 (s), 1083 (s), 1010 (m), 879 (m), 825 (m), 751 (s), 662 (s); elemental analysis calcd (%) for $C_{14}H_{22}N_8$: C 55.64, H 7.34, N 37.06; found: C 53.02, H 7.43, N 33.10.

***Preparation of [1-butyl-3-methylimidazolium][5-(2-(1,2,4-triazol-1-yl)ethyl)tetrazolate]* (1[6]):** Compound **1[6]** was prepared from **1[N_3]** (0.788 g, 4.4 mmol) and **4** (0.665 g, 5.4 mmol). Amber liquid, water soluble (95%); ^{1}H NMR (500 MHz, DMSO-*d6*) δ ppm 9.21 (s, 1H), 8.41 (s, 1H), 7.91 (s, 1H), 7.79 (d, 1H), 7.72 (d, 1H), 4.49 (t, 2H), 4.15 (t, 2H), 3.85 (s, 3H), 3.12 (t, 2H), 1.75 (m, 2H), 1.24 (m, 2H), 0.89 (t, 3H); ^{13}C NMR (125 MHz, DMSO-*d6*) δ ppm 157.4, 151.0, 143.8, 136.5, 123.6, 122.2, 48.5, 48.3, 35.7, 31.3, 26.5, 13.2. FT-IR (ν_{max} in cm^{-1}): 3392 (bw), 3101 (m), 2961 (w), 2963 (w), 2875 (w), 2482 (w), 1962 (w), 1571 (s), 1508 (s), 1461 (m), 1364 (s), 1269 (vs), 1207 (m), 1168 (s), 1138 (s), 1004 (s), 958 (w), 877m(s), 753 (m), 681 (s); elemental analysis calcd (%) for $C_{13}H_{21}N_9$: C 51.50, H 6.98, N 41.56; found: C 49.89, H 7.38, N 37.31.

***Preparation of [4-amino-1-butyl-1,2,4-triazolium][5-(2-(1,2,4-triazol-1-yl)ethyl)-tetrazolate]* (2[6]):** Compound **2[6]** was prepared from **2[N_3]** (0.722 g, 3.9 mmol) and **4** (0.612 g,

5.0 mmol). Amber liquid, water soluble (90%); ^{1}H NMR (500 MHz, DMSO-*d6*) $\boldsymbol{\delta}$ ppm 10.26 (s, 1H), 9.21 (s, 1H), 8.58 (d, 1H), 7.92 (s, 1H), 7.08 (s, 2H), 4.50 (t, 2H), 4.37 (t, 2H), 3.17 (t, 2H), 1.80 (m, 2H), 1,26 (m, 2H), 0.89 (t, 3H); ^{13}C NMR (125 MHz, DMSO-*d6*) $\boldsymbol{\delta}$ ppm 151.7, 145.7, 144.4, 143.1, 52.0, 48.2, 30.5, 26.2, 19.1, 13.7. FT-IR ($\boldsymbol{\nu}_{max}$ in cm^{-1}): 3417 (w), 3205 (w), 3109 (s), 2962 (s), 2875 (w), 2749 (w), 1631 (s), 1561 (m), 1508 (vs), 1460 (s), 1404 (m), 1370 (m), 1272 (vs), 1207 (m), 1165 (s), 1138 (s), 1072 (m), 1003 (s), 990 (s), 876 (s), 755 (w), 717 (w), 680 (s); elemental analysis calcd (%) for $C_{11}H_{19}N_{11}$: C 43.29, H 6.28, N 50.47; found: C 41.58, H 6.18, N 48.25.

***Preparation of 1-(2-(5-tetrazolidyl)ethyl)-3H-imidazolium* (7):** Compound **7** was prepared from **2[N_3]** (0.210 g, 1.2 mmol) and **3** (0.184 g, 1.5 mmol). White solid, water soluble (70%); ^{1}H NMR (500 MHz, DMSO-*d6*) $\boldsymbol{\delta}$ ppm 7.68 (s, 1H), 7.17 (s, 1H), 6.90 (s, 1H), 4.42 (t, 2H), 3.35 (t, 2H); ^{13}C NMR (125 MHz, DMSO-*d6*) $\boldsymbol{\delta}$ ppm 154.0, 137.1, 127.7, 119.4, 43.9, 25.4. FT-IR ($\boldsymbol{\nu}_{max}$ in cm^{-1}): 3707 (w), 3116 (w), 3006 (w), 2973 (s), 2939 (w), 2923 (w), 2866 (w), 2844 (w), 2826 (w), 2348 (bw), 1921 (bw), 1599 (w), 1526 (w), 1511 (w), 1455 (w), 1398 (w), 1345 (w), 1295 (w), 1271 (w), 1240 (w), 1197 (w), 1056 (vs), 1032 (s), 1014 (s), 935 (m), 855 (m), 757 (s), 683 (w); elemental analysis calcd (%) for $C_6H_8N_6$: C 43.92, H 4.92, N 51.20; found: C 43.79, H 5.07, N 48.96.

This research was supported by the Air Force Office of Scientific Research (Grant FA9550-10-1-0521).

References

1 Han, X.; Armstrong, D. W. *Org. Lett.* **2005**, *7*, 4205.

2 (*a*) Wang, R.; Zeng, Z.; Twamley, B.; Piekarski, M. M.; Shreeve, J. M. *Eur. J. Org. Chem.* **2007**, 655; (*b*) Leclercq, L.; Suisse, I.; Nowogrocki, G.; Agbossou-Niedercorn, F. *Green Chem.* **2007**, *9*, 1097.

3 Pernak, J.; Skrzypczak, A.; Lota, G.; Frackowiak, E. *Chem. –Eur. J.* **2007**, *13*, 3106.

4 (*a*) Schmidt, A.; Mordhorst, T.; Nieger, M. *Org. Biomol. Chem.* **2005**, *3*, 3788; (*b*) Wang, R.; Piekarski, M. M.; Shreeve, J. M. *Org. Biomol. Chem.* **2006**, *4*, 1878.

5 Wang, R.; Gao, H.; Ye, C.; Shreeve, J. M. *Chem. Mater.* **2007**, *19*, 144.

6 (*a*) Holbrey, J. D.; Visser, A. E.; Spear, S. K.; Reichert, W. M.; Swatloski, R. P.; Broker, G. A.; Rogers, R. D. *Green Chem.* **2003**, *5*, 129; (*b*) Zeng, Z.; Phillips, B. S.; Xiao, J. –C.; Shreeve, J. M. *Chem. Mater.* **2008**, *20*, 2719.

7 Jin, C. –M.; Ye, C.; Piekarski, C.; Twamley, B.; Shreeve, J. M. *Eur. J. Inorg. Chem.* **2005**, 3760.

8 Anderson, J. L.; Ding, R.; Ellern, A.; Armstrong, D. W. *J. Am. Chem. Soc.* **2005**, *127*, 593.

9 Ni, B.; Headley, A. D. *Chem. –Eur. J.* **2010**, *16*, 4426.

10 Patil, M. L.; Rao, C. V. L.; Takizawa, S.; Takenaka, K.; Onitsuka, K.; Sasai, H. *Tetrahedron* **2007**, *63*, 12702.

11 Demko, Z. P.; Sharpless, K. B. *J. Org. Chem.* **2001**, *66*, 7945.

12 Drab, D. M.; Shamshina, J. L.; Smiglak, M.; Hines, C. C.; Cordes, D. B.; Rogers, R. D. *Chem. Commun.* **2010**, *46*, 3544.

13 Smiglak, M.; Holbrey, J. D.; Griffin, S. T.; Reichert, W. M.; Swatloski, R. P.; Katritzky, A. R.; Yang, H.; Zhang, D.; Kirichenko, K.; Rogers, R. D. *Green Chem.* **2007**, *9*, 90.

14 Fuller, J.; Carlin, R. T.; De Long, H. C.; Haworth, D. J. *J. Chem. Soc., Chem. Commun.* **1994**, 299.

15 Landini, D.; Maia, A. *Tetrahedron Lett.* **2005**, *46*, 3961.

16 (*a*) Betti, C.; Landini, D.; Maia, A. *Tetrahedron* **2008**, *64*, 1689; (*b*) D'Anna, F.; Marullo, S.; Noto, R. *J. Org. Chem.* **2008**, *73*, 6224; (*c*) D'Anna, F.; Marullo, S.; Noto, R. *J. Org. Chem.* **2010**, *75*, 767.

17 Ranu, B. C.; Adak, L.; Banerjee, S. *Can. J. Chem.* **2007**, *85*, 366.

18 (*a*) Schneider, S.; Hawkins, T.; Rosander, M.; Mills, J.; Vaghjiani, G.; Chambreau, S. *Inorg. Chem.* **2008**, *47*, 6082; (*b*) Chambreau, S. D.; Schneider, S.; Rosander, M.; Hawkins, T.; Gallegos, C. J.; Pastewait, M. F.; Vaghjiani, G. L. *J. Phys. Chem. A* **2008**, *112*, 7816; (*c*) Bedrov, D.; Borodin, O. *J. Phys. Chem. B* **2010**, *114*, 12802.

19 Smiglak, M.; Metlen, A.; Rogers, R. D. *Acc. Chem. Res.* **2007**, *40*, 1182.

20 (*a*) Katritzky, A. R.; Singh, S.; Kirichenko, K.; Smiglak, M.; Holbrey, J. D.; Reichert, W. M.; Spear, S. K.; Rogers, R. D. *Chem. – Eur. J.* **2006**, *12*, 4630; (*b*) Smiglak, M.; Bridges, N. J.; Dilip, M.; Rogers, R. D. *Chem. – Eur. J.*,**2008**, *14*, 11314; (*c*) Smiglak, M.; Hines, C. C.; Wilson, T. B.; Singh, S.; Vincek, A. S.; Kirichenko, K.; Katritzky, A. R.; Rogers, R. D. *Chem. – Eur. J.* **2010**, *16*, 1572.

21 Xue, H.; Gao, Y.; Twamley, B.; Shreeve, J. M. *Inorg. Chem.* **2005**, *44*, 5068.

22 Bonhôte, P.; Dias, A. –P.; Papageorgiou, N.; Kalyanasundaram, K.; Grätzel, M. *Inorg. Chem.* **1996**, *35*, 1168.

23 Astleford, B. A.; Goe, G. L.; Keay, J. G.; Scriven, E. F. V. *J. Org. Chem.* **1989**, *54*, 731.

24 Finnegan, W. G.; Henry, R. A.; Lofquist, R. *J. Am. Chem. Soc.* **1958**, *80*, 3908.

25 (*a*) Schmidt, B.; Meid, D.; Kieser, D. *Tetrahedron* **2007**, *63*, 492; (*b*) Gutmann, B.; Roduit, J. –P.; Roberge, D.; Kappe, C. O. *Angew. Chem., Int. Ed.* **2010**, *49*, 7101; (*c*) Zlotin, S. G.; Makhova, N. N. *Russ. Chem. Rev.* **2010**, *79*, 543.

26 Catalan, J.; Abboud, J. L. M.; Elguero, J. *Adv. Heterocycl. Chem.* **1986**, *41*, 187.

27 (*a*) Trohalaki, S.; Pachter, R.; Drake, G. W.; Hawkins, T. *Energy Fuels* **2005**, *19*, 279; (*b*) Schwarzler, A.; Laus, G.; Kahlenberg, V.; Wurst, K.; Gelbrich, T.; Kreutz, H.; Kopacka, H.; Bonn, G.; Schottenberger, H. *Z. Naturforsch., B: J. Chem. Sci.* **2009**, *64*, 603.

28 Xue, H.; Arritt, S. W.; Twamley, B.; Shreeve, J. M. *Inorg. Chem.* **2004**, *43*, 7972; (*b*) Xue, H.; Twamley, B.; Shreeve, J. M. *J. Mater. Chem.* **2005**, *15*, 3459.

29 Fredlake, C. P.; Crosthwaite, J. M.; Hert, D. G.; Aki, S. N. V. K.; Brennecke, J. F. *J. Chem. Eng. Data* **2004**, *49,* 954.

30 Kun, D.; Suojiang, Z.; Daxi, W.; Xiaoqian, Y. *J. Phys. Chem. A* **2006**, *110,* 9775.

CHAPTER 7

CONCLUSIONS

Multi-heterocyclic ionic liquids (MHILs) are an emerging class of compounds capable of modification at numerous levels. In part from the increased scrutiny of bridged MHILs in recent years, there persists a demand for a deeper understanding of MHIL chemistry (i) to target performance requirements in properties for specific applications (e.g., energetic materials) as well as (ii) to examine fundamental questions regarding the nature of MHILs, such as how compounds can be made to exhibit IL behavior when featuring multi-heterocyclic base structures. The work compiled in this dissertation has addressed each of these challenges through the synthesis of MHILs and their precursors as well as in the development of novel synthetic methods that expand the structural scope and current techniques for MHIL preparation.

Work began with the synthesis and characterization of *N*-cyanoalkyl-functionalized imidazolium salts (Chapter 2), where structural modifications were made for both *N*-alkyl (methyl, butyl, and 2-cyanoethyl) and *N*-cyanoalkyl ($(CH_2)_nCN$, where n = 1-6, and $CH(CH_3)CN$) chain lengths as well as type of anion present (original halide, or exchanged nitrate or dicyanamide by either anion exchange resin or silver salt metathesis, respectively). Throughout this study, all halide salt precursors were obtained using literature protocols by the alkylation of *N*-alkylimidazoles with different commercially available haloalkylnitriles, and

nitrate and dicyanamide analogues were prepared *via* nitrate anion exchange resin or silver dicyanamide metathesis, respectively. From the characterization data of the 41 salts prepared, patterns in phase transitions were observed that depended upon the *N*-substituent length and the type of anion. For example, it was found that increasing the *N*-alkyl and *N*-cyanoalkyl substituent lengths resulted in reduced $\boldsymbol{T}_g$ and $\boldsymbol{T}_m$ values, where an effect of the anion on $\boldsymbol{T}_g$ values was also suggested ($\boldsymbol{T}_g$: $[N(CN)_2]^- < [NO_3]^- < [X]^-$).

In addition to phase transition behavior, thermal stabilities estimated by TGA experiments were compared between series of salts showing that shorter *N*-cyanoalkyl-functionalized cations (e.g., *N*-$(CH_2)_nCN$, where n = 1-2, and *N*-$CH(CH_3)CN$) were less stable (as assessed by comparing $\boldsymbol{T}_{5\%onset}$ values) compared to analogous cations having longer *N*-cyanoalkyl chains. Interestingly, this trend was strongly directed by the type of anion present, where the presence of the nitrate anion appeared to destabilize the shorter *N*-cyanoalkyl-functionalized salts, and the dicyanamide anion was most destabilizing in the presence of *N*-(2-cyanoalkyl)-functionalized cations. Thus, it was concluded that the length of the *N*-cyanoalkyl chain and type of anion influenced the observed thermal stability of the salts, contributing to information that can be used for the future design of ILs. How cation stabilities change as a function of *N*-alkyl and *N*-cyanoalkyl groups would later be used in rationalizing the differences in reactivity of *N*-cyanoalkyl-functionalized imidazolium salts for both click synthesis of bi-heterocyclic targets (Chapters 4 and 5) as well as in the selective reactivity of these same cations for either hydrolysis or cycloaddition to tetrazolates when eluted on an azide anion exchange resin column (Chapter 5).

Overall, this investigation showed how the thermal properties of *N*-cyanoalkyl-functionalized imidazolium salts could be targeted by systematic changes in cation and anion structure, where these results might be applied for future EIL design. Additional evidence for the production of carbonaceous char (formed upon heating in the TGA experiment), also depending on the structure of the cation substituents and anion, points towards potential applications for the directed fabrication of mesoporous carbon-based solid supports for various applications (e.g., catalysis, chemical separations, *etc.*). In subsequent chapters, the dual-functional nature of *N*-cyanoalkyl-functionalized imidazolium salts would contribute towards the design of new MHILs (Chapter 3) and their precursors (Chapters 4 and 5).

The synthesis of MHILs and their precursors was initiated *via* a new design platform (Chapter 3) that utilized a general click synthetic strategy to access bi- and tri-heterocyclic compounds by sequentially functionalizing azoles with *N*-cyanoalkyl substituents followed by reaction of the nitrile component with azide anion to form a new tetrazole moiety. The first part of this effort had resulted in the preparation of new compounds that varied systematically in charge (zwitterion, anion, and cation) and structure (different heterocycles and bridge units). However, none of these products were ILs by definition (e.g., mp < 100 ^{o}C). It was in the second effort of this work that the design space was shown to accommodate the formation of MHILs from multi-heterocycle precursors, highlighted by the synthesis of a zwitterionic bi-tetrazole-functionalized tri-heterocycle that could be further modified into *either* the cationic or anionic component of new MHILs by one-step transformations based upon IL chemical principles. Thus, it was concluded that this platform was both general in scope and unique in its approach to obtain singly-charged MHIL ions or their precursors. Although these initial results were very promising, it was evident that there was a full range of synthetic possibilities that awaited further

exploration. The remaining chapters of this work report efforts that were made to fulfill this call, but other applications that could benefit from utilizing the MHIL design platform include areas such as surface functionalization, poly(MHIL) synthesis, pharmaceutical synthesis, and supramolecular chemistry, to name but a few.

Many of the cations introduced in Chapter 2 were employed as click-reactive precursors in more recent studies. For example, the synthesis of a homologous series of Zn-complexed 1-(5-tetrazolidyl)alkyl-3-alkylimidazolium zwitterions (Chapter 4) were obtained by synthetic methods described in Chapter 3. An NMR kinetic study showed that *N*-cyanoalkyl-functionalized cations are optimal for click synthesis of tetrazoles with azide anion, as they were often high yielding under ambient conditions and faster reaction times in comparison with neutral nitrile precursors. Additionally, the single-crystal XRD analysis of *catena*-poly[(bromochlorozinc)-μ-[1-(5-tetrazolato)methyl-3-methylimidazolium]-N_1:N_4] shows a coordination polymer structure that supports the potential use of these zwitterions as organometallic ligands with variable *N*-alkyl and *N*-alkyl bridge lengths. As the separation of Zn was demonstrated in the initial work (Chapter 3), these compounds can provide access to zwitterions capable of further modification into MHILs or utilization as ligands for new coordination chemistry.

The reactivity of *N*-cyanoalkyl-functionalized imidazolium halides was addressed by observing the products of their elution down an azide anion exchange resin column (Chapter 5). Competing hydration (amide product) and [3+2] dipolar cycloaddition (tetrazole product) were observed, where product ratios were found to vary from precursors with different (i) *N*-alkyl chain length, (ii) distance and substitution of α-carbon next to nitrile group and (iii) type of

halide. Electronic effects (aromatic alkyl induction, proximity of nitrile reactive site to the imidazolium ring, *etc.*) were proposed to explain the differences in product formation, where it was concluded that tetrazole-based products might be directed by the shorter *N*-cyanoalkyl chain length (higher polarization for dipolar cycloaddition), longer *N*-alkyl substituents on the imidazolium ring (higher alkyl inductive effect), and halide anion in precursor that has greater selectivity for the anion exchange resin (e.g., bromide vs. less selective chloride) to increase promote azide exchange. Further study would provide more conclusive results, however, the initial findings suggest a fast and convenient synthetic technique which might be directed for improved protocols to synthesize commodity chemicals: amides (for pharmaceutical design) and tetrazoles (towards EILs or other MHIL synthesis) obtained under ambient, metal- and solvent-free conditions.

The dual-functional nature of ILs was captured in the synthesis of azolium azolate-based MHILs (Chapter 6), where the modular combination of azolium azides with neutral nitriles with acetic acid to form room temperature MHILs featuring a 5-(2-(azolyl)ethyl)tetrazolate bi-heterocyclic anion. The synthetic protocol benefits from (i) a metal- and solvent-free synthetic protocol, (ii) an azolium azide IL precursor that is both an azide source as well as a modular azolium component in the final MHIL and (iii) a neutral nitrile that may be structurally modified in type of heterocycle, substituents, and *N*-cyanoalkyl chain length. This work exemplifies how each component of an MHIL may be strategically formed in a compartmentalized fashion, and future exploration of new synthetic variants waits. For example, one can envision a similar reaction for two equivalents of azolium azide with one equivalent of a dinitrile-functionalized heterocycle to yield a [azolium]$_2$[ditetrazolate] product. Such 'double-click' reactivity had been previously shown in Chapter 3, however, the methodology could be improved by employing the

dual-functional nature of IL design to incorporate an azolium into the final MHIL product if azolium azide were used rather than an inorganic azide source.

The field of IL research has already grown into regions where the design of ILs on the molecular level can be effectively put to use nano- and mesoscale architectures, and continuing to develop the chemistry introduced here provides an effective way to 'bridge the gap'. The discovery of new MHIL structures and methods for their design may provide significant direction for both revealing new insight into the fundamentals of IL chemistry as well as identifying possible applications valuable for high-performance applications in academia as well as industry. Likewise, as new strides are made in different disciplines, IL chemical theory and practice will in turn gain from the feedback provided by such discoveries, which we may find as effective tools to address the challenges of tomorrow.